

Chem, Volume 5

Supplemental Information

**An Auxiliary Approach
for the Stereoselective Synthesis
of Topologically Chiral Catenanes**

Mathieu Denis, James E.M. Lewis, Florian Modicom, and Stephen M. Goldup

Supplemental Experimental Procedures

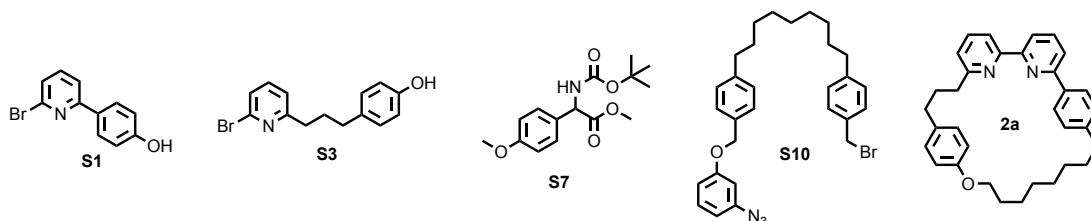
1. General Experimental	2
2. Syntheses of macrocycles 2b and 2c.....	3
S2.....	3
S4.....	7
2b.....	10
S5.....	13
S6.....	16
2c.....	19
3. Syntheses of U-shapes 1 and S11.....	23
(R)-1	32
(S)-1.....	36
S11.....	37
4. Syntheses of catenanes 3 and 6.....	40
(R,S _{mt})-3b and (R,R _{mt})-3b.....	44
(S,S _{mt})-3b and (S,R _{mt})-3b.....	53
(R,R/S _{mt})-3c.....	54
rac-6b	55
(S _{mt})-6b	59
(R _{mt})-6b	60
5. Syntheses of triazole-functionalised macrocycles S12 and S13	61
S12.....	61
S13.....	65
6. Chiral Stationary Phase HPLC analysis of catenane 6b, S8 and S9.....	68
7. Single Crystal X-ray Analysis of Catenane (S*,R* _{mt})-3b.....	71
8. Preliminary Molecular Modelling of the AT-CuAAC Reaction Between (R)-1 and 2b ...	74
9. Supplemental References.....	78

1. General Experimental

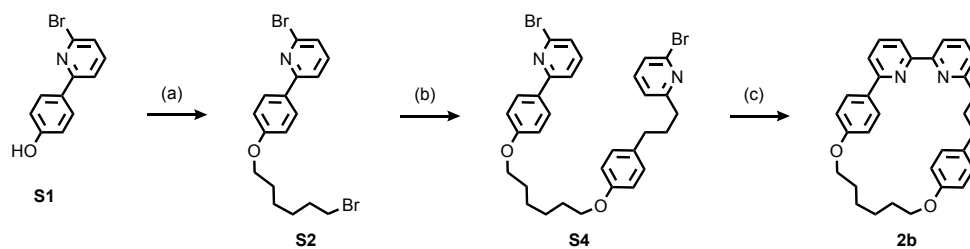
Synthesis: Unless otherwise stated, all reagents, including anhydrous solvents, were purchased from commercial sources and used without further purification. All reactions were carried out under an atmosphere of N₂ using anhydrous solvents unless otherwise stated. Petrol refers to the fraction of petroleum ether boiling in the range 40-60 °C. Flash column chromatography was performed using Biotage Isolera-4 automated chromatography system, employing Biotage SNAP or ZIP cartridges. Analytical TLC was performed on precoated silica gel plates (0.25 mm thick, 60F254, Merck, Germany) and observed under UV light.

Analysis: NMR spectra were recorded on Bruker AV400, AV3-400 or AV500, at a constant temperature of 298 K. Chemical shifts are reported in parts per million from low to high field and referenced to residual solvent. ¹³C data were typically recorded as phased JMOD experiments. Coupling constants (J) are reported in Hertz (Hz). Standard abbreviations indicating multiplicity were used as follows: m = multiplet, quint = quintet, q = quartet, t = triplet, d = doublet, s = singlet, app. = apparent, br = broad. Signal assignment was carried out using 2D NMR methods (HSQC, HMBC, COSY, NOESY) where necessary. In the case of some complex multiplets with contributions from more than one signal absolute assignment was not possible. Here indicative either/or assignments are provided. All melting points were determined using a Griffin apparatus. Low resolution mass spectrometry was carried out by the mass spectrometry services at the University of Southampton (Waters TQD mass spectrometer equipped with a triple quadrupole analyser with UHPLC injection [BEH C18 column; MeCN-hexane gradient {0.2% formic acid}]). High resolution mass spectrometry was carried out by the mass spectrometry services at the University of Southampton (MaXis, Bruker Daltonics, with a Time of Flight (TOF) analyser; samples were introduced to the mass spectrometer via a Dionex Ultimate 3000 autosampler and uHPLC pump in a gradient of 20% acetonitrile in hexane to 100% acetonitrile (0.2% formic acid) over 5 min at 0.6 mL min; column: Acquity UPLC BEH C18 (Waters) 1.7 micron 50 × 2.1mm). As accurate mass measurements are of limited value for compounds with Mw >1000 Da, in these cases a graphical comparison of the observed isotope pattern and the predicted isotopic distribution is provided.

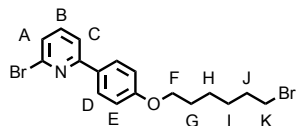
The following compounds were synthesized according to literature procedures: S1, S3, macrocycle 2a,¹ S7,² S10.³



2. Syntheses of macrocycles **2b** and **2c**



Scheme S1 Synthesis of macrocycle **2b**. Conditions: (a) 1,6-dibromohexane, K_2CO_3 , MeCN, reflux, 18 h, 68%; (b) **S3**, K_2CO_3 , MeCN, reflux, 86%; (c) $Ni(PPh_3)_2Br_2$, PPh_3 , Mn, Et_4NI , DMF/THF, 50 °C, 6 h, 71%.



S2

To a solution of **S1** (1 g, 4 mmol, 1 eq.) in MeCN (20 mL) was added K_2CO_3 (2.2 g, 16 mmol, 4 eq.) as a solid. After stirring for 30 minutes, 1,6-dibromohexane (1.53 mL, 2.5 mmol, 2.5 eq.) was added and the reaction was stirred at reflux for 18 h. The cooled reaction mixture was filtered through celite. The solvent was removed *in vacuo*. The residue was purified by column chromatography (Petrol with a gradient from 0 to 50% CH_2Cl_2) to give **S2** as a white solid (1.1 g, 68%). m.p. 94–96 °C. 1H NMR (400 MHz, $CDCl_3$) δ : 7.94 (d, J = 8.9, 2H, H_D), 7.61 (dd, J = 7.7, 0.9, 1H, H_C), 7.54 (t, J = 7.7, 1H, H_B), 7.34 (dd, J = 7.7, 0.9, 1H, H_A), 6.96 (d, J = 8.9, 2H, H_E), 4.02 (t, J = 6.4, 2H, H_F), 3.43 (t, J = 6.7, 2H, H_K), 1.97–1.87 (m, 2H, H_J), 1.87–1.77 (m, 2H, H_G), 1.60–1.45 (m, 4H, H_H , H_I). ^{13}C NMR (101 MHz, $CDCl_3$) δ : 160.6, 158.4, 142.2, 139.0, 130.3, 128.5, 125.6, 118.2, 114.8, 68.0, 33.9, 32.8, 29.2, 28.1, 25.4. HR-ESI-MS m/z = 411.9910 $[M+H]^+$ (calc. for $C_{17}H_{20}Br_2NO$ 411.9906).

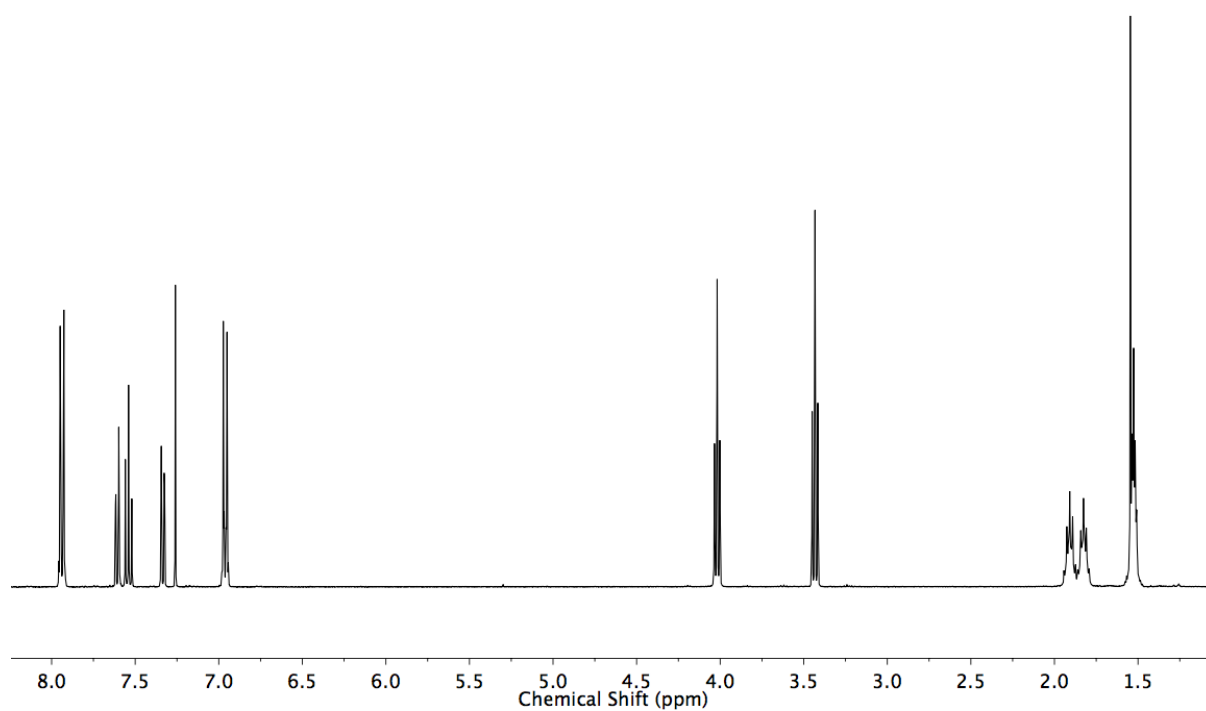


Figure S1 ^1H NMR (400 MHz, CDCl_3) of S2.

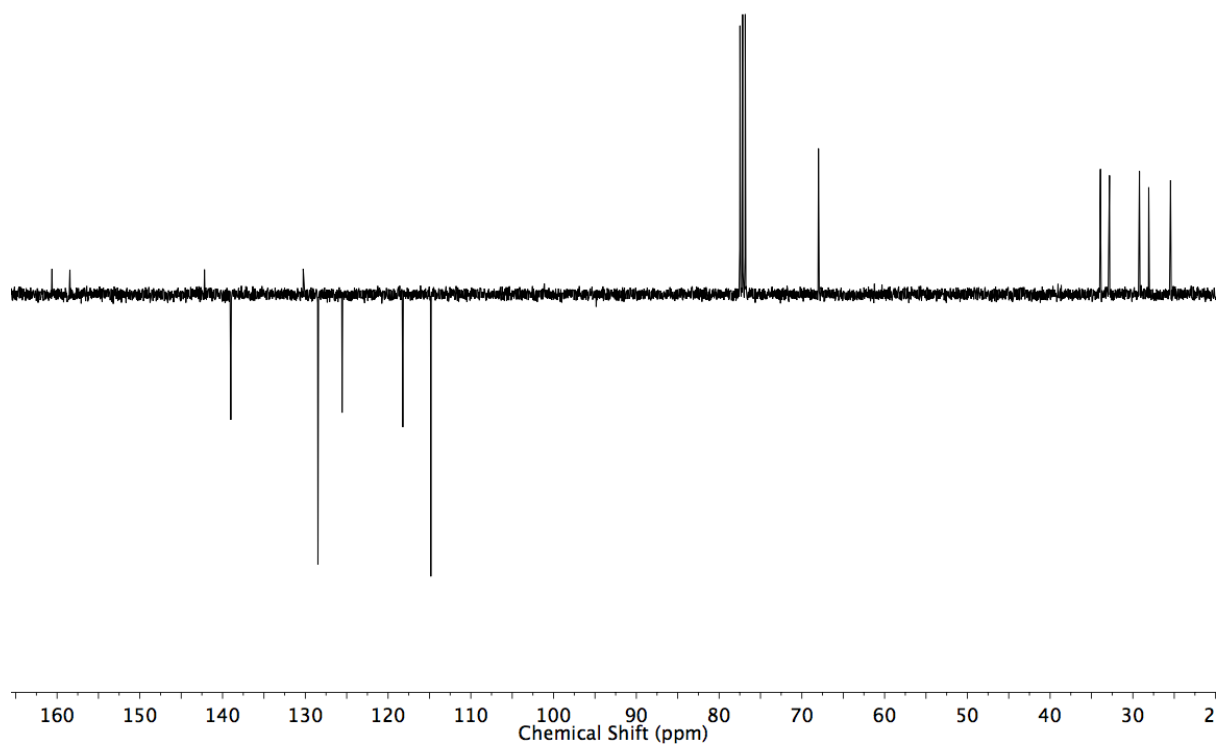


Figure S2 JMOD NMR (101 MHz, CDCl_3) of S2.

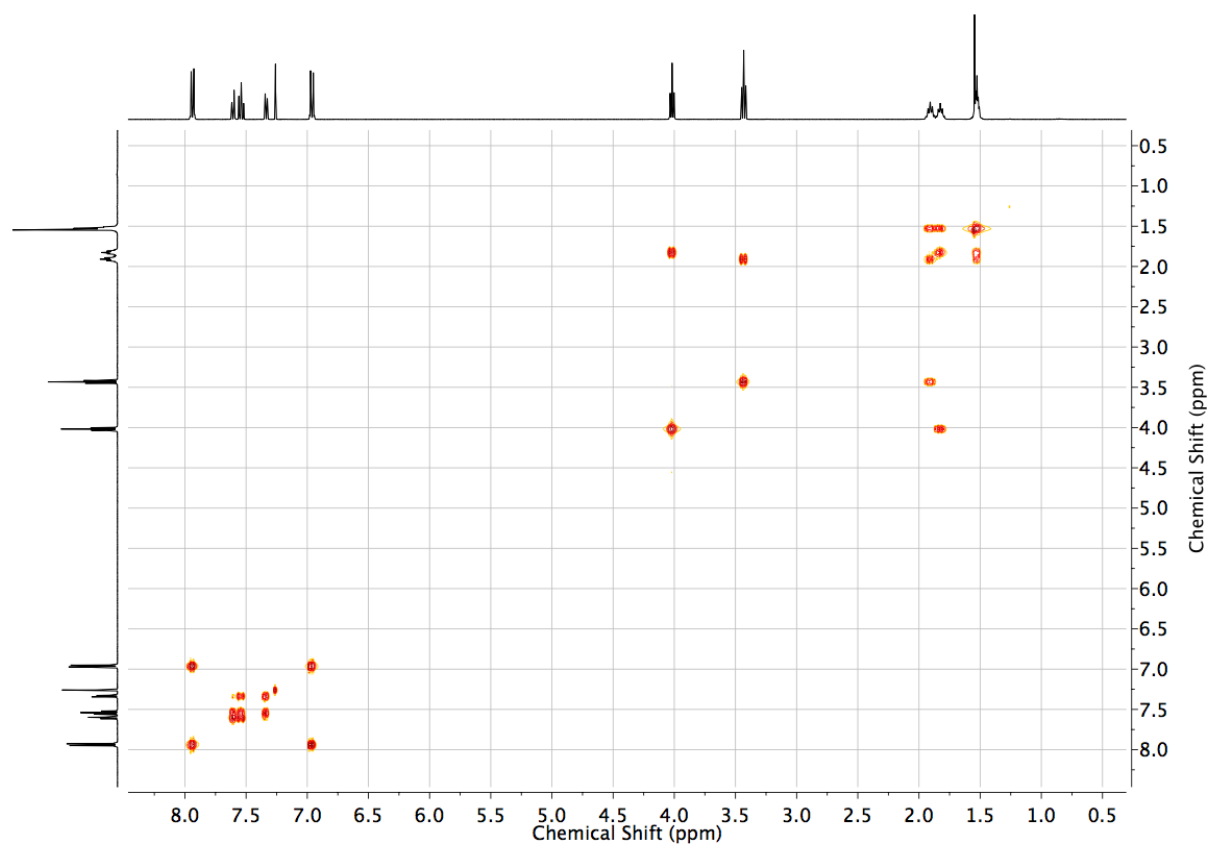


Figure S3 COSY NMR (CDCl₃) of S2.

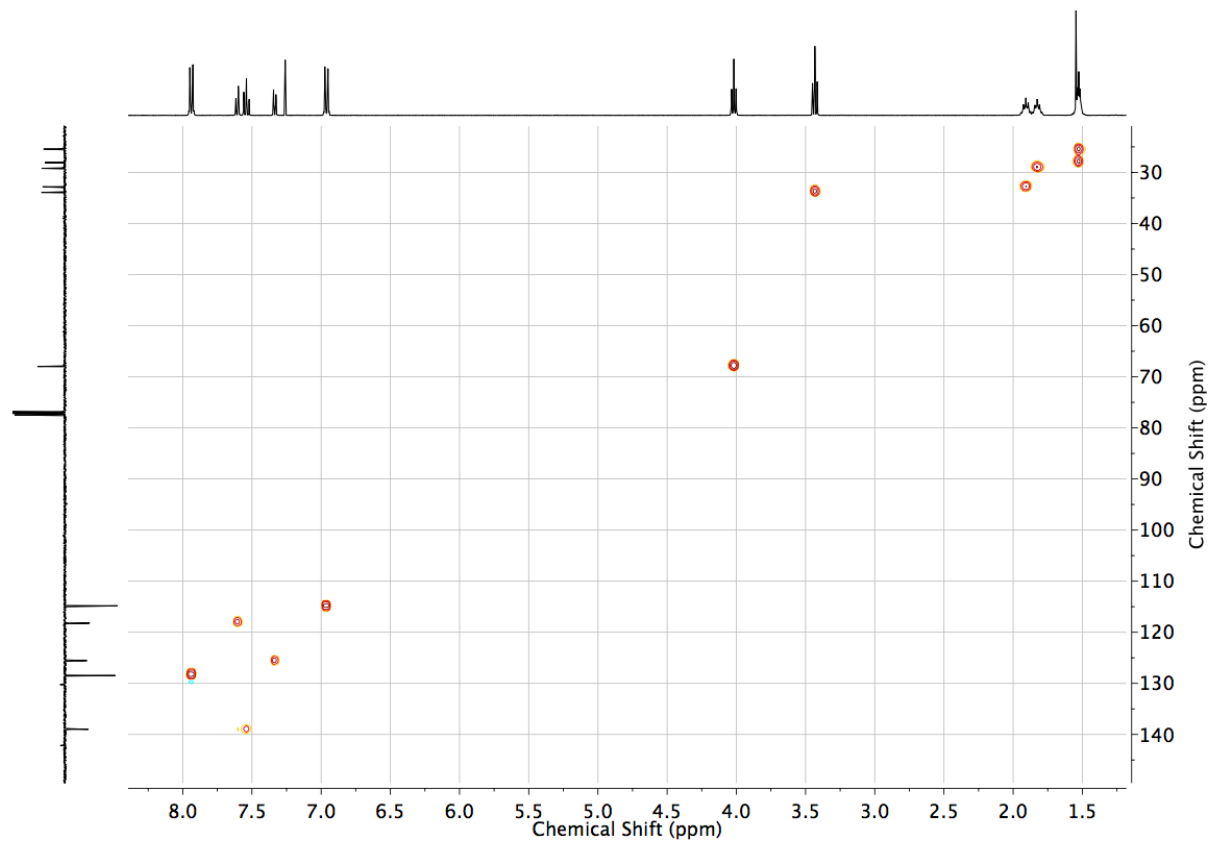


Figure S4 HSQC NMR (CDCl₃) of S2.

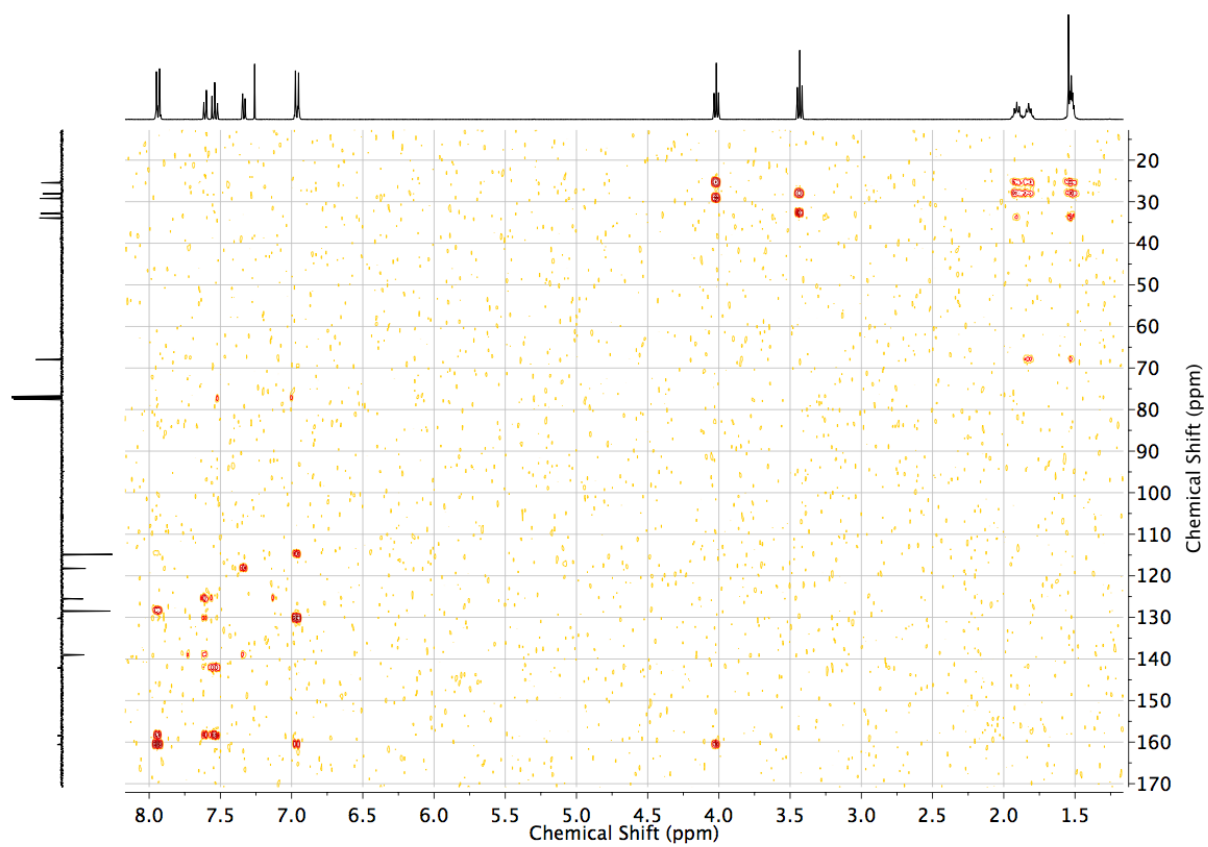
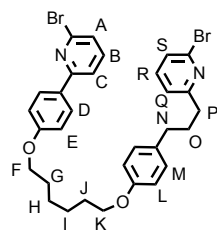


Figure S5 HMBC NMR (CDCl_3) of **S2**.



S4

To a solution of **S3** (4.5 g, 15.3 mmol, 1.2 eq.) in MeCN (70 mL) was added K_2CO_3 (2.76 g, 20.0 mmol, 1.7 eq.) as a solid. After stirring for 30 minutes, **S2** (5.0 g, 12.1 mmol, 1.0 eq.) was added as a solid and the reaction stirred at reflux for 18 h. The solvent was removed *in vacuo* and the resultant solid dissolved in CH_2Cl_2 (500 mL), washed with H_2O (100 mL) and brine (100 mL), dried ($MgSO_4$), filtered and the solvent removed *in vacuo*. After purification by column chromatography (Petrol/ CH_2Cl_2 1/1 with a gradient to 80% CH_2Cl_2), **S4** (6.5 g, 86%) was obtained as a white solid. m.p. 96-98 °C. 1H NMR (400 MHz, $CDCl_3$) **S4**: 7.94 (d, $J = 8.8$, 2H, H_D), 7.60 (dd, $J = 7.7$, 0.9, 1H, H_C), 7.54 (t, $J = 7.7$, 1H, H_B), 7.43 (t, $J = 7.7$, 1H, H_R), 7.33 (dd, $J = 7.7$, 0.9, 1H, H_A), 7.29 (dd, $J = 7.7$, 0.9, 1H, H_S), 7.13-7.04 (m, 4H, H_M , H_Q), 6.96 (d, $J = 8.9$, 2H, H_E), 6.82 (d, $J = 8.5$, 2H, H_L), 4.02 (t, $J = 6.5$, 2H, H_P), 3.95 (t, $J = 6.4$, 2H, H_K), 2.78 (t app, $J = 7.8$, 2H, H_P), 2.61 (t app, $J = 7.6$, 2H, H_N), 2.07-1.95 (m, 2H, H_O), 1.90-1.76 (m, 4H, H_G , H_J), 1.61-1.50 (m, 4H, H_H , H_I). ^{13}C NMR (101 MHz, $CDCl_3$) **S4**: 164.0, 160.7, 158.5, 157.5, 142.2, 141.7, 139.0, 138.7, 134.0, 130.2, 129.5, 128.5, 125.5, 125.4, 121.6, 118.2, 114.8, 114.6, 68.1, 68.0, 37.6, 34.7, 31.7, 29.4, 29.3, 26.1. HR-ESI-MS $m/z = 623.0907$ $[M+H]^+$ (calc. for $C_{31}H_{33}Br_2N_2O_2$ 623.0903).

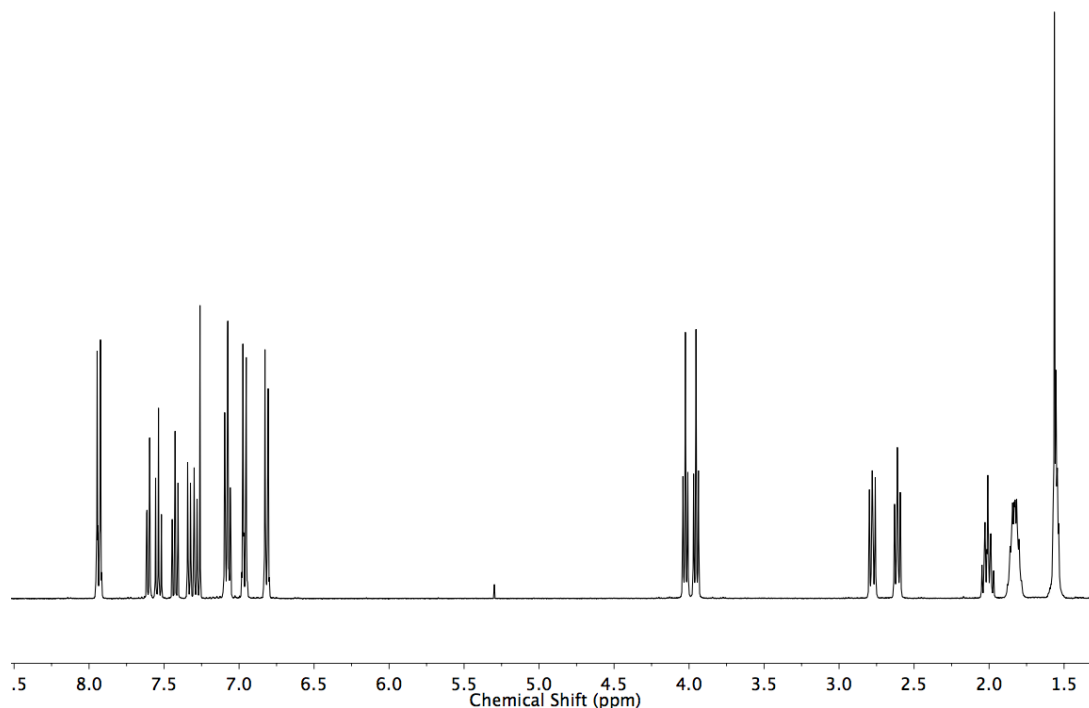


Figure S6 1H NMR (400 MHz, $CDCl_3$) of **S4**.

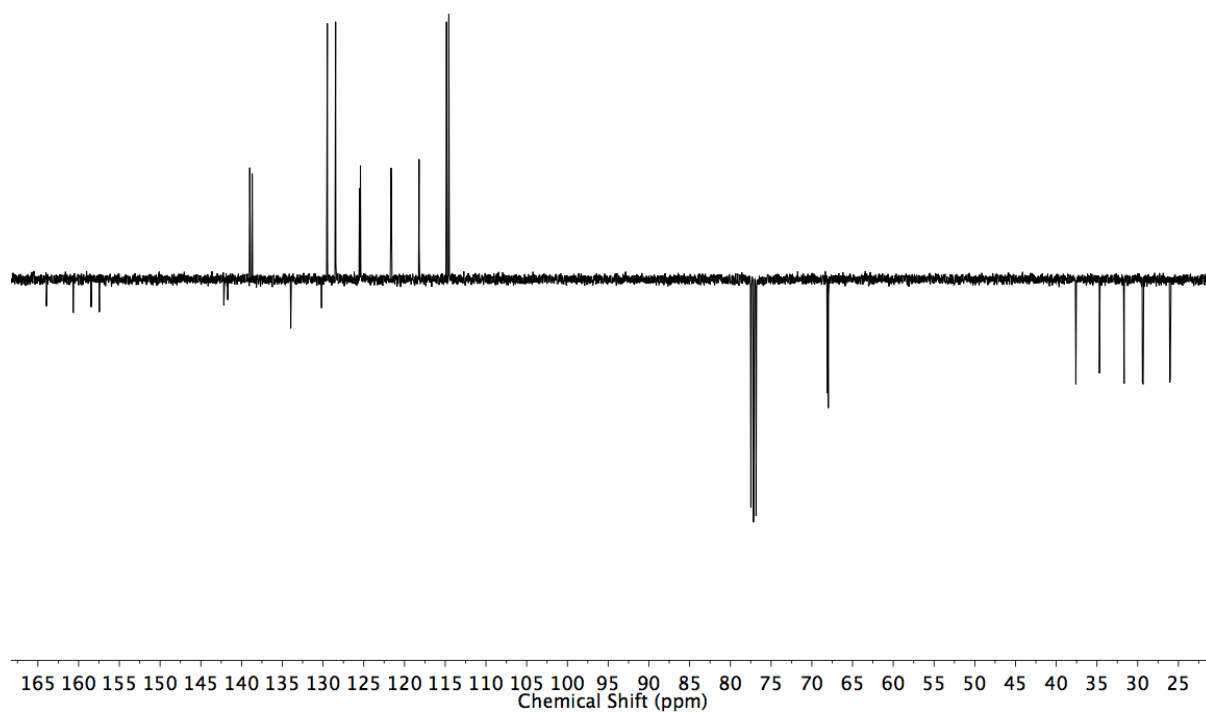


Figure S7 JMOD NMR (101 MHz, CDCl₃) of S4.

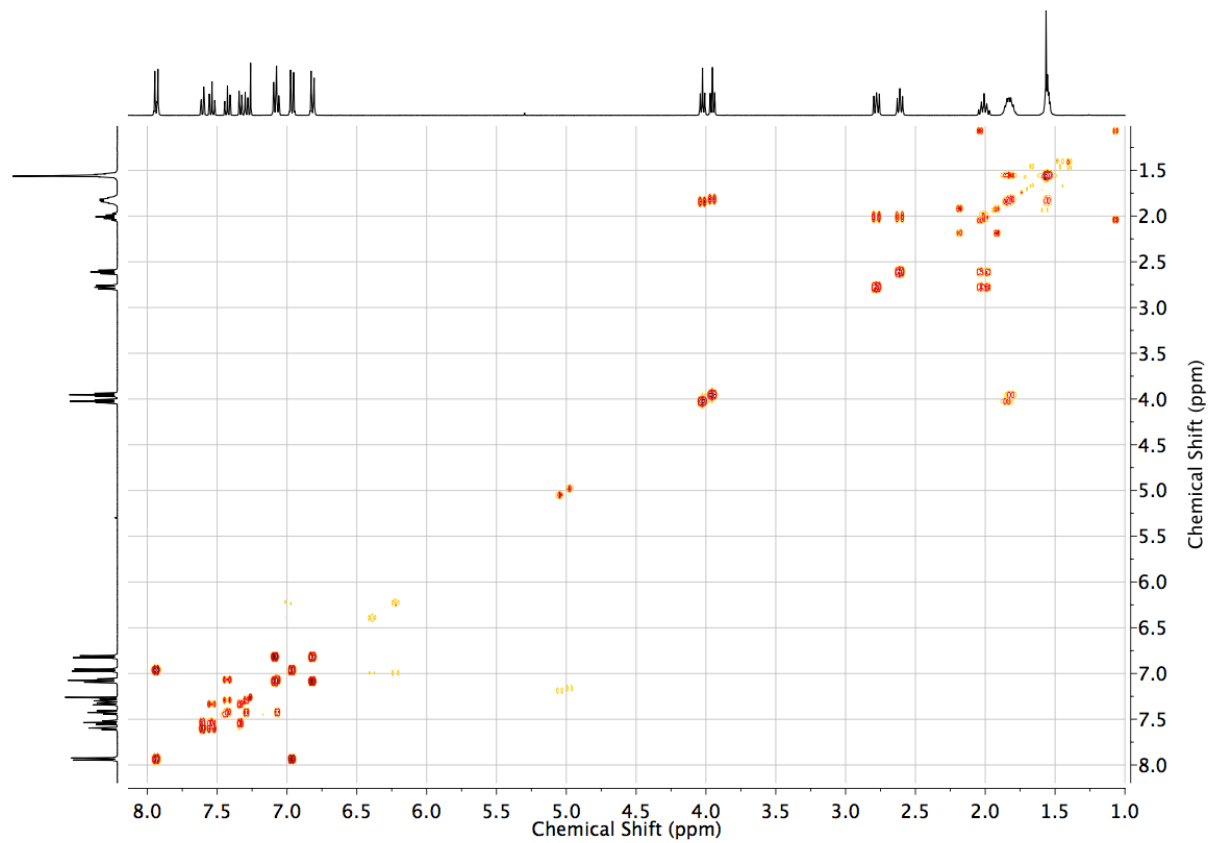


Figure S8 COSY NMR (CDCl₃) of S4.

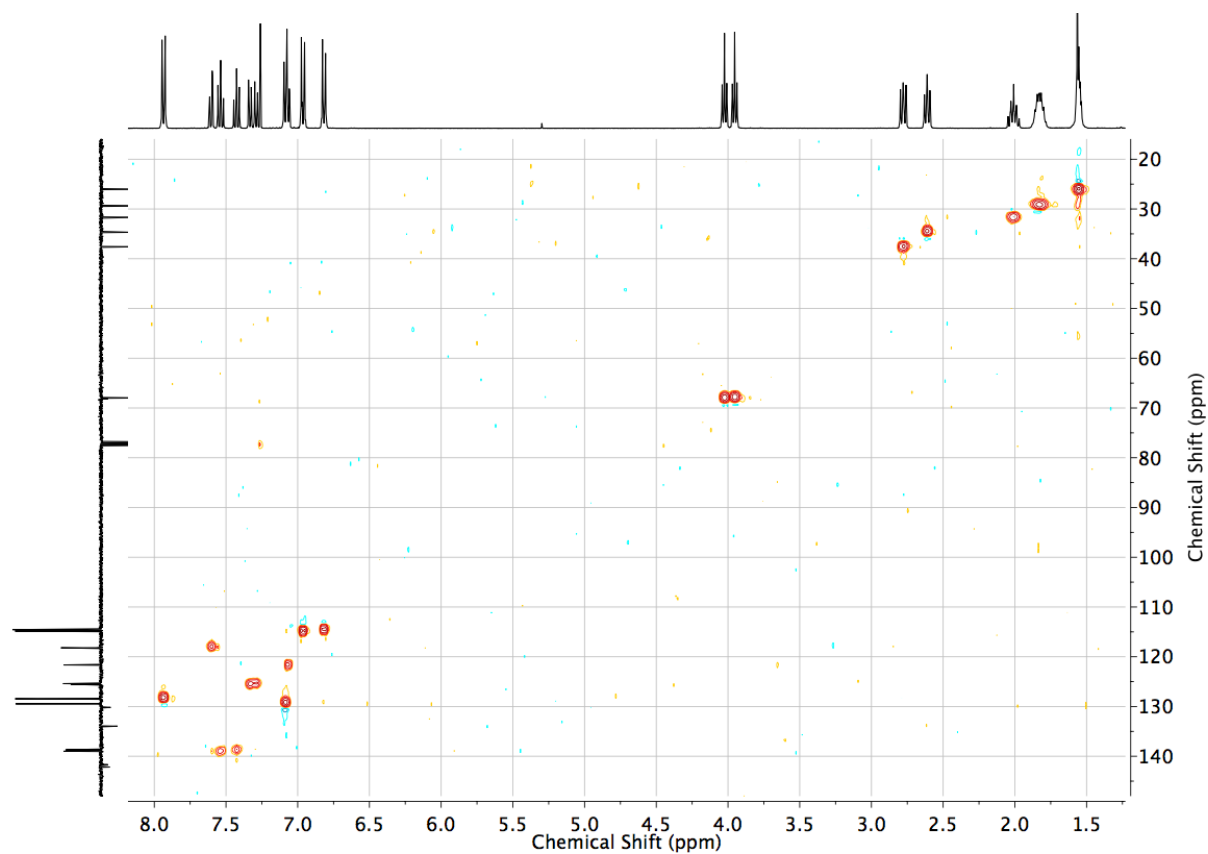


Figure S9 HSQC NMR (CDCl_3) of **S4**.

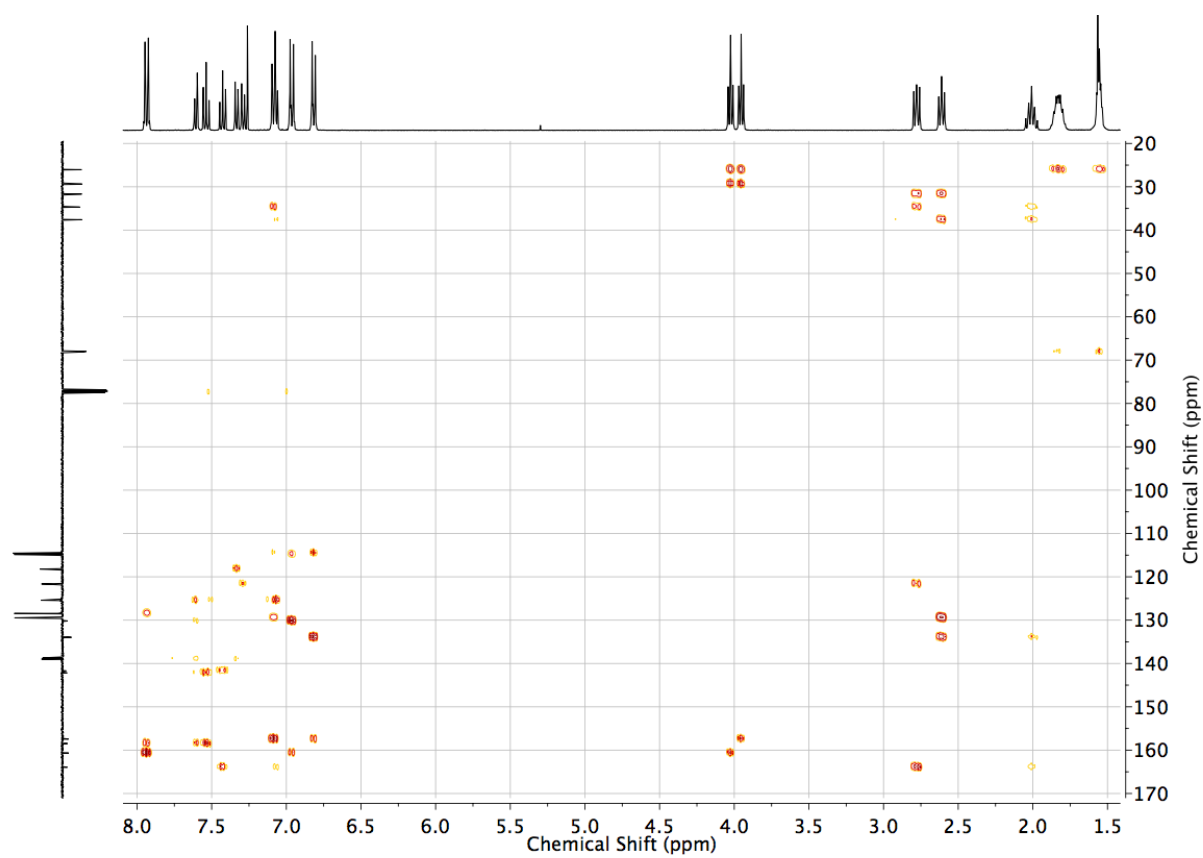
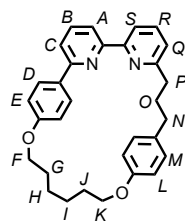


Figure S10 HMBC NMR (CDCl_3) of **S4**.



2b

[Ni(PPh₃)₂Br₂] (1.49 g, 2.00 mmol, 1 eq.), PPh₃ (1.05 g, 4.00 mmol, 2 eq.), Mn (1.10 g, 20.0 mmol, 10 eq.) and NEt₄I (0.514 g, 2.00 mmol, 1 eq.) in DMF (20 mL) were sonicated for 10 min, followed by stirring at 50 °C for 1 h. To this catalyst mixture was added **S4** (1.25 g, 2.00 mmol, 1 eq.) in DMF (20 mL) via syringe over 4 h, followed by additional stirring of the reaction for 1 h. To the cooled reaction was added CH₂Cl₂ (100 mL) and EDTA-NH₃ solution (100 mL). After filtering through a pad of Celite the organic phase was washed with water (2 × 100 mL) and brine (100 mL), and the combined aqueous phases extracted with CH₂Cl₂ (50 mL). The combined organic phases were dried (MgSO₄), filtered and the solvent removed *in vacuo*. The crude product was purified by column chromatography (Petrol with a gradient of 0 to 60% CHCl₃ + 0.2% EtOH) yielded **2b** as white solid (0.653 g, 71%). m.p. 130-132 °C. ¹H NMR (500 MHz, CDCl₃) **δ**: 8.08 (d, *J* = 9.0, 2H, H_D), 7.80 (t, *J* = 7.8, 1H, H_B), 7.71 (t, *J* = 7.8, 1H, H_R), 7.70 (dd, *J* = 7.7, 0.9, 1H, H_C), 7.65 (dd, *J* = 7.7, 0.9, 1H, H_A), 7.62 (dd, *J* = 7.9, 0.9, 1H, H_S), 7.31 (d, *J* = 8.7, 2H, H_M), 7.22 (dd, *J* = 7.6, 0.9, 1H, H_Q), 6.85 (d, *J* = 9.0, 2H, H_E), 6.78 (d, *J* = 8.7, 2H, H_I), 4.10 (t, *J* = 6.7, 2H, H_F), 3.98 (t, *J* = 6.1, 2H, H_K), 3.00 (t, *J* = 7.2, 2H, H_P), 2.73 (dd, *J* = 8.8, 6.6, 2H, H_N), 2.41-2.20 (m, 2H, H_O), 1.79 (m, 4H, H_G, H_J), 1.66-1.51 (m, 4H, H_H, H_L). ¹³C NMR (126 MHz, CDCl₃) **δ**: 162.5, 160.0, 157.5, 157.4, 156.7, 156.4, 137.5, 136.9, 135.2, 132.2, 130.1, 128.8, 122.8, 119.5, 119.4, 118.7, 115.3, 114.9, 68.1, 67.7, 37.0, 34.3, 31.4, 28.6, 28.2, 24.8, 24.5. HR-ESI-MS *m/z* = 465.2535 [M+H]⁺ (calc. for C₃₁H₃₃N₂O₂ 465.2537).

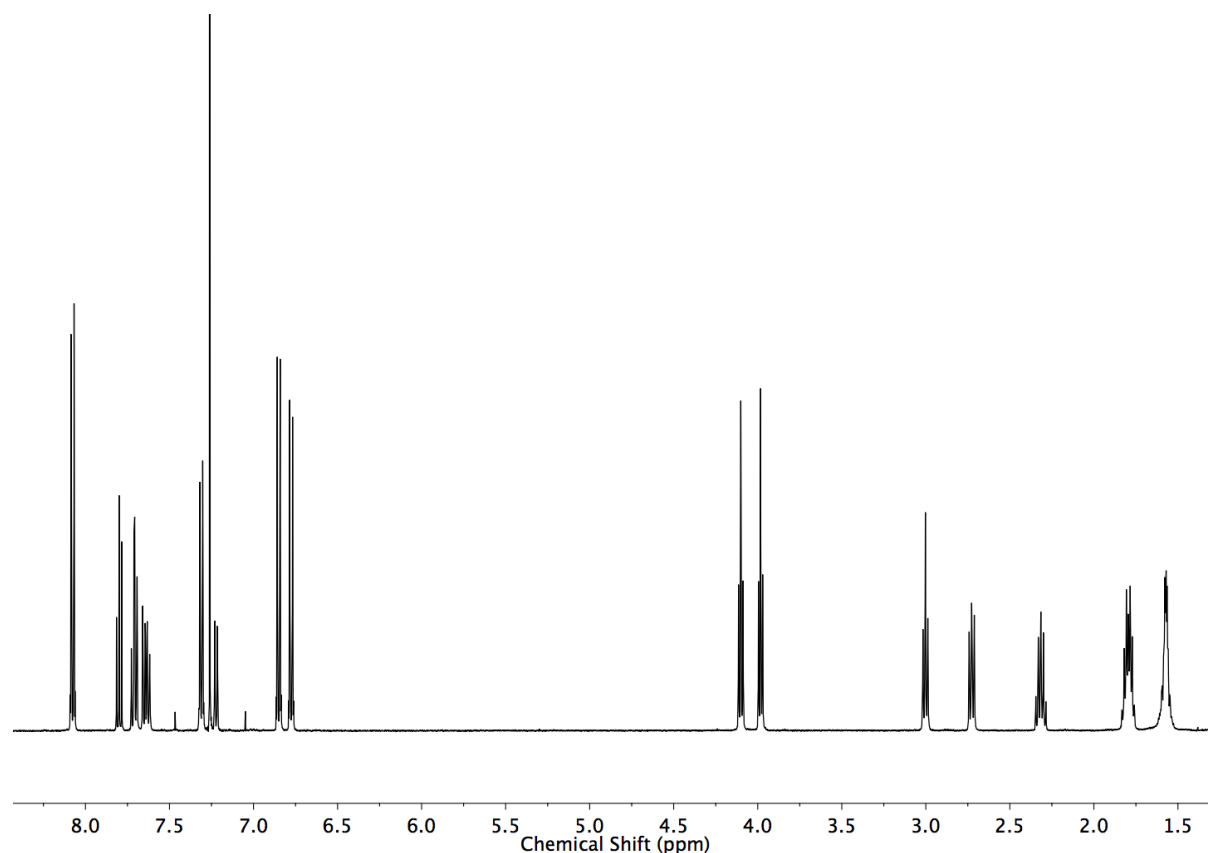


Figure S11 ¹H NMR (500 MHz, CDCl₃) of **2b**.

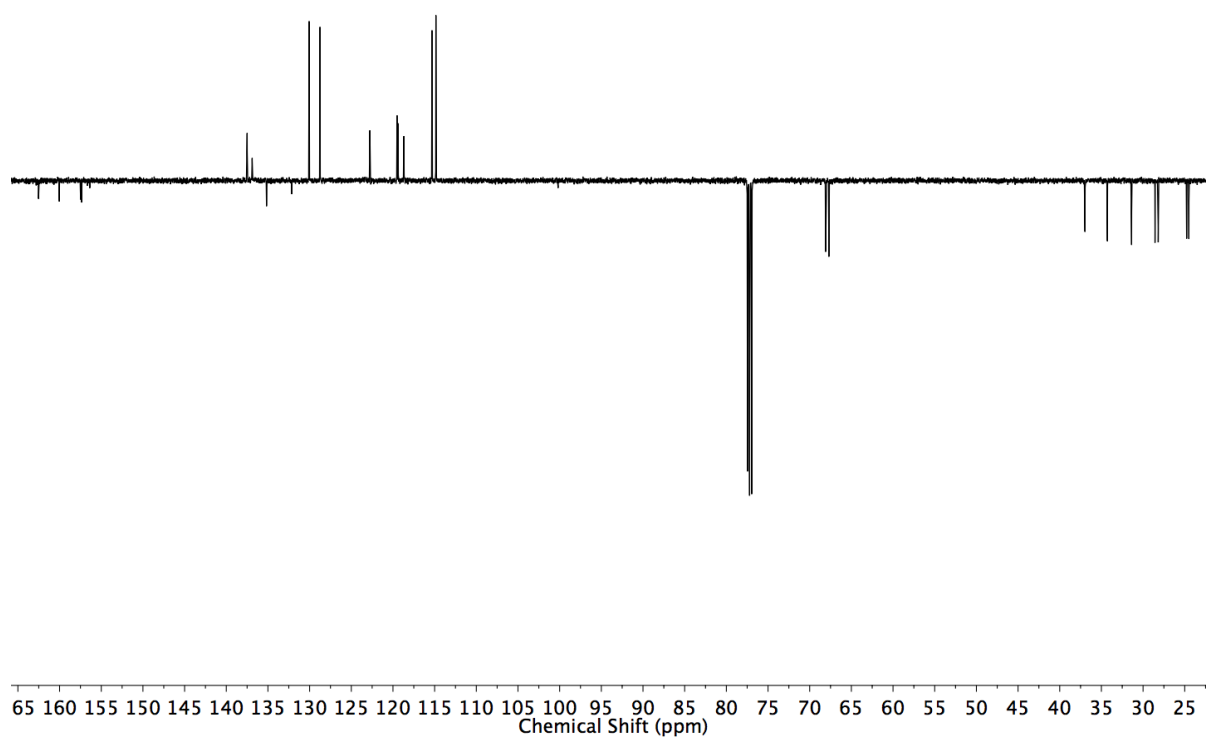


Figure S12 JMOD NMR (126 MHz, CDCl_3) of **2b**.

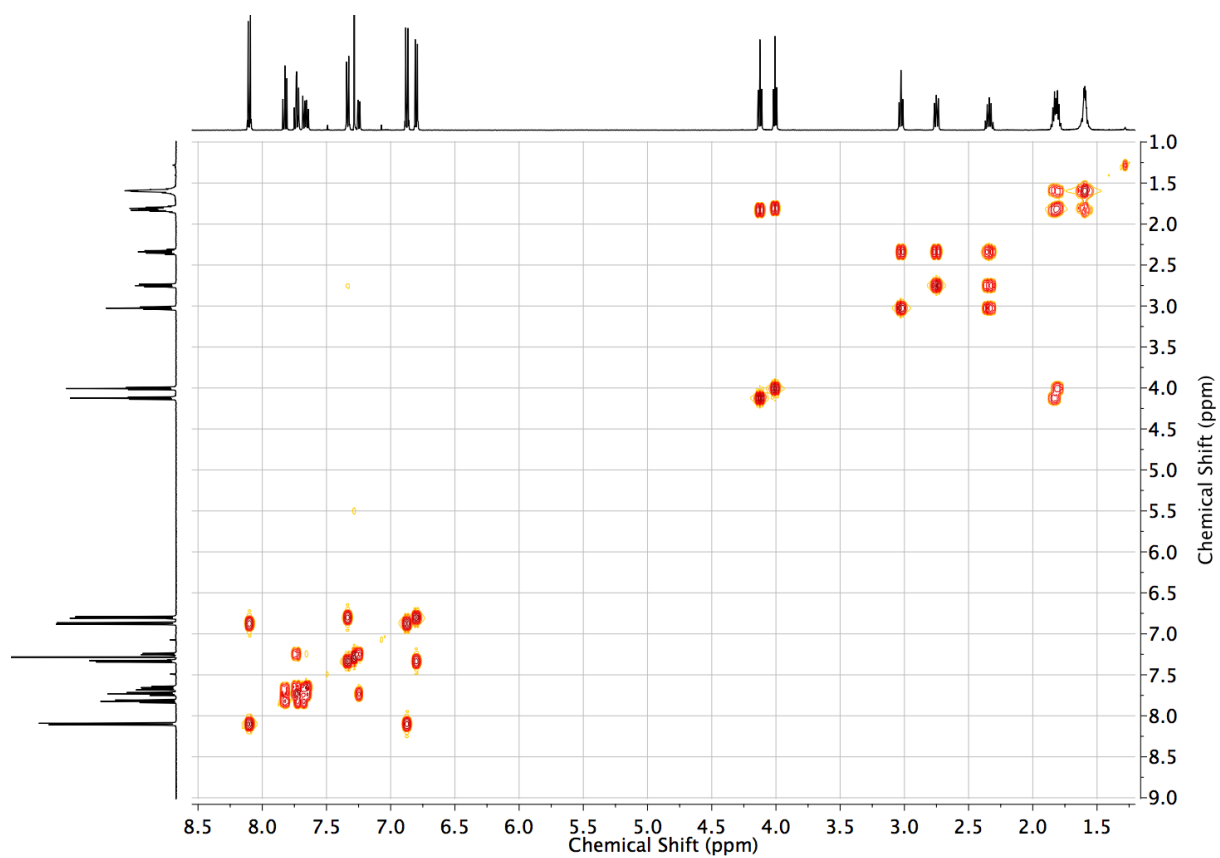


Figure S13 COSY NMR (CDCl_3) of **2b**.

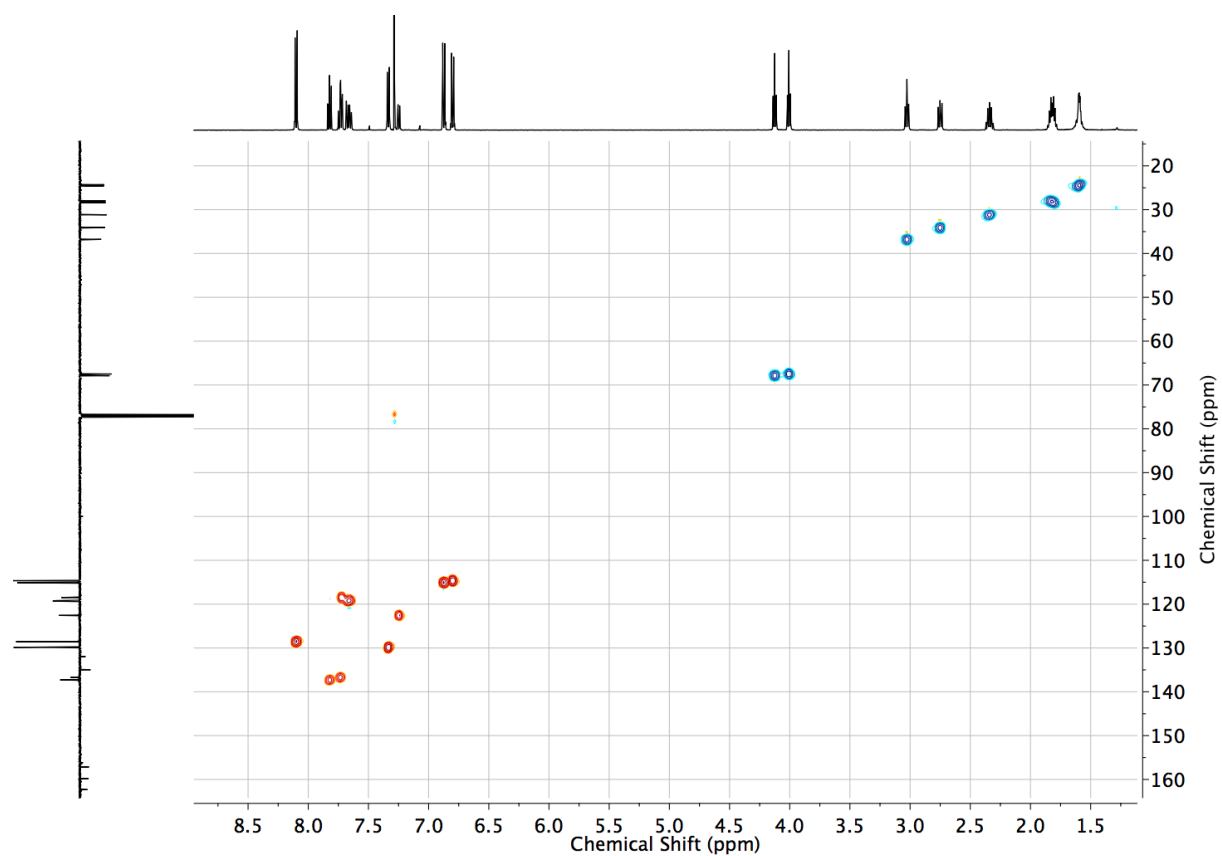


Figure S14 HSQC NMR (CDCl_3) of **2b**.

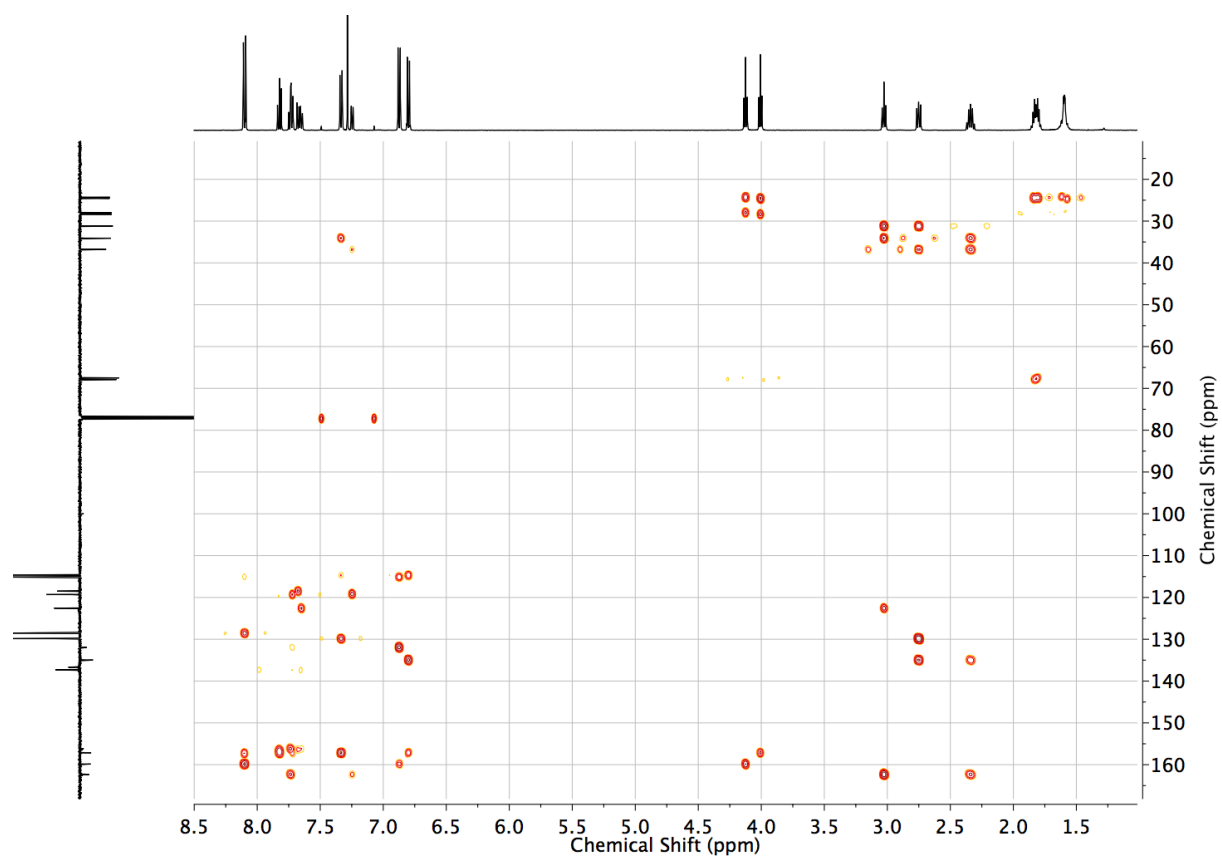
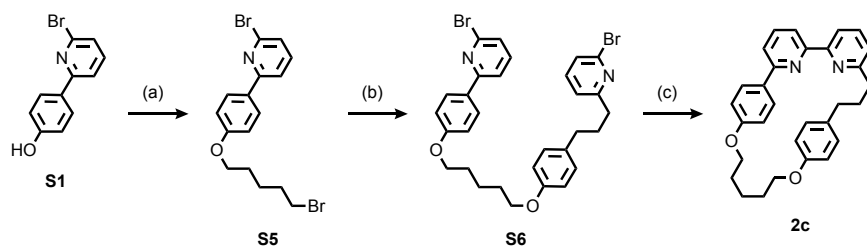
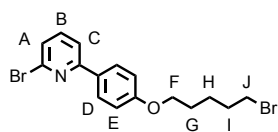


Figure S15 HMBC NMR (CDCl_3) of **2b**.



Scheme S2 Synthesis of macrocycle **2c**. Conditions: (a) 1,5-dibromoheptane, K_2CO_3 , MeCN, reflux, 18 h, 69%; (b) **S3**, K_2CO_3 , MeCN, reflux, 80%; (c) $Ni(PPh_3)_2Br_2$, PPh_3 , Mn, Et_4NI , DMF/THF, 50 °C, 6 h, 38%.



S5

To a solution of **S1** (1 g, 4 mmol, 1 eq.) in MeCN (20 mL) was added K_2CO_3 (2.2 g, 16 mmol, 4 eq.) as a solid. After stirring for 30 minutes, 1,6-dibromopentane (1.35 mL, 2.5 mmol, 2.5 eq.) was added and the reaction was stirred at reflux for 18 h. The cooled reaction mixture was filtered through celite. The solvent was removed *in vacuo*. The residue was purified by column chromatography (Petrol with a gradient from 0 to 50% CH_2Cl_2) to give **S5** as a white solid (1.1 g, 69%). m.p. 70-72 °C 1H NMR (400 MHz, $CDCl_3$) **δ**: 7.94 (d, J = 8.9, 2H, H_D), 7.60 (dd, J = 7.7, 0.9, 1H, H_C), 7.54 (t, J = 7.7, 1H, H_B), 7.33 (dd, J = 7.7, 0.9, 1H, H_A), 6.96 (d, J = 8.9, 2H, H_E), 4.02 (t, J = 6.3, 2H, H_F), 3.45 (t, J = 6.7, 2H, H_K), 2.01-1.90 (m, 2H, H_I), 1.89-1.78 (m, 2H, H_G), 1.70-1.60 (m, 2H, H_H). ^{13}C NMR (101 MHz, $CDCl_3$) **δ**: 160.5, 158.4, 142.2, 139.0, 130.3, 128.5, 125.6, 118.2, 114.8, 67.8, 33.7, 32.6, 28.5, 25.0. HR-ESI-MS m/z = 397.9752 $[M+H]^+$ (calc. for $C_{16}H_{18}Br_2NO$ 397.9750).

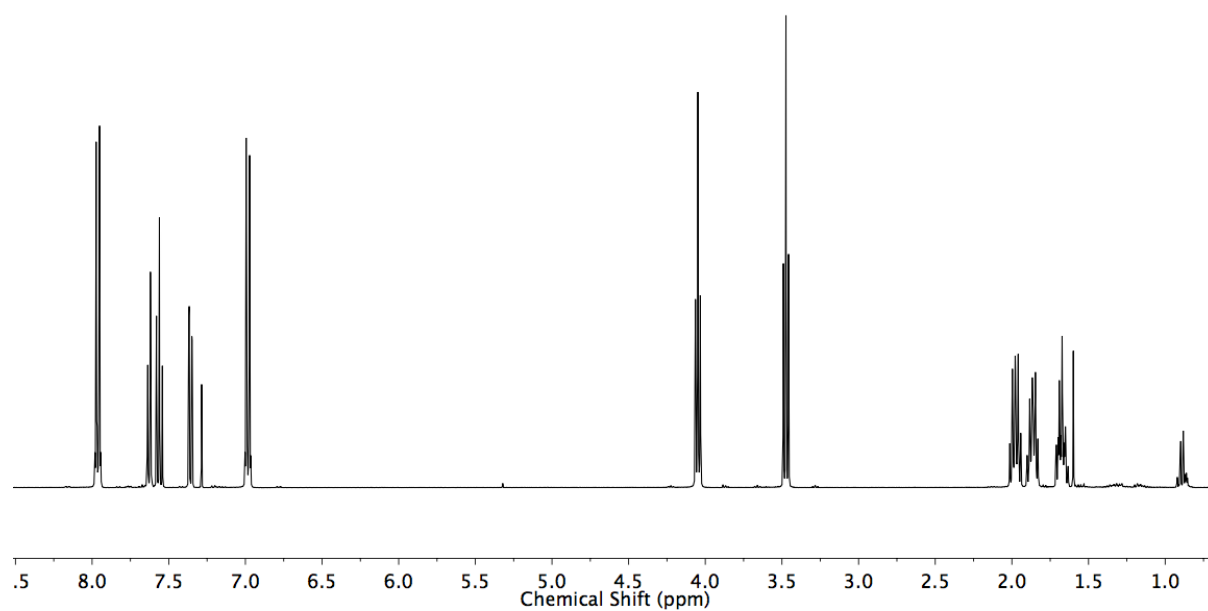


Figure S16 ¹H NMR (400 MHz, CDCl₃) of S5.

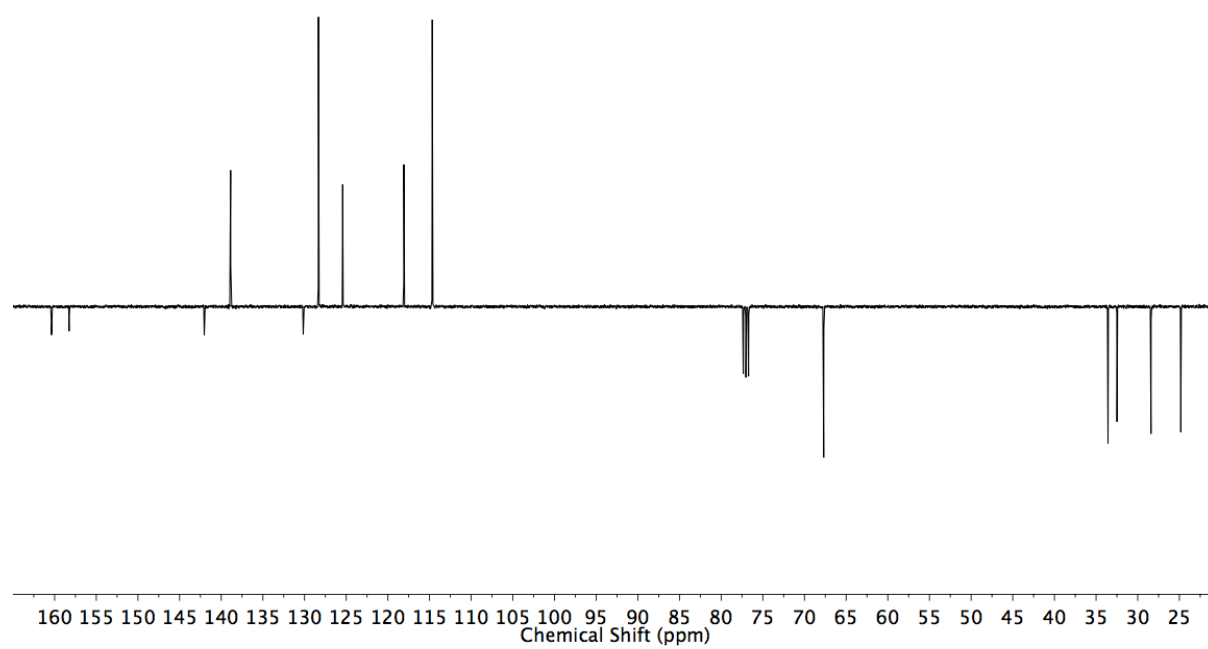


Figure S17 JMOD NMR (101 MHz, CDCl₃) of S5.

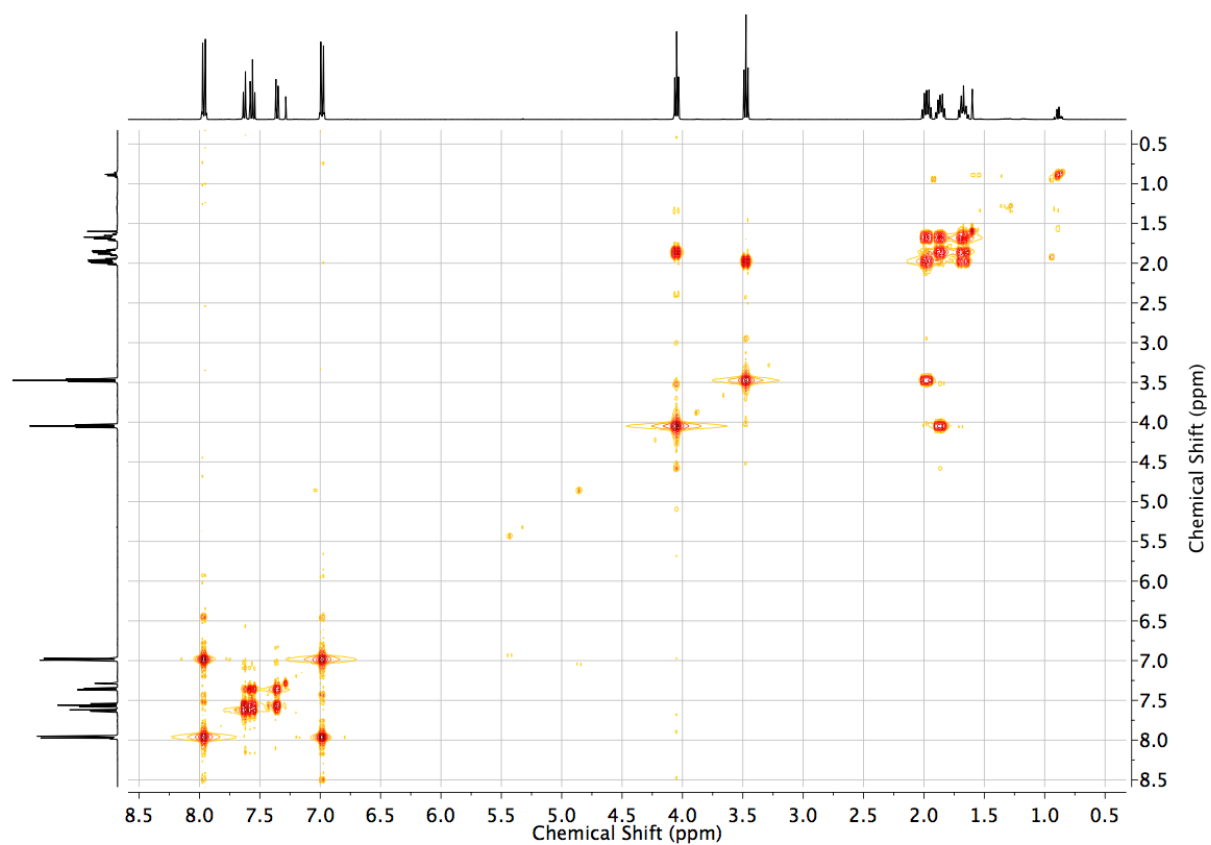


Figure S18 COSY NMR (CDCl₃) of S5.

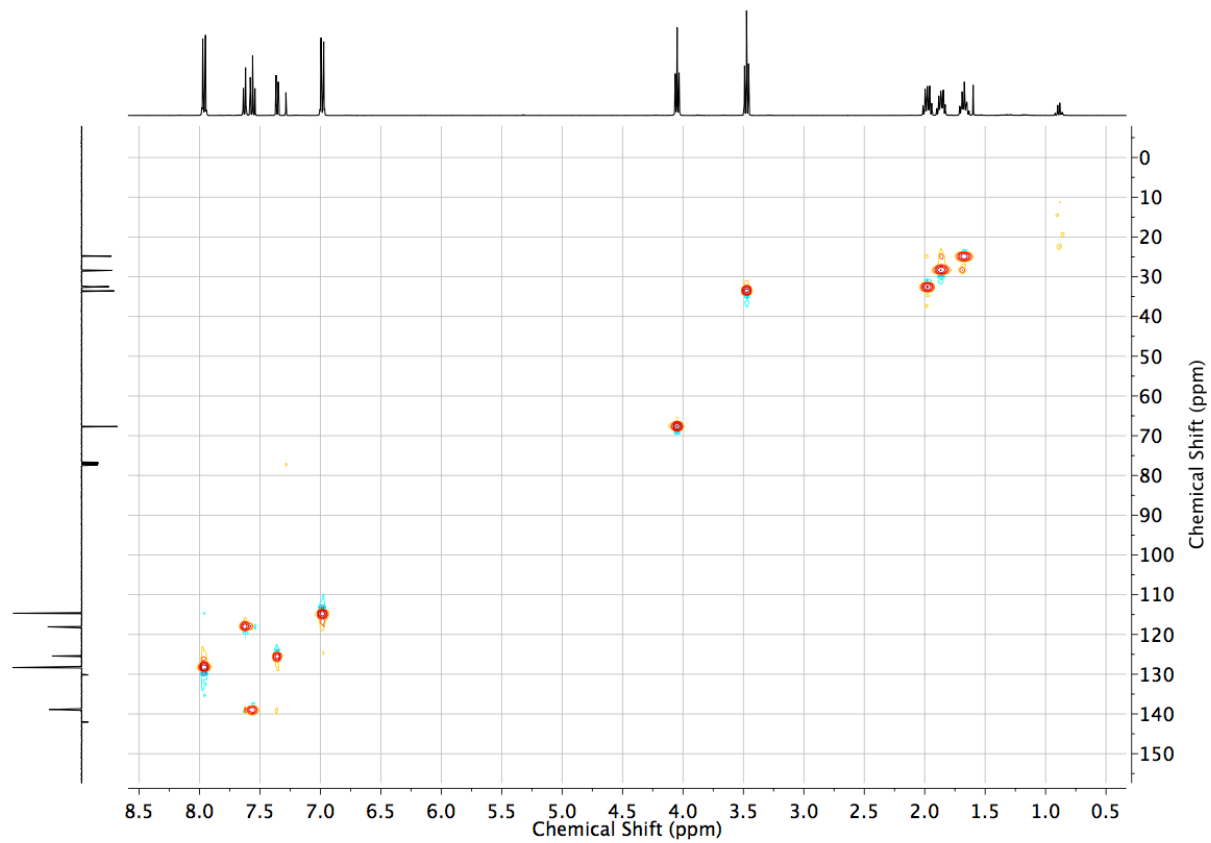


Figure S19 HSQC NMR (CDCl₃) of S5.

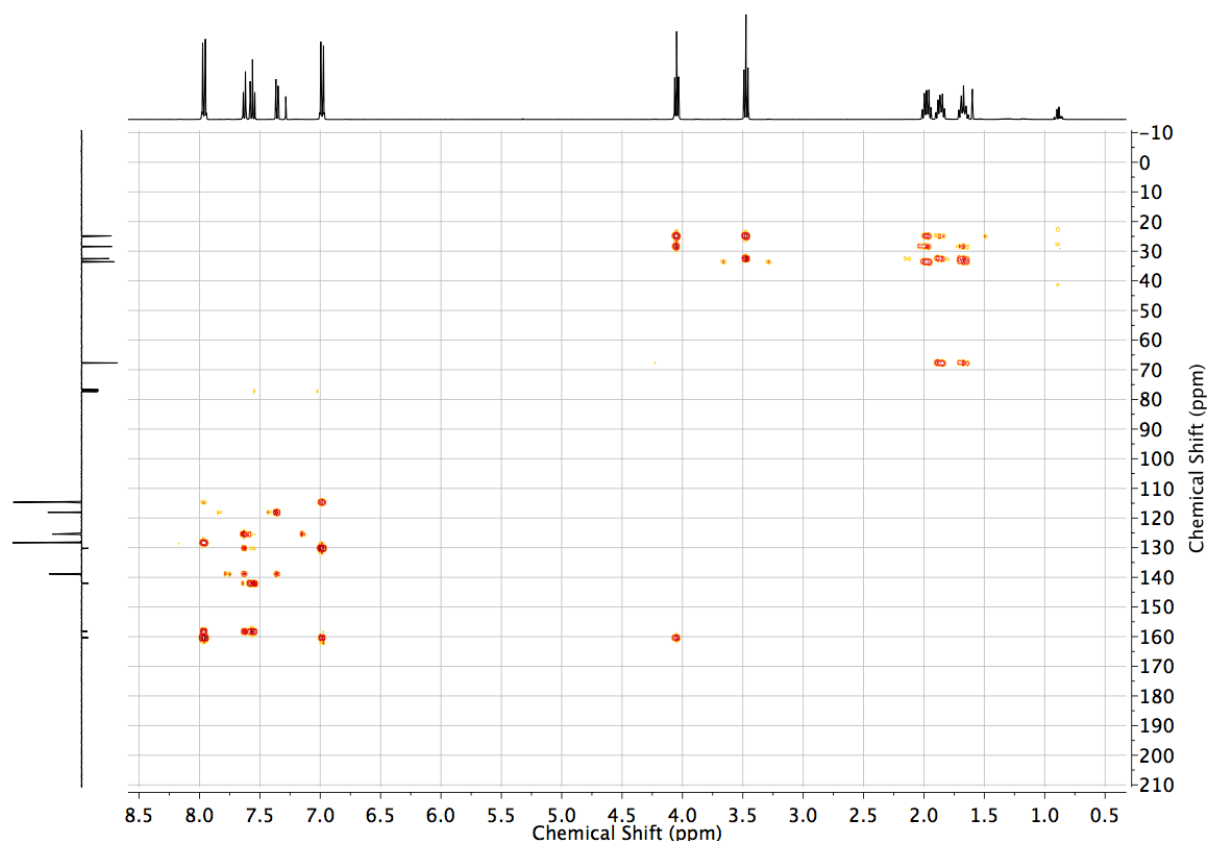
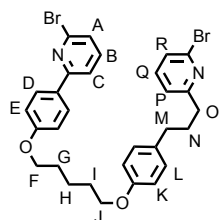


Figure S20 HMBC NMR (CDCl₃) of **S5**.



S6

To a solution of **S3** (0.88 g, 3 mmol, 1.2 eq.) in MeCN (10 mL) was added K₂CO₃ (1.38 g, 10 mmol, 4 eq.) as a solid. After stirring for 30 minutes, **S5** (1.0 g, 2.5 mmol, 1.0 eq.) was added as a solid and the reaction stirred at reflux for 18 h. The solvent was removed *in vacuo* and the resultant solid dissolved in CH₂Cl₂ (75 mL), washed with H₂O (20 mL) and brine (20 mL), dried (MgSO₄), filtered and the solvent removed *in vacuo*. After purification by column chromatography (Petrol/CH₂Cl₂ 1/1 with a gradient to 80% CH₂Cl₂), **S6** (1.4 g, 90%) was obtained as a white solid. m.p. 82-84 °C. ¹H NMR (400 MHz, CDCl₃) **S6**: 7.93 (d, *J* = 8.8, 2H, H_D), 7.60 (dd, *J* = 7.8, 0.9, 1H, H_C), 7.54 (t, *J* = 7.7, 1H, H_B), 7.43 (t, *J* = 7.7, 1H, H_D), 7.33 (dd, *J* = 7.7, 0.9, 1H, H_A), 7.29 (dd, *J* = 7.7, 0.9, 1H, H_R), 7.12-7.03 (m, 4H, H_L, H_P), 6.96 (d, *J* = 8.9, 2H, H_E), 6.82 (d, *J* = 8.6, 2H, H_K), 4.02 (t, *J* = 6.4, 2H, H_F), 3.95 (t, *J* = 6.4, 2H, H_J), 2.78 (t app, *J* = 7.8, 2H, H_O), 2.61 (t app, *J* = 7.6, 2H, H_M), 2.07-1.95 (m, 2H, H_N), 1.93-1.81 (m, 4H, H_G, H_I), 1.73-1.62 (m, 2H, H_H). ¹³C NMR (101 MHz, CDCl₃) **S6**: 163.9, 160.6, 158.5, 157.4, 142.2, 141.7, 139.0, 138.7, 134.0, 130.2, 129.5, 128.5, 125.5, 125.4, 121.6, 118.2, 114.8, 114.6, 68.0, 67.9, 37.6, 34.7, 31.7, 29.2, 29.1, 22.9. HR-ESI-MS *m/z* = 609.0736 [M+H]⁺ (calc. for C₃₀H₃₁Br₂N₂O₂ 609.0747).

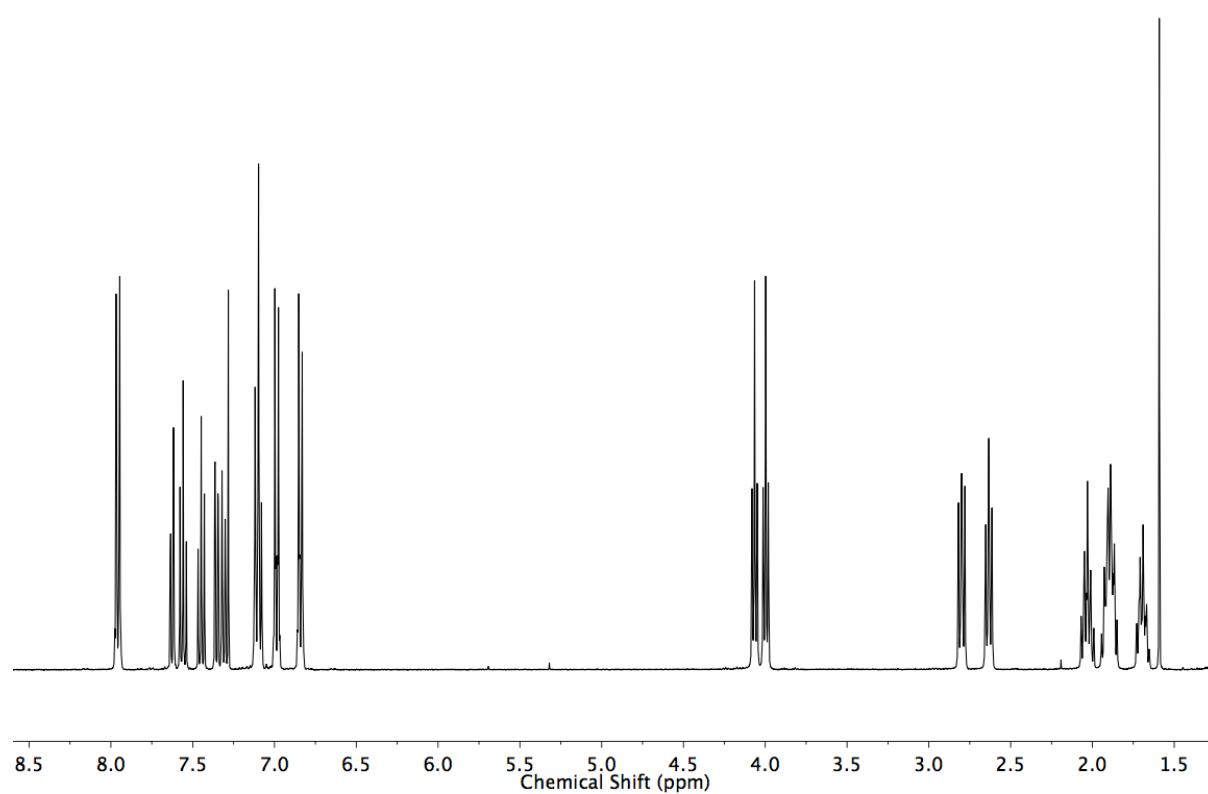


Figure S21 ^1H NMR (400 MHz, CDCl_3) of **S6**.

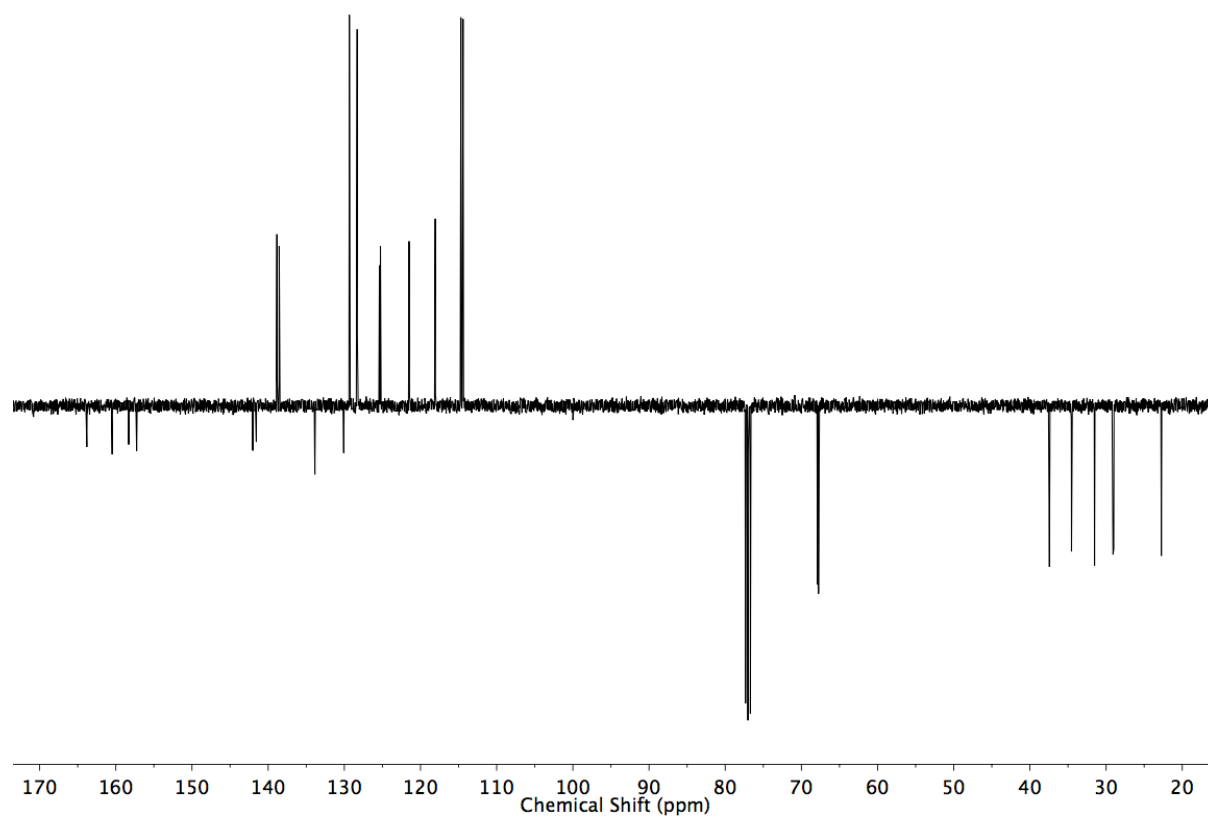


Figure S22 JMOD NMR (101 MHz, CDCl_3) of **S6**.

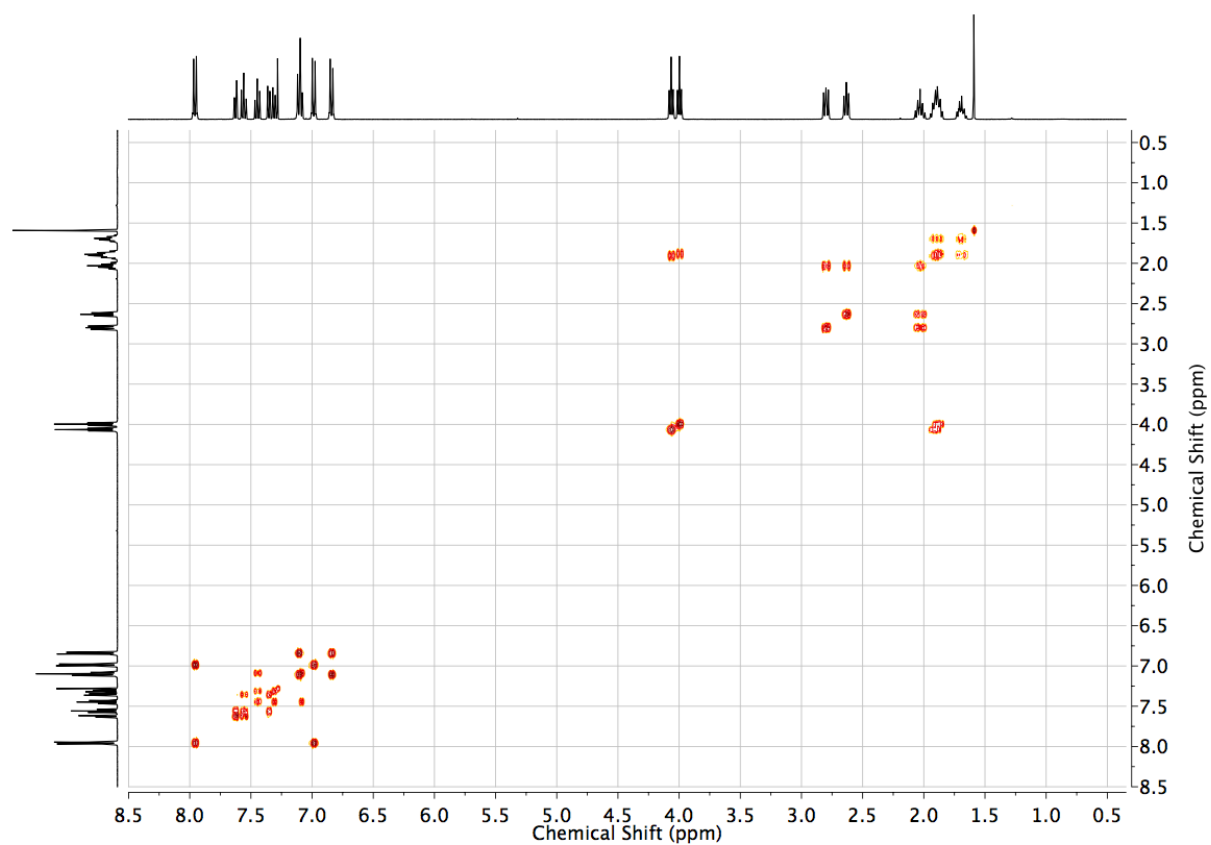


Figure S23 COSY NMR (CDCl_3) of **S6**.

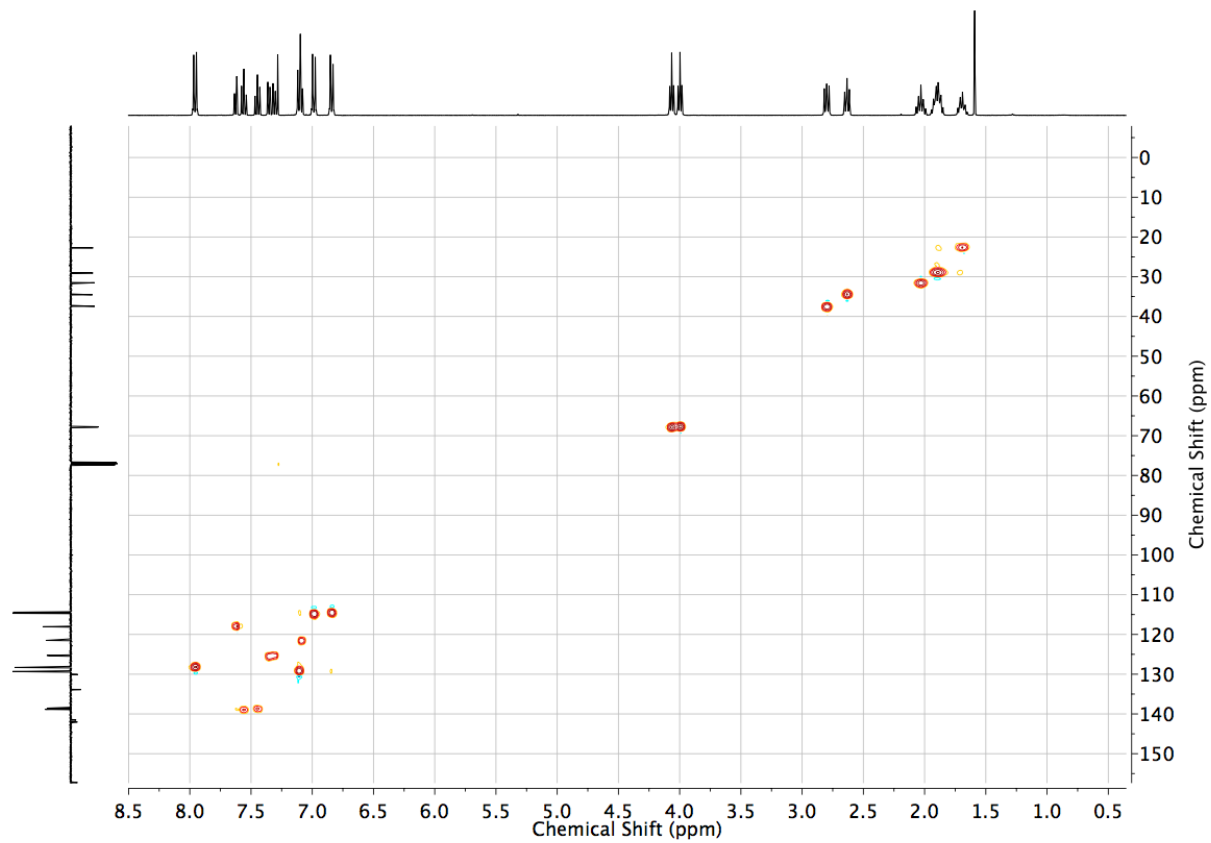


Figure S24 HSQC NMR (CDCl_3) of **S6**.

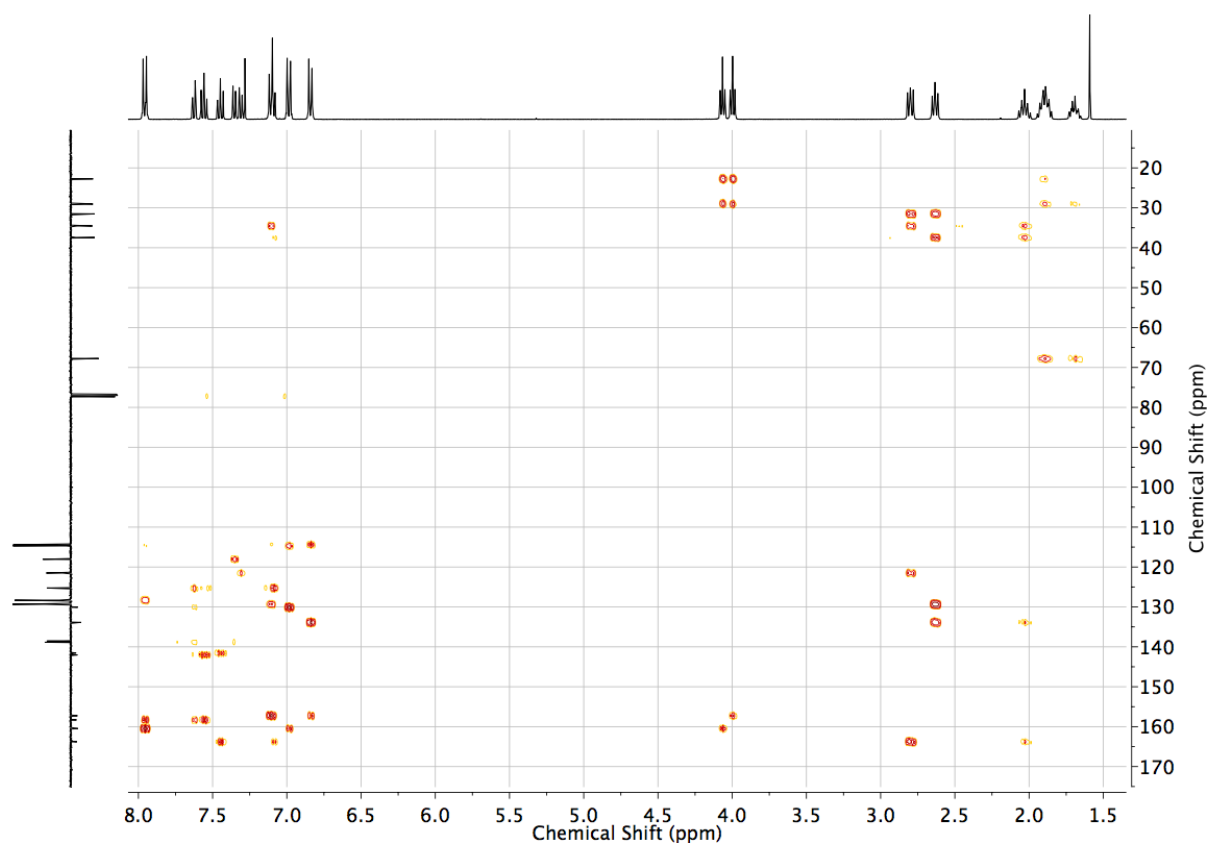
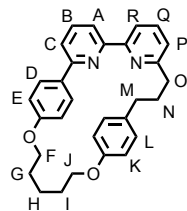


Figure S25 HMBC NMR (CDCl_3) of **S6**.



2c

[Ni(PPh_3) $_2\text{Br}_2$] (1.49 g, 2.00 mmol, 1 eq.), PPh_3 (1.05 g, 4.00 mmol, 2 eq.), Mn (1.10 g, 20.0 mmol, 10 eq.) and NEt_4I (0.514 g, 2.00 mmol, 1 eq.) in DMF (20 mL) were sonicated for 10 min, followed by stirring at 50 °C for 1 h. To this catalyst mixture was added **S6** (1.22 g, 2.00 mmol, 1 eq.) in DMF (20 mL) via syringe over 4 h, followed by additional stirring of the reaction for 1 h. To the cooled reaction was added CH_2Cl_2 (100 mL) and EDTA- NH_3 solution (100 mL). After filtering through a pad of Celite the organic phase was washed with water (2 \times 100 mL) and brine (100 mL), and the combined aqueous phases extracted with CH_2Cl_2 (50 mL). The combined organic phases were dried (MgSO_4), filtered and the solvent removed *in vacuo*. The crude product was purified by column chromatography (CH_2Cl_2 with 1% acetone) yielded **2c** as white solid (0.340 g, 38%). m.p. 138-140 °C. ^1H NMR (400 MHz, CDCl_3) δ : 8.04 (d, J = 8.8, 2H, H_D), 7.79 (t, J = 7.8, 1H, H_B), 7.75-7.67 (m, 2H, H_C , H_O), 7.70 (dd, J = 7.7, 0.9, 1H, H_S), 7.66 (dd, J = 7.7, 0.9, 1H, H_A), 7.63 (dd, J = 7.8, 1.0, 1H, H_R), 7.30 (d, J = 8.7, 2H, H_I), 7.22 (dd, J = 7.6, 1.0, 1H, H_P), 6.93-6.70 (m, 4H, H_E , H_K), 4.12 (t, J = 7.3, 2H, H_F), 4.03 (t, J = 6.1, 2H, H_J), 3.01 (t, J = 7.3, 2H, H_O), 2.70 (dd, J = 8.8, 6.6, 2H, H_M), 2.39-2.27 (m, 2H, H_N), 1.91-1.78 (m, 4H, H_G , H_I), 1.72-1.62 (m, 2H, H_H). ^{13}C NMR (126 MHz, CDCl_3) δ : 162.3, 159.5, 157.3, 156.9, 156.3, 156.0, 137.3, 136.7, 135.3, 132.0, 129.9, 128.6, 122.6, 119.2, 119.1, 118.5, 115.3, 114.9, 68.4, 67.3, 36.8, 34.2, 31.2, 27.9, 27.2, 21.3. HR-ESI-MS m/z = 451.2386 [$\text{M}+\text{H}$] $^+$ (calc. for $\text{C}_{30}\text{H}_{31}\text{N}_2\text{O}_2$ 451.2380).

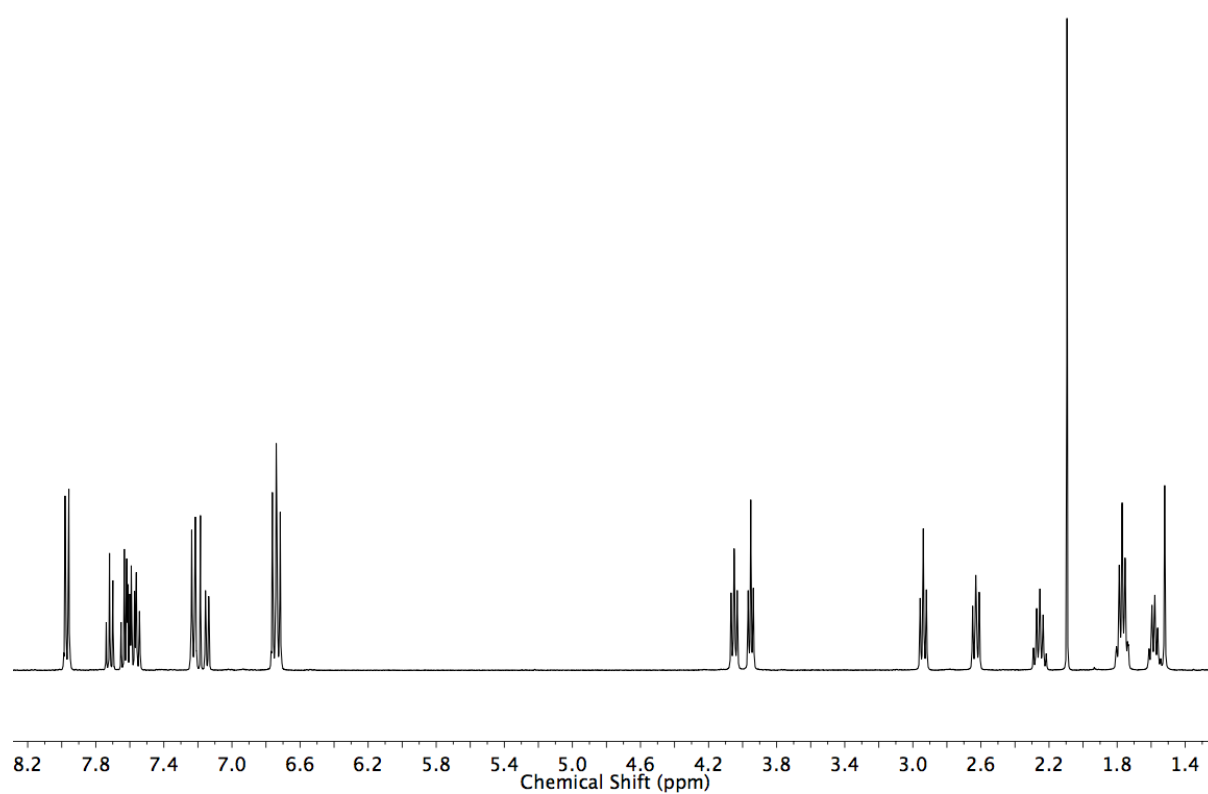


Figure S26 ^1H NMR (400 MHz, CDCl_3) of **2c**.

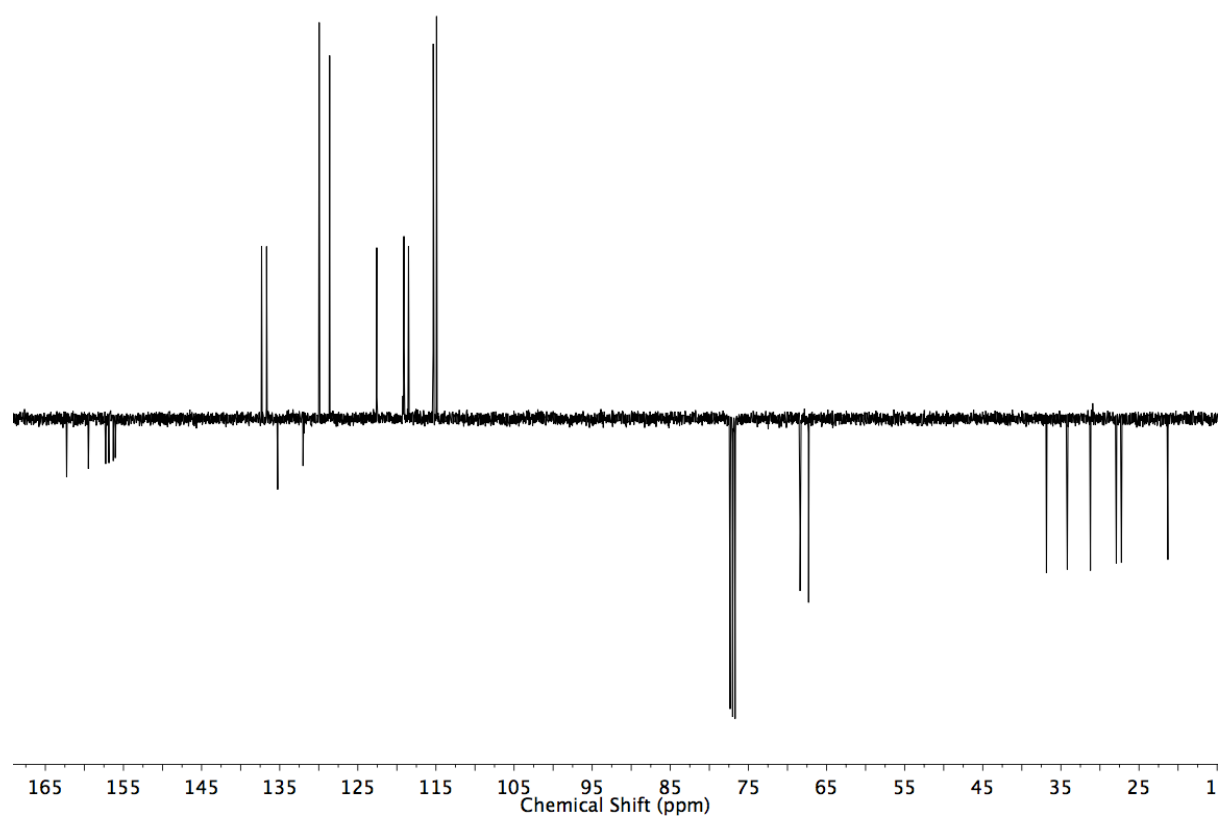


Figure S27 JMOD NMR (101 MHz, CDCl_3) of **2c**.

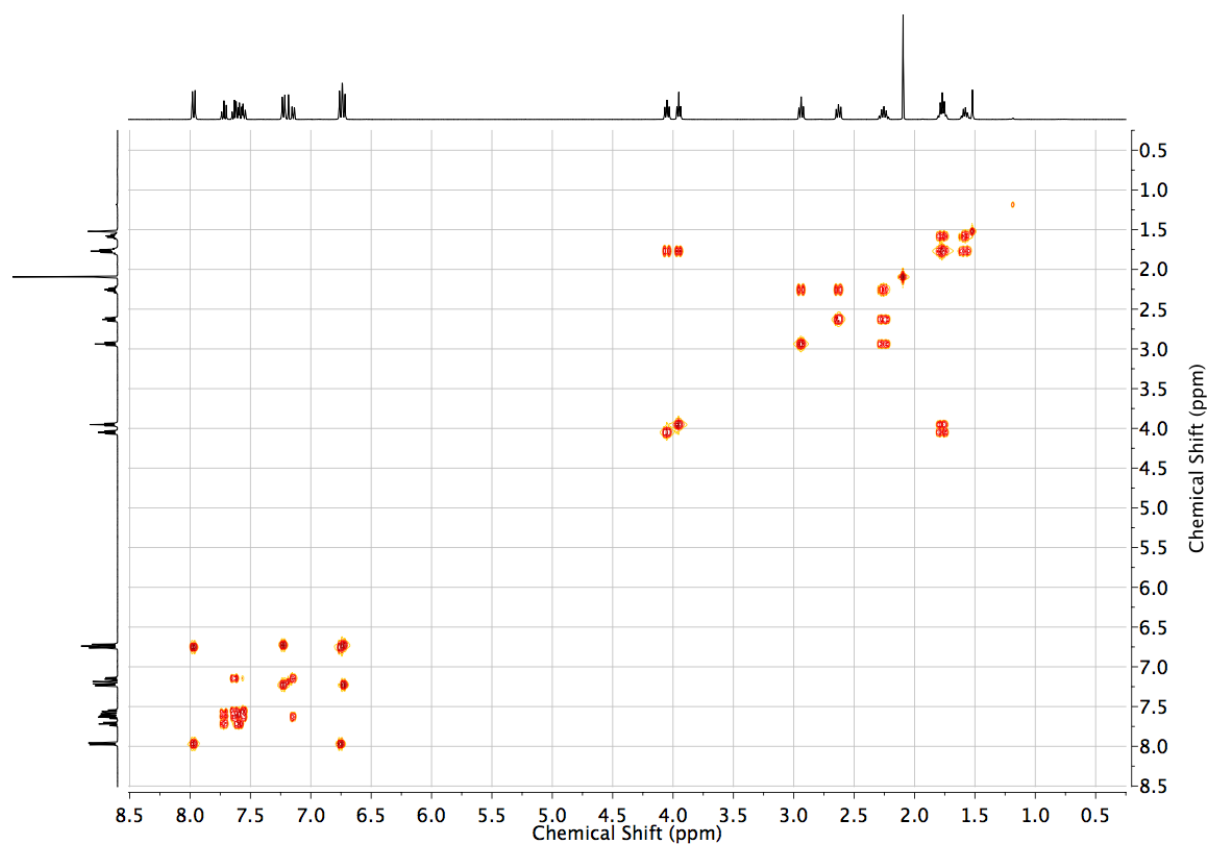


Figure S28 COSY NMR (CDCl₃) of 2c.

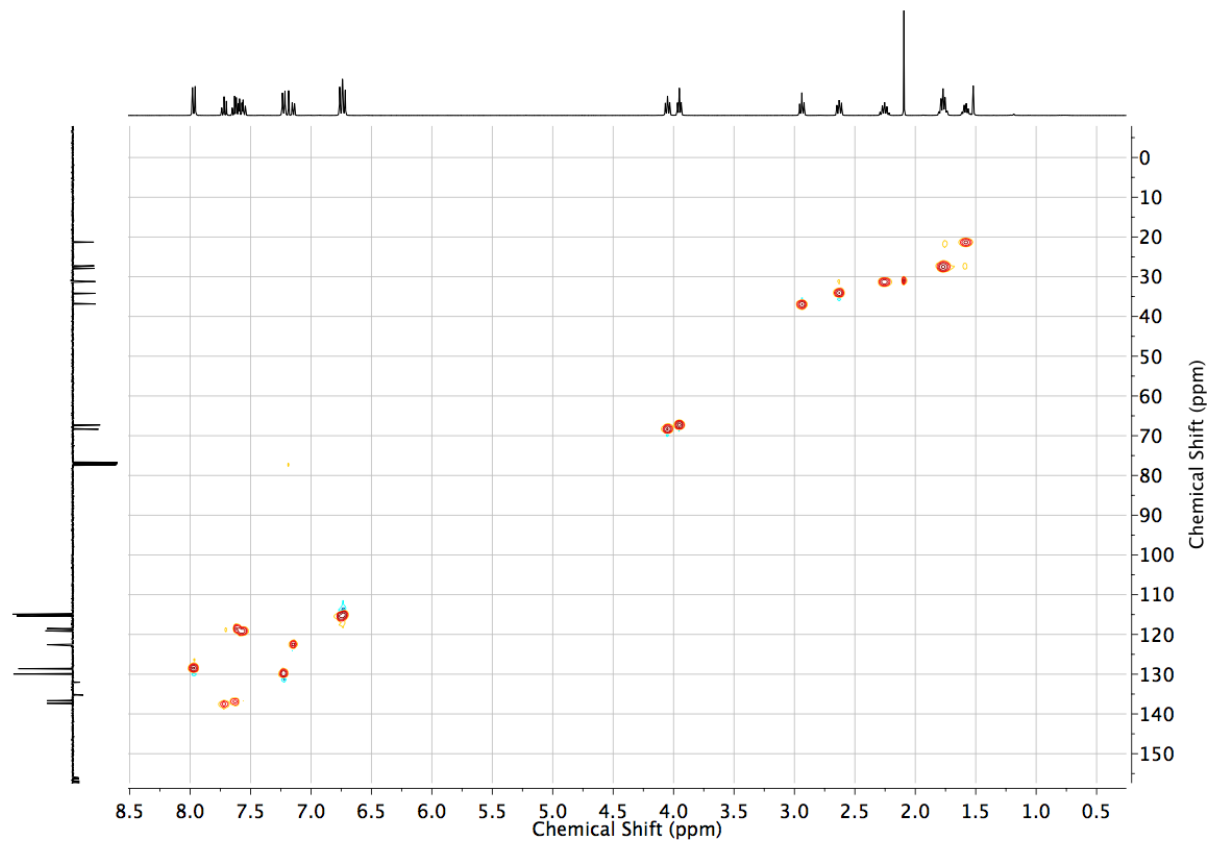


Figure S29 HSQC NMR (CDCl₃) of 2c.

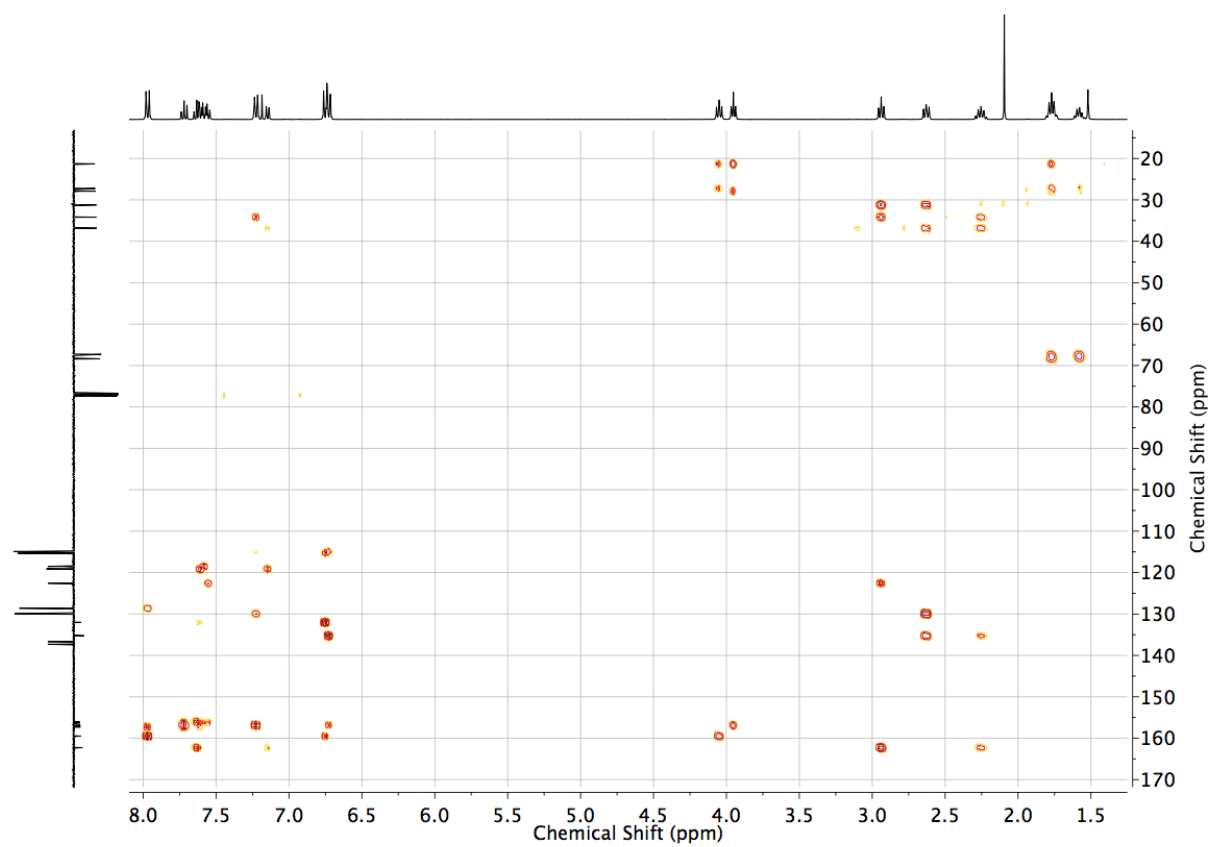
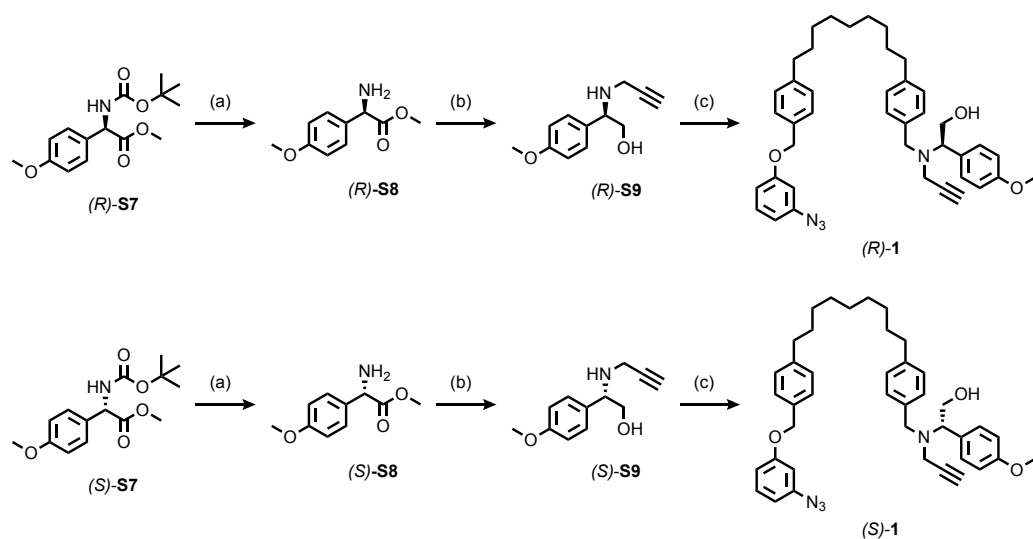
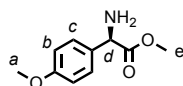


Figure S30 HMBC NMR (CDCl₃) of 2c.

3. Syntheses of U-shapes 1 and S11.



Scheme S3 Syntheses of U-shapes (*R*)-1 and (*S*)-1. Conditions: (a) HCl, dioxane, r.t., 16 h, 26% (*R*) and 60% (*S*) after recrystallisation; (b) LiAlH₄, THF, 0 °C to r.t., 2 h, then propargylbromide, K₂CO₃, MeCN, r.t., 16 h, 43% (*R*) and 40% (*S*) over two steps; (c) **S11**, K₂CO₃, MeCN, reflux, 20 h, 99% (*R*) and 90% (*S*).



(*R*)-S8

Boc-protected amine (*R*)-S7 (31.9 g, 108 mmol, 1 eq.) was stirred in 4N HCl in dioxane (162 mL, 648 mmol, 6 eq) for 16 h. Et₂O (160 mL) was added and the precipitate was recovered *via* vacuum filtration, washed with more Et₂O and dried in a desiccator. The ammonium salt (22.8 g, 98.4 mmol) was recrystallized from a refluxing solution of EtOAc/MeOH, affording 6.5 g (26%) of salt with an ee > 99%. The latter was treated with saturated NaHCO₃ (50 mL) and the aqueous layer was extracted with CH₂Cl₂ (2 × 50 mL). The combined organics were dried (MgSO₄), filtered and the solvent evaporated *in vacuo* to give amine (*R*)-S8 as a colourless oil (5.37 g, 98%). ¹H NMR (400 MHz, CDCl₃) **δ**: 7.29 (d, *J* = 8.8, 2H, H_c), 6.88 (d, *J* = 8.8, 2H, H_b), 4.58 (s, 1H, H_d), 3.80 (s, 3H, H_a), 3.70 (s, 3H, H_e), 1.88 (br s, 2H, -NH-). ¹³C NMR (101 MHz, CDCl₃) **δ**: 174.8, 159.5, 132.5, 128.1, 114.3, 58.2, 55.4, 52.5. HPLC: Whelk-O 1 (hexane/*i*-PrOH, 90:10), flow rate 2.0 mL.min⁻¹, λ = 275 nm, t_{major} = 19.6, ee > 99%).

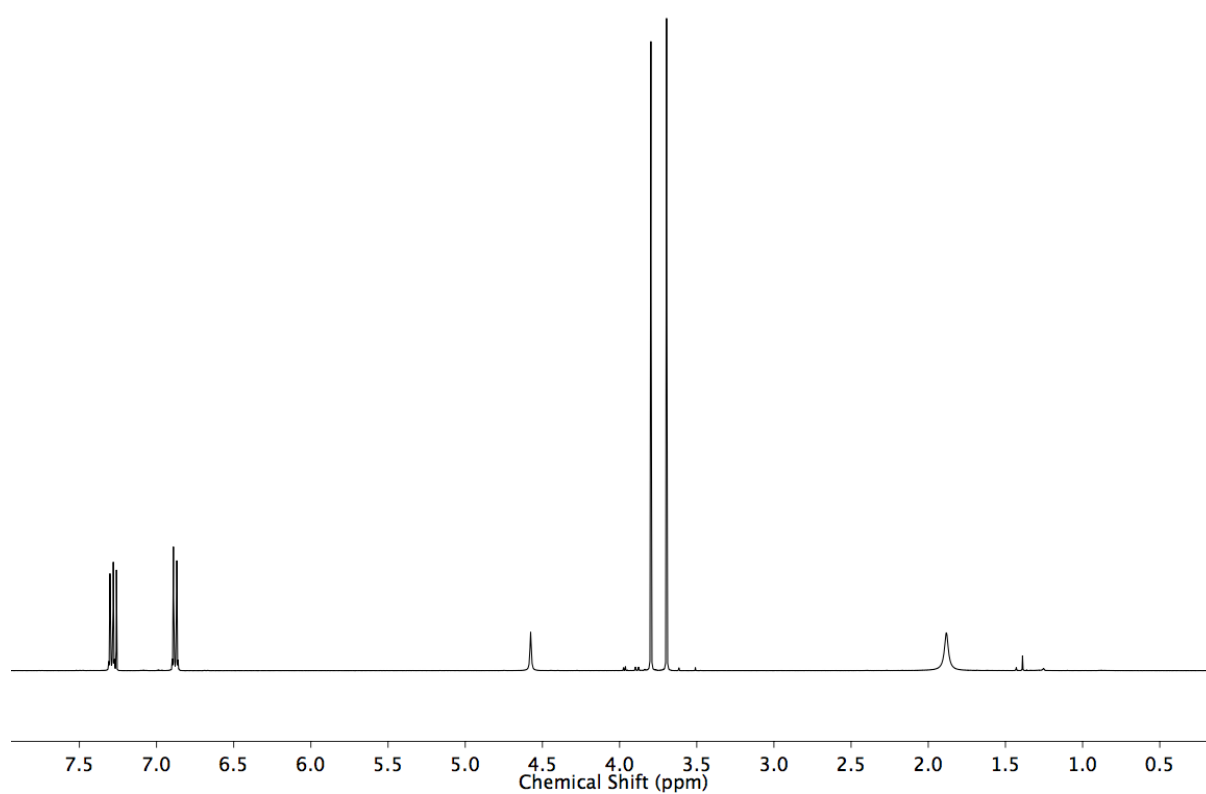


Figure S31 ^1H NMR (400 MHz, CDCl_3) of (*R*)-S8.

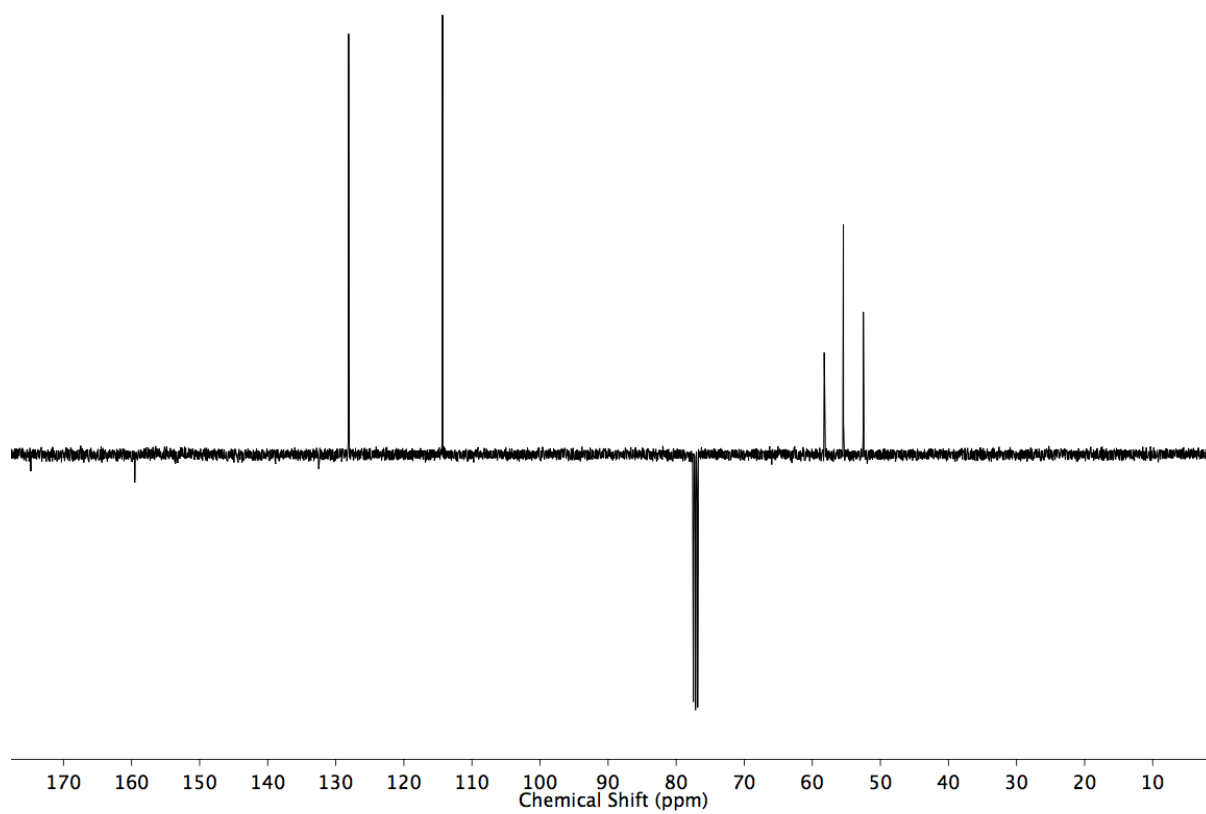


Figure S32 JMOD NMR (101 MHz, CDCl_3) of (*R*)-S8.

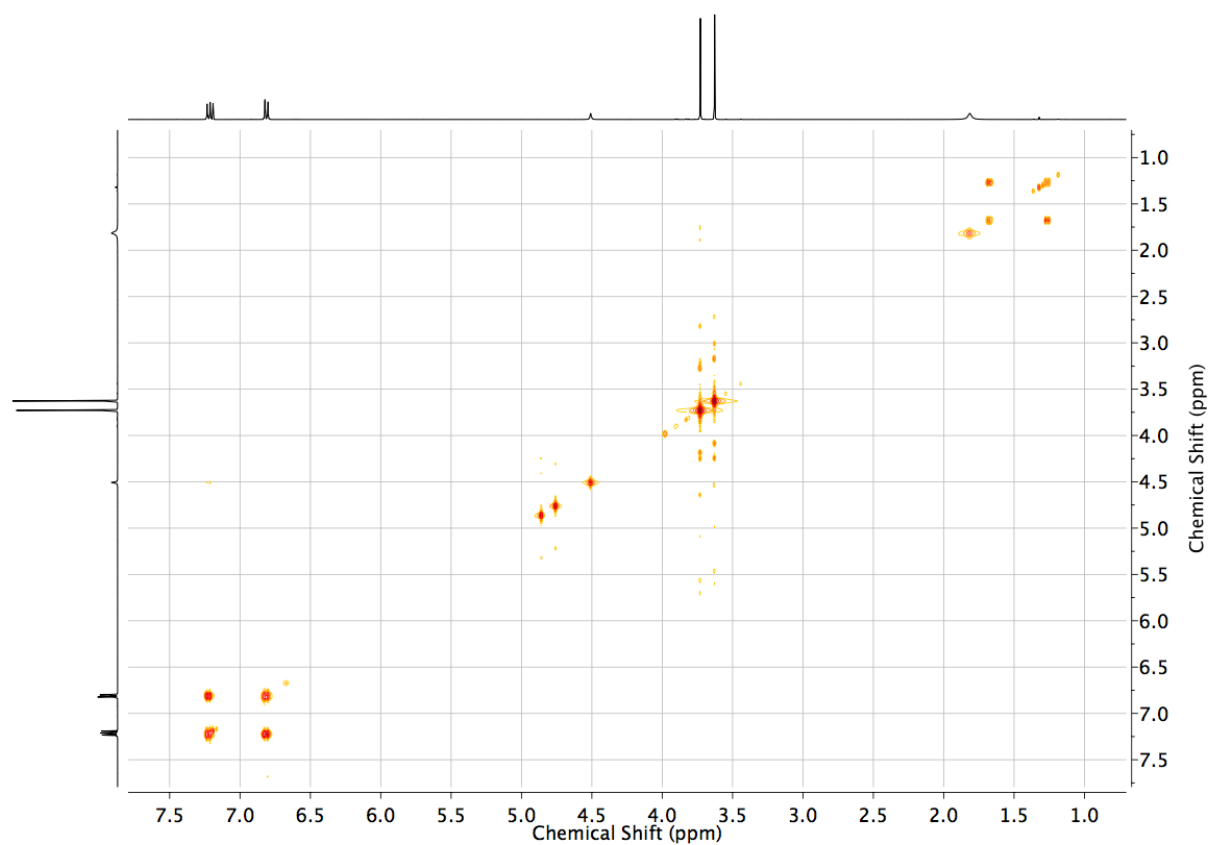


Figure S33 COSY NMR (CDCl_3) of (*R*)-S8.

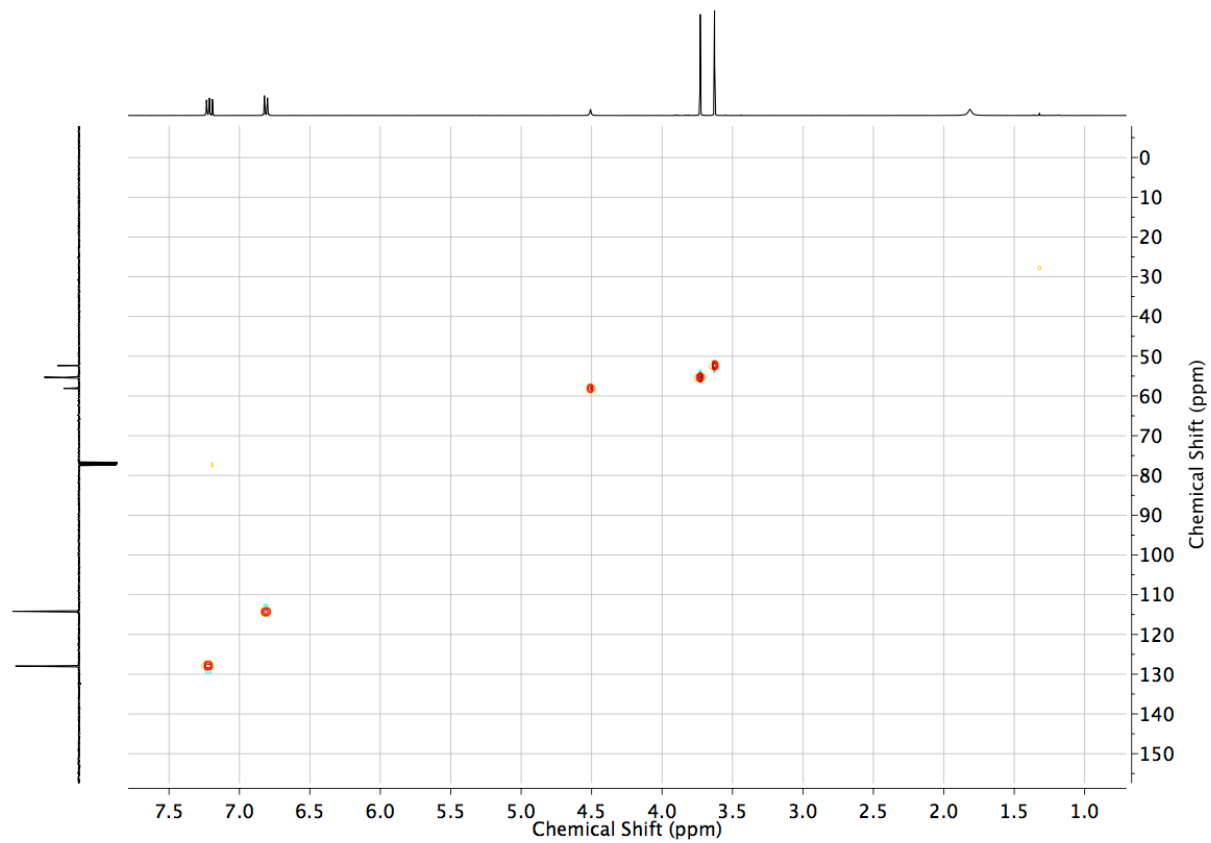


Figure S34 HSQC NMR (CDCl_3) of (*R*)-S8.

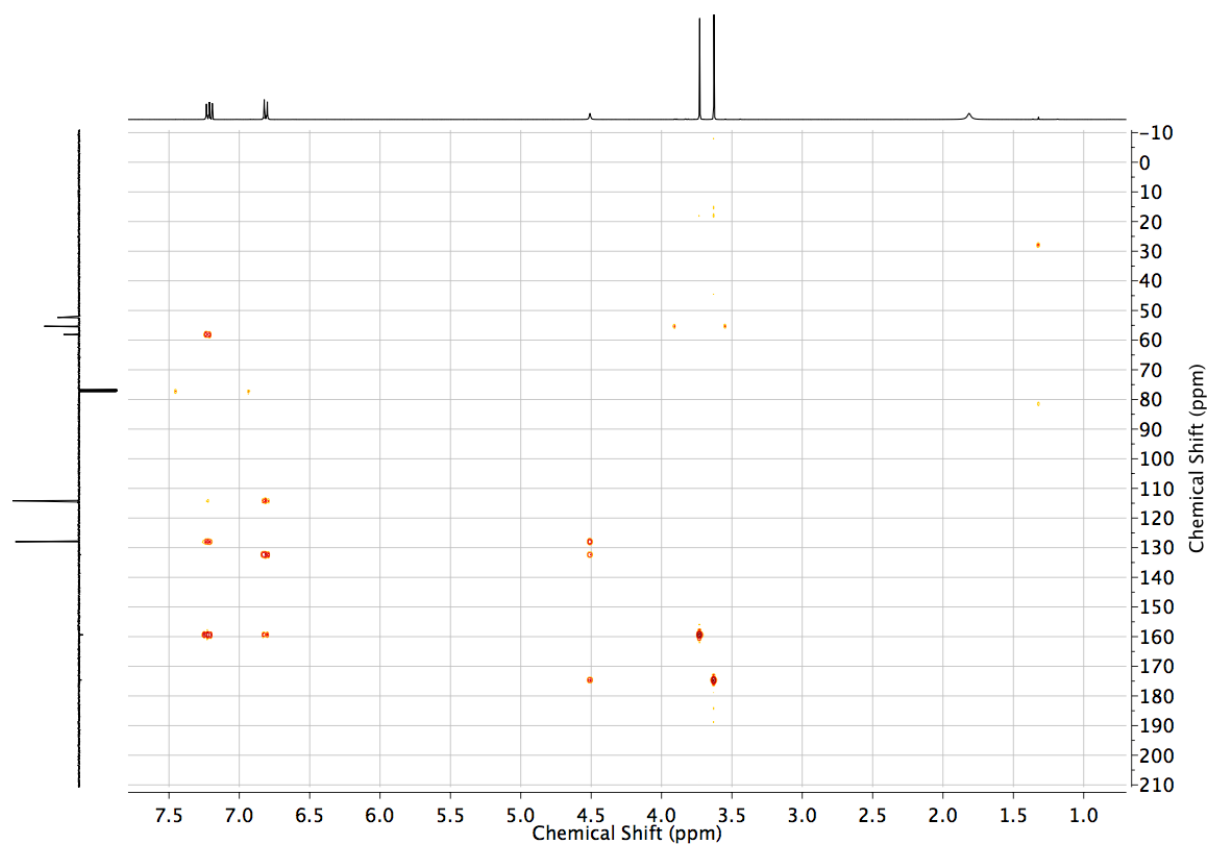


Figure S35 HMBC NMR (CDCl_3) of (*R*)-**S8**.

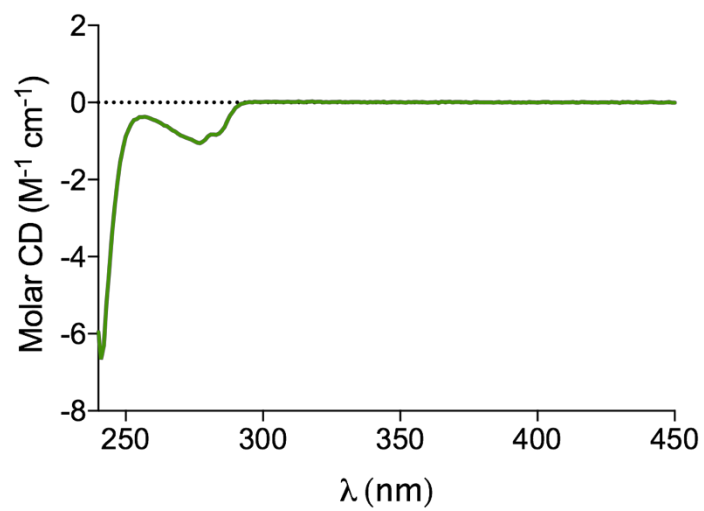
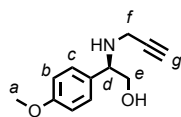


Figure S36 Circular dichroism spectrum of (*R*)-**S8** (200.0 μM in CHCl_3 , 293 K).



(R)-S9

To a suspension of LAH (0.751 g, 19.0 mmol, 1.5 eq.) in THF (100 mL) at 0 °C was added dropwise (*R*)-**S8** (2.470 g, 12.7 mmol, 1 eq.) as a solution in THF (10 mL) after which the reaction mixture was allowed to stir at r.t. for 2 h. Water (3 mL) was carefully added to the mixture at 0 °C followed by 10 M aq NaOH (2 mL) and the crude stirred for an additional 30 min. The suspension was then filtered through MgSO₄ with THF and the filtrate concentrated. The crude pale yellow solid (1.78 g, 10.7 mmol, 1 eq.) was dissolved in MeCN (50 mL) at r.t. and to this solution was added K₂CO₃ (2.222 g, 16.1 mmol, 1.5 eq.) followed after 15 min by propargyl bromide (80 wt. % in toluene, 1.19 mL, 10.7 mmol, 1 eq.). The resulting mixture was stirred for 16 h then filtered through celite and concentrated *in vacuo*. The crude residue was purified via flash column chromatography on silica gel with a step-wise gradient of EtOAc in petrol 0 - 15 - 40%, providing the pure product (*R*)-**S9** as pale yellow oil (1.120 g, 43% over 2 steps). ¹H NMR (400 MHz, CDCl₃) **δ**: 7.26 (d, *J* = 8.7, 2H, H_c), 6.89 (d, *J* = 8.7, 2H, H_b), 3.96 (dd, *J* = 8.3, 4.5, 1H, H_d), 3.80 (s, 3H, H_a), 3.73 (dd, *J* = 10.8, 4.5, 1H, H_e), 3.60 (dd, *J* = 10.7, 8.3, 1H, H_e), 3.42 (dd, *J* = 17.0, 2.4, 1H, one of H_f), 3.20 (dd, *J* = 17.0, 2.4, 1H, one of H_f), 2.21 (t, *J* = 2.4, 1H, H_g), 1.79 (s, 1H, -NH-). ¹³C NMR (400 MHz, CDCl₃) **δ**: 159.4, 131.6, 128.8, 114.2, 82.1, 71.6, 67.0, 62.4, 55.4, 35.8. HR-ESI-MS *m/z* = 206.1173 [M+H]⁺ (calc. for C₁₂H₁₆NO₂ 206.1173). HPLC: RegisPack (hexane/EtOH, 97:3), flow rate 1.5 mL.min⁻¹, λ = 275 nm, t_{major} = 15.3, ee > 99%).

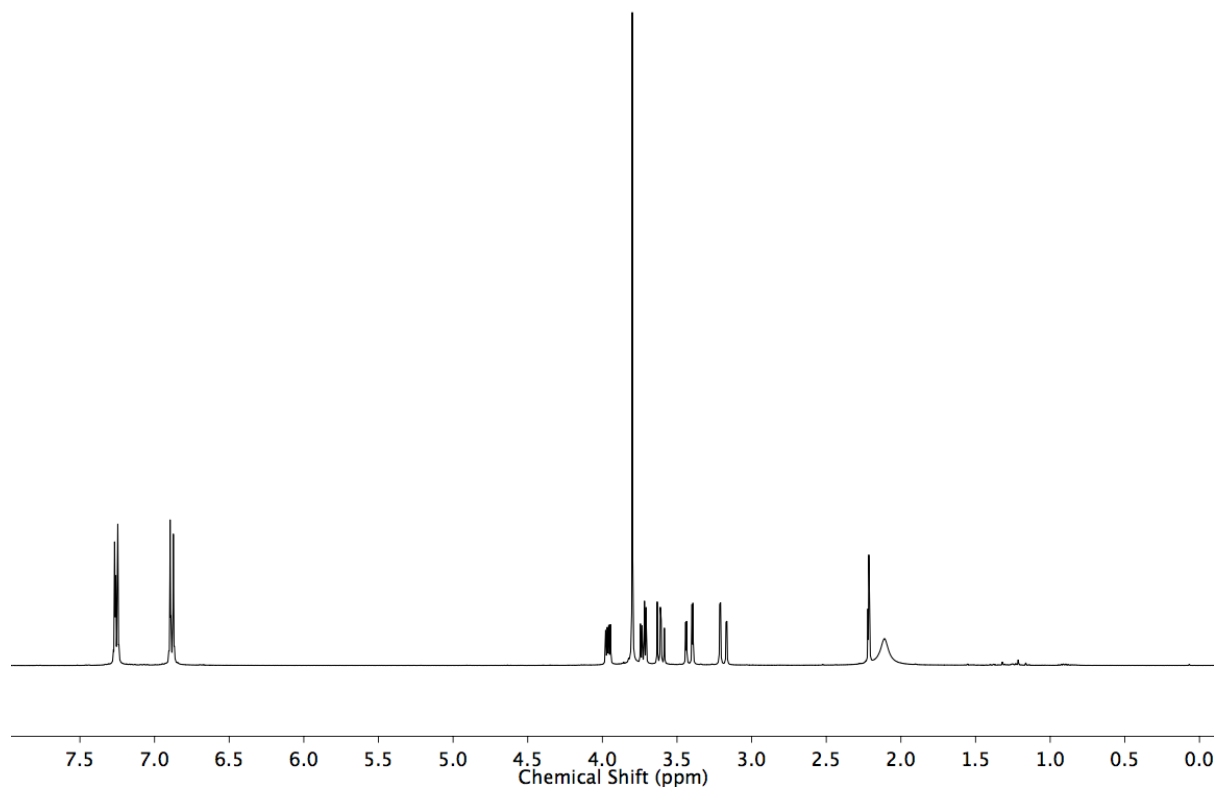


Figure S37 ¹H NMR (400 MHz, CDCl₃) of (*R*)-**S9**.

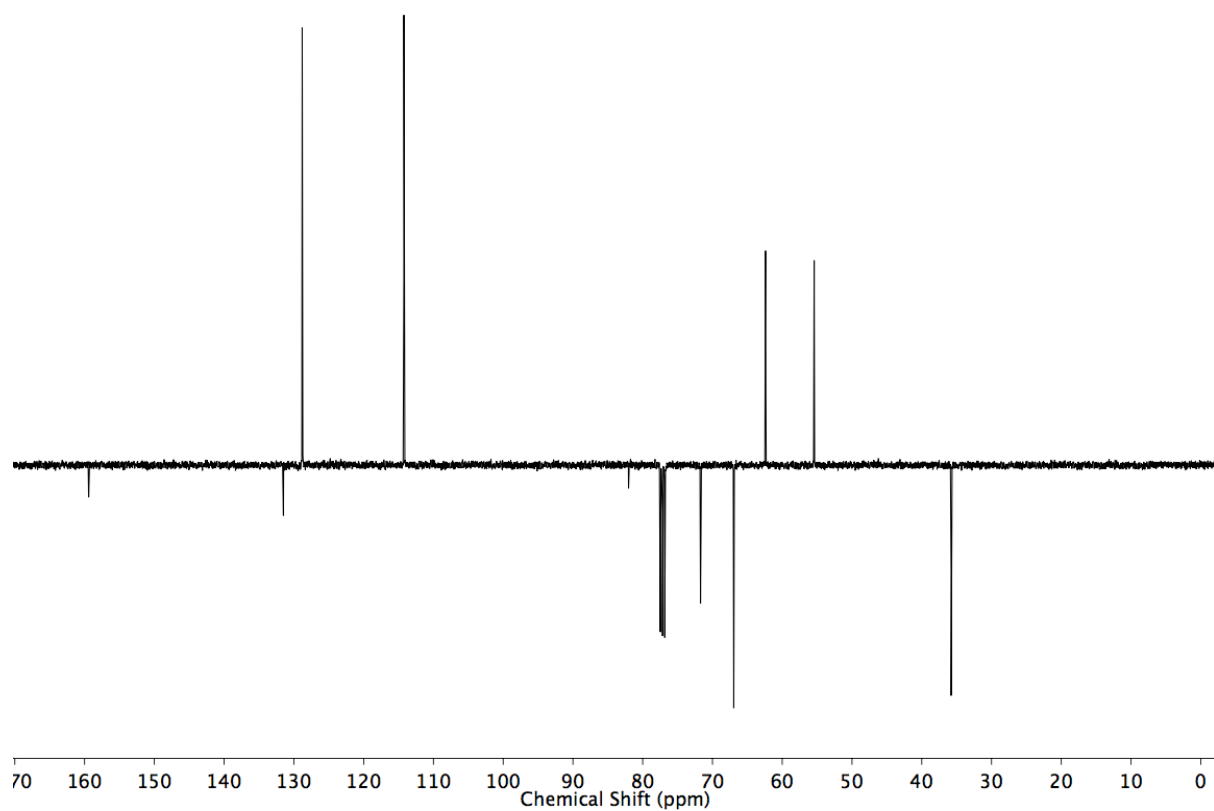


Figure S38 JMOD NMR (101 MHz, CDCl_3) of *(R)*-S9.

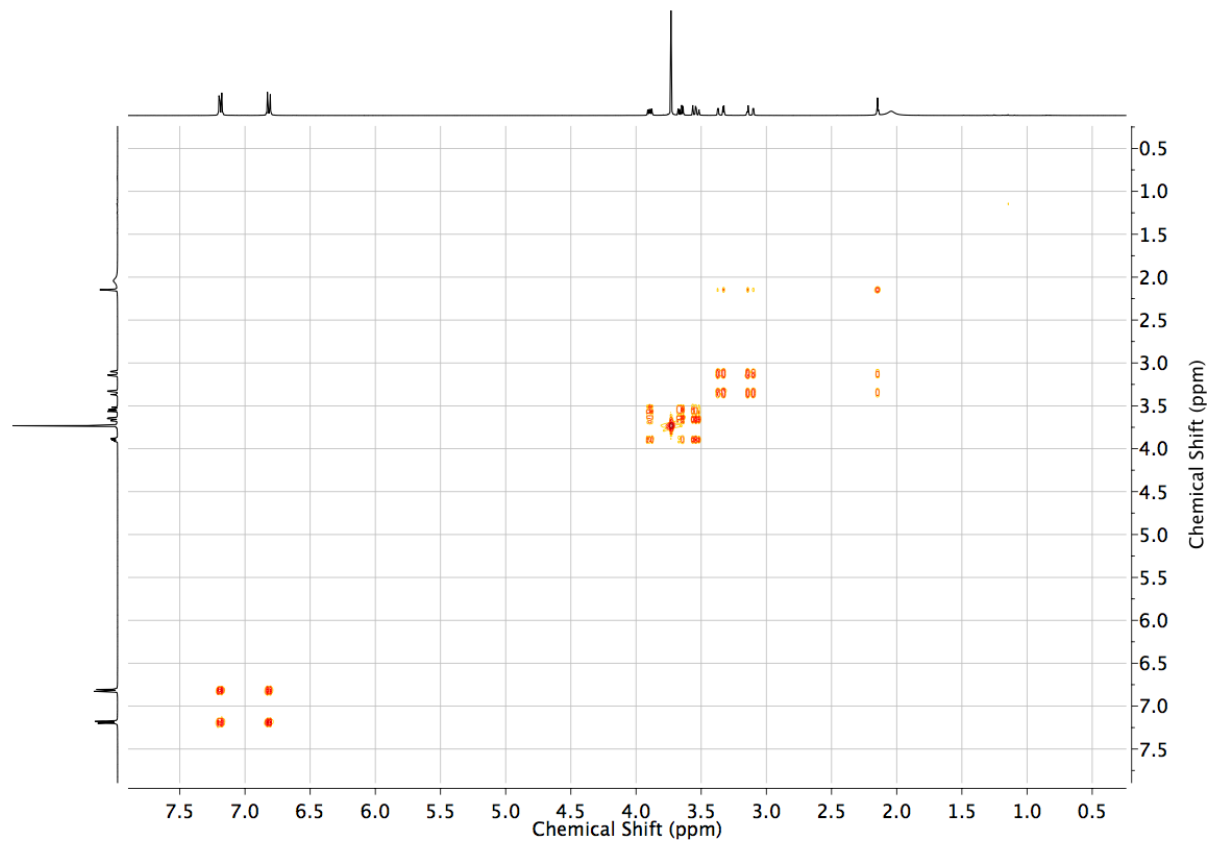


Figure S39 COSY NMR (CDCl_3) of *(R)*-S9.

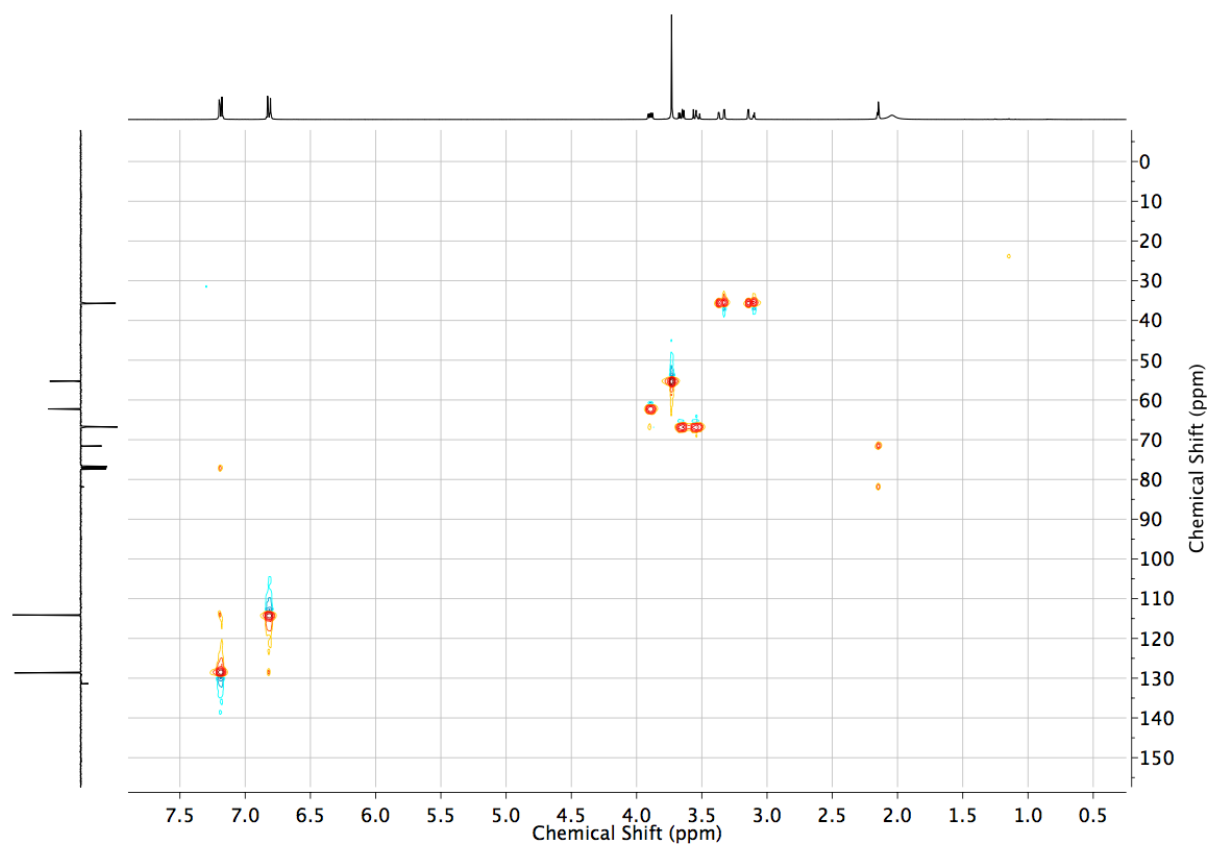


Figure S40 HSQC NMR (CDCl₃) of (R)-S9.

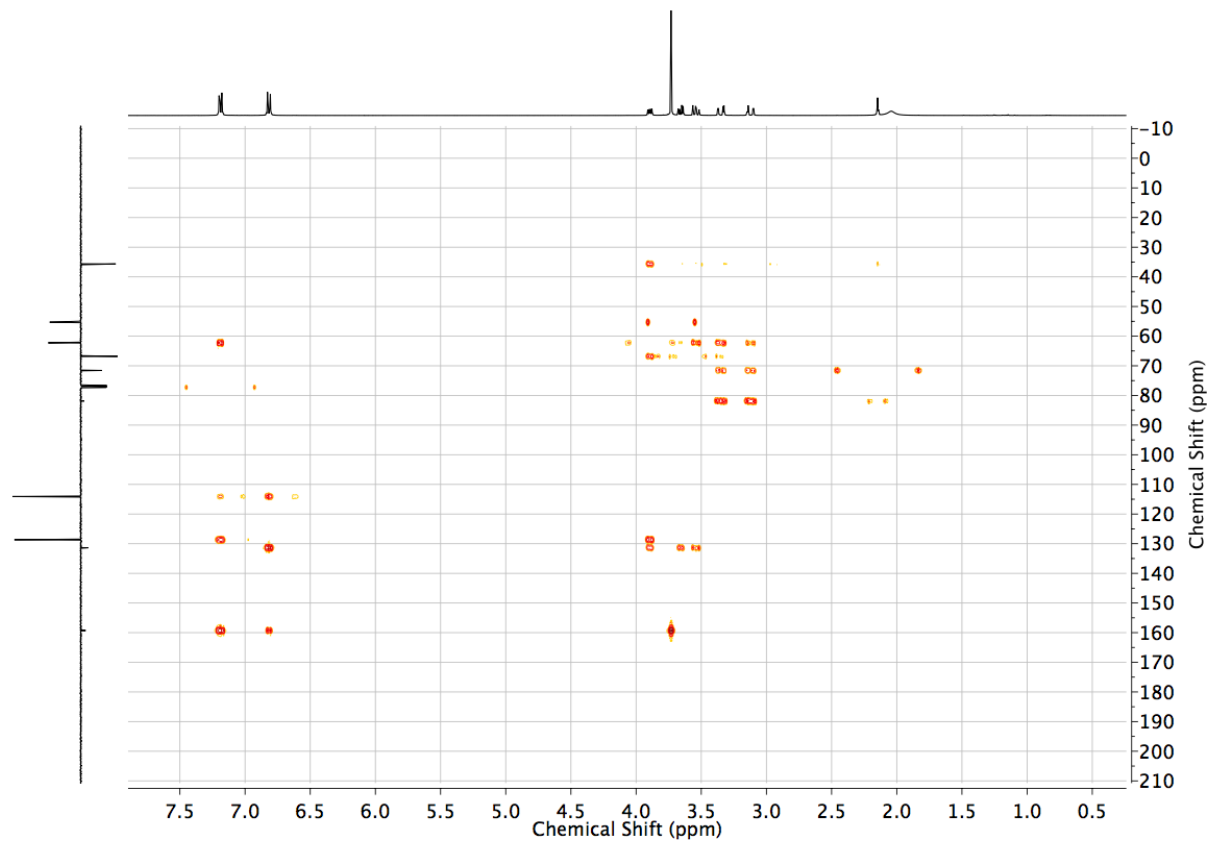


Figure S41 HMBC NMR (CDCl₃) of (R)-S9.

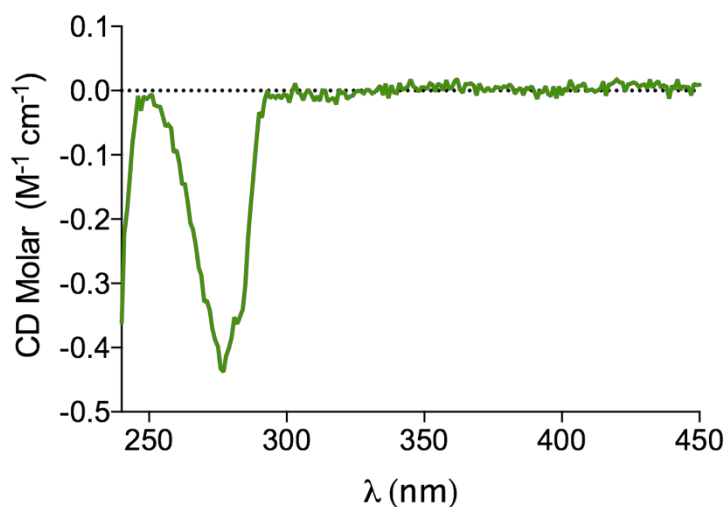
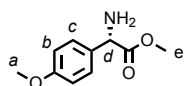


Figure S42 Circular dichroism spectrum of (*R*)-**S9** (200.0 μ M in CHCl_3 , 293 K).



(*S*)-S8

Boc-protected amine (*S*)-**S7** (30.1 g, 102 mmol, 1 eq.) was stirred in 4N HCl in dioxane (152 mL, 611 mmol, 6 eq) for 16 h. Et_2O (150 mL) was added and the precipitate was recovered via vacuum filtration, washed with more Et_2O and dried in a desiccator. The ammonium salt (22.8 g, 98.4 mmol) was recrystallized from a refluxing solution of EtOAc/MeOH . The process was repeated twice using the filtrate of the previous recrystallization, affording a combined mass of 14.9 g (60%) of salt with an ee > 99%. The latter was treated with saturated NaHCO_3 (150 mL) and the aqueous layer was extracted with CH_2Cl_2 (2×100 mL). The combined organics were dried (MgSO_4), filtered and the solvent evaporated *in vacuo* to give amine (*S*)-**S8** as a colourless oil (12.2 g, 98%). HPLC: Whelk-O 1 (hexane/*i*-PrOH, 90:10), flow rate 2.0 mL.min⁻¹, $\lambda = 275$ nm, $t_{\text{major}} = 15.5$, ee > 99%). Spectroscopic data were identical to those reported for (*R*)-**S8** with the exception of the circular dichroism spectra.

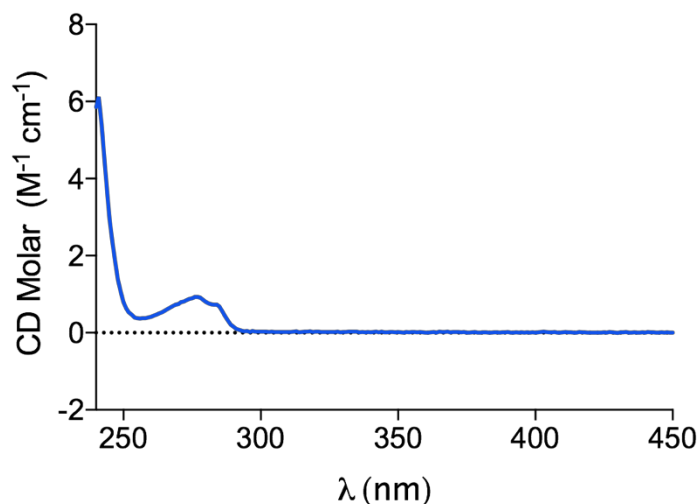
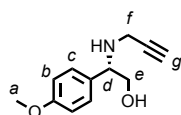


Figure S43 Circular dichroism spectrum of (*S*)-**S8** (200.0 μ M in CHCl_3 , 293 K).



(*S*)-**S9**

To a suspension of LAH (87 mg, 2.20 mmol, 1.5 eq.) in THF (11 mL) at 0 °C was added dropwise (*S*)-**S8** (285 mg, 1.46 mmol, 1 eq.) as a solution in THF (1 mL) after which the reaction mixture was allowed to stir at r.t. for 2 h. Water (0.5 mL) was carefully added to the mixture at 0 °C followed by 10 M aq NaOH (0.5 mL) and the crude stirred for an additional 30 min. The suspension was then filtered through MgSO_4 with THF and the filtrate concentrated. The crude pale yellow solid (230 mg, 1.40 mmol, 1 eq.) was dissolved in MeCN (5 mL) at r.t. and to this solution was added K_2CO_3 (291 mg, 2.10 mmol, 1.5 eq.) followed after 15 min by propargyl bromide (80 wt. % in toluene, 0.16 mL, 1.40 mmol, 1 eq.). The resulting mixture was stirred for 16 h then filtered through celite and concentrated *in vacuo*. The crude residue was purified via flash column chromatography on silica gel with a step-wise gradient of EtOAc in petrol 0 - 15 - 40%, providing the pure product (*S*)-**S9** as pale yellow oil (181 mg, 40% over 2 steps). HPLC: RegisPack (hexane/EtOH, 97:3), flow rate 1.5 mL.min⁻¹, λ = 275 nm, t_{major} = 13.3, ee > 99%. Spectroscopic data were identical to those reported for (*R*)-**S9** with the exception of the circular dichroism spectra.

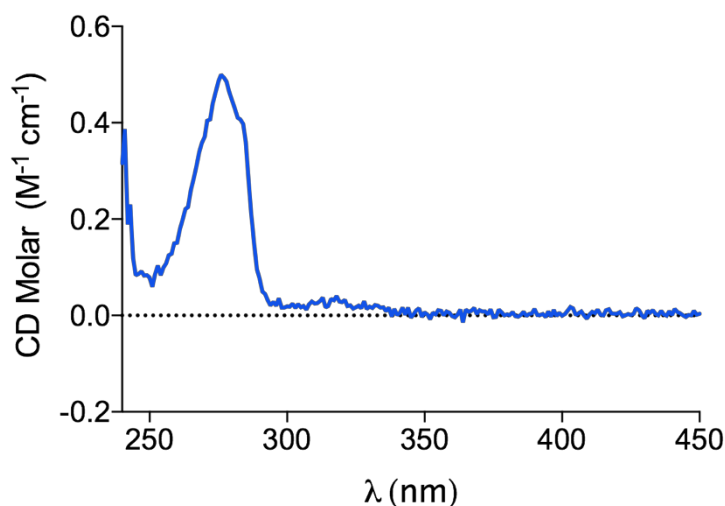
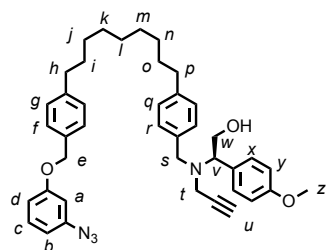


Figure S44 Circular dichroism spectrum of (*S*)-**S9** (200.0 μ M in CHCl_3 , 293 K).



(*R*)-**1**

S10 (0.296 g, 0.568 mmol, 1 eq.), (*R*)-**S9** (0.140 g, 0.682 mmol, 1.2 eq.) and K_2CO_3 (0.785 g, 5.68 mmol, 10 eq.) were stirred at 80 °C in MeCN (25 mL) under air in a sealed vial for 20 h. The cooled reaction mixture was filtered through celite and purified by column chromatography (Petrol/ CH_2Cl_2 1/1 with a gradient from 0 to 10% EtOAc) to give the product (*R*)-**1** as a colorless oil (0.362 g, 99%). ^1H NMR (500 MHz, CDCl_3) **1**: 7.33-7.30 (m, 4H, H_f , H_x), 7.26-7.19 (m, 5H, H_c , H_g , H_l), 7.12 (d, $J = 8.1$, 2H, H_q), 6.91 (d, $J = 8.8$, 2H, H_y), 6.76 (ddd, $J = 8.3$, 2.3, 0.9, 1H, H_b or H_d), 6.66-6.63 (m, 2H, H_a , H_b or H_d), 5.01 (s, 2H, H_e), 4.01-3.97 (m, H_v , H_w), 3.84-3.77 (m, 5H, H_s , H_w , H_z), 3.41-3.37 (m, 1H, H_t), 3.31 (d, $J = 13.3$, 1H, H_s), 3.13 (dd, $J = 17.2$, 2.4, 1H, H_t), 2.62-2.56 (m, 4H, H_h , H_i), 2.23 (app. t, $J = 2.4$, 1H, H_u), 1.63-1.55 (m, 4H, H_i , H_o), 1.30 (br. m, 10H, H_j , H_k , H_l , H_m , H_n). ^{13}C NMR (126 MHz, CDCl_3) **1**: 160.2, 159.5, 143.2, 142.1, 141.4, 135.8, 133.8, 130.6, 130.0, 129.8, 129.0, 128.8, 128.6, 127.8, 114.1, 111.6 ($\times 2$), 106.1, 79.6, 73.3, 70.3, 65.4, 62.8, 55.4, 53.9, 39.0, 35.9, 35.8, 31.7, 31.6, 29.6 ($\times 3$), 29.5, 29.4. HR-ESI-MS $m/z = 645.3799$ [$\text{M}+\text{H}$] $^+$ (calc. for $\text{C}_{41}\text{H}_{49}\text{N}_4\text{O}_3$ 645.3799).

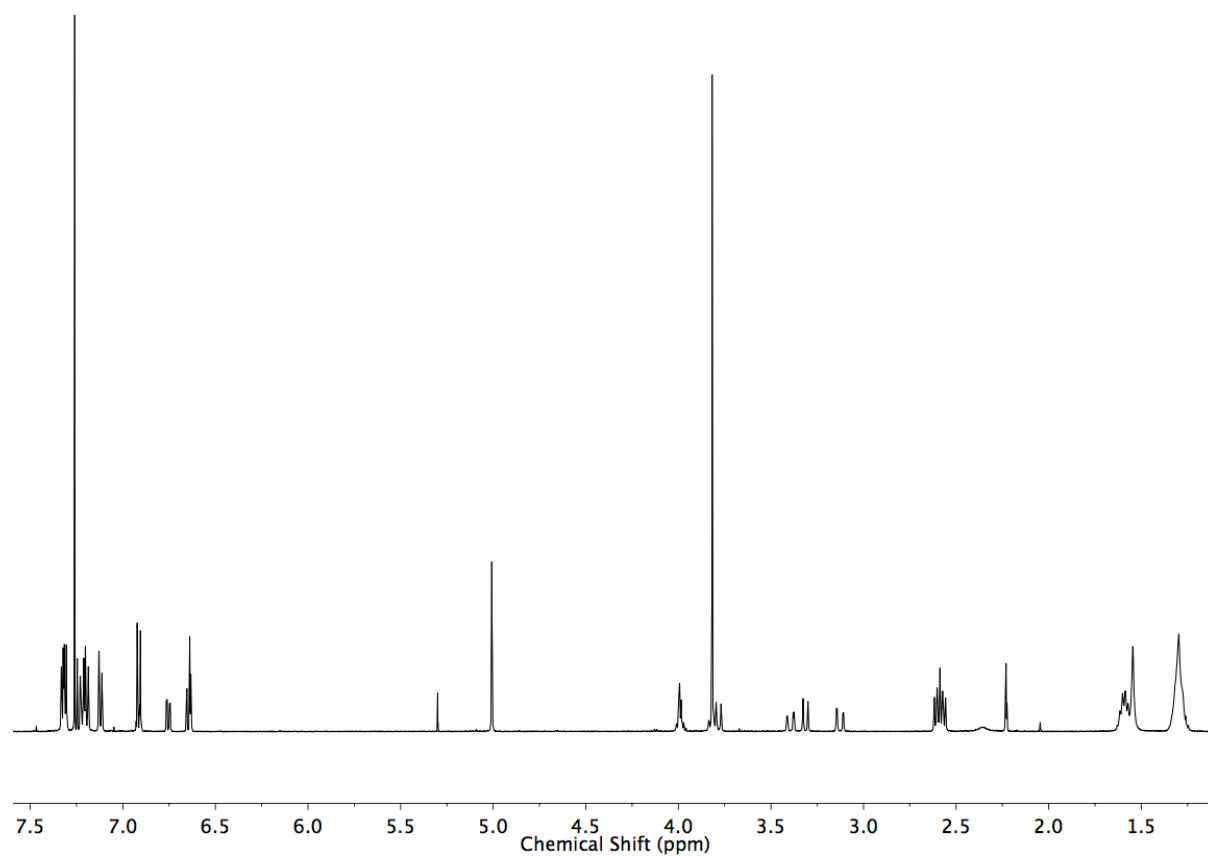


Figure S45 ^1H NMR (500 MHz, CDCl_3) of (R)-1.

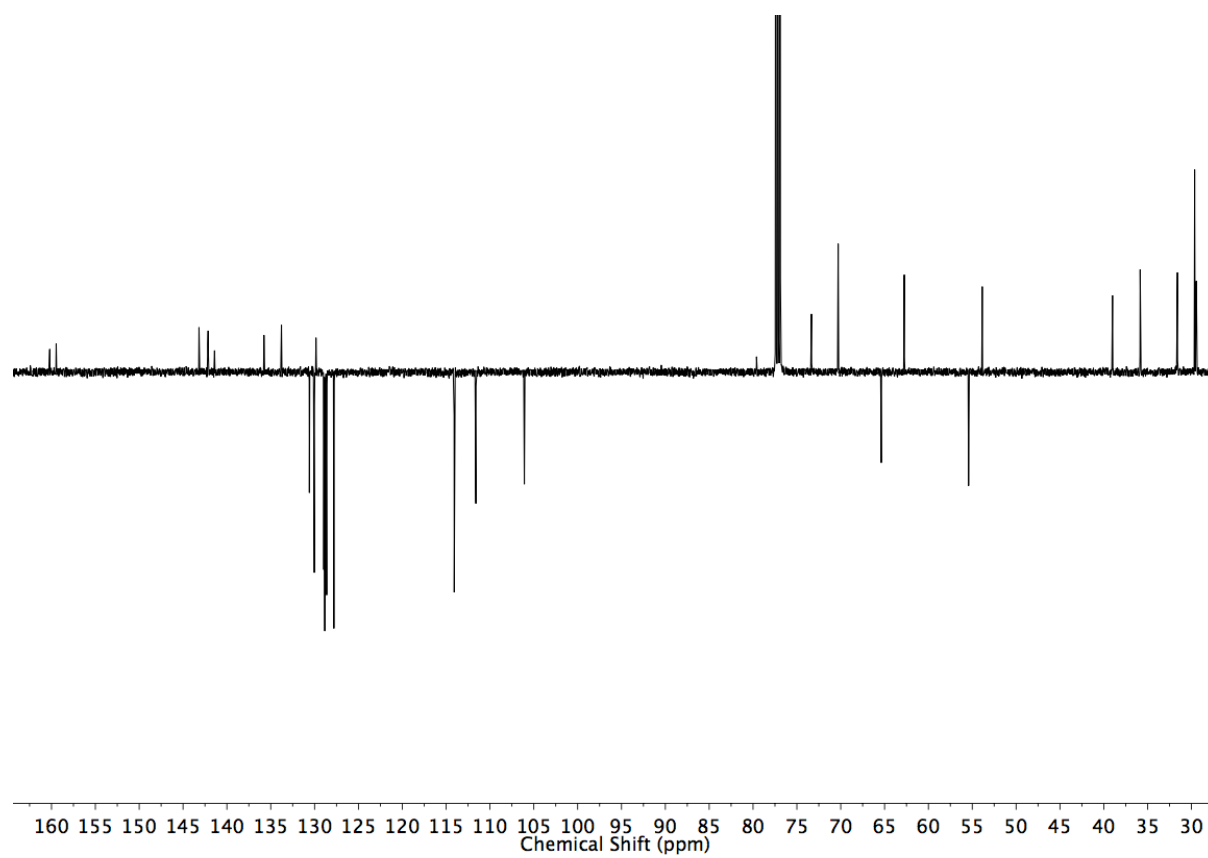


Figure S46 JMOD NMR (126 MHz, CDCl_3) of (R)-1.

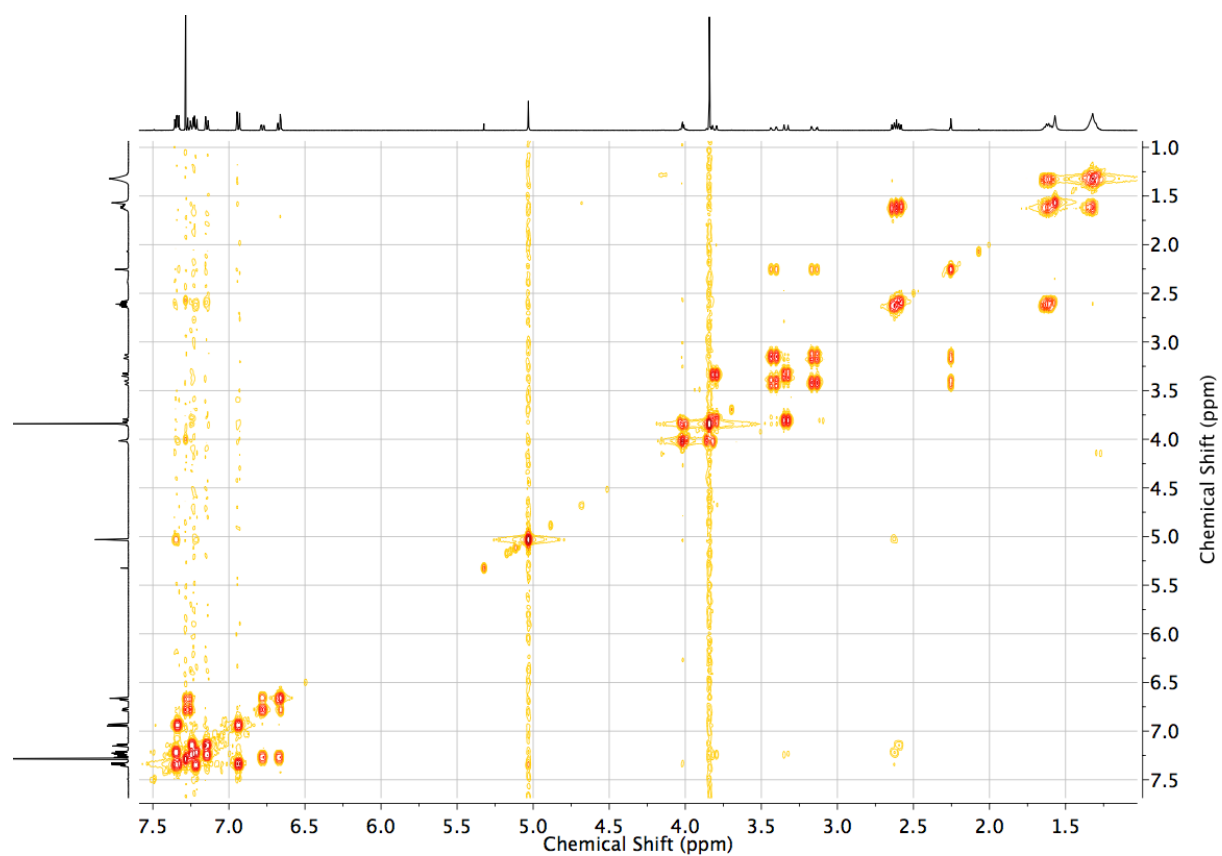


Figure S47 COSY NMR (CDCl_3) of (*R*)-1.

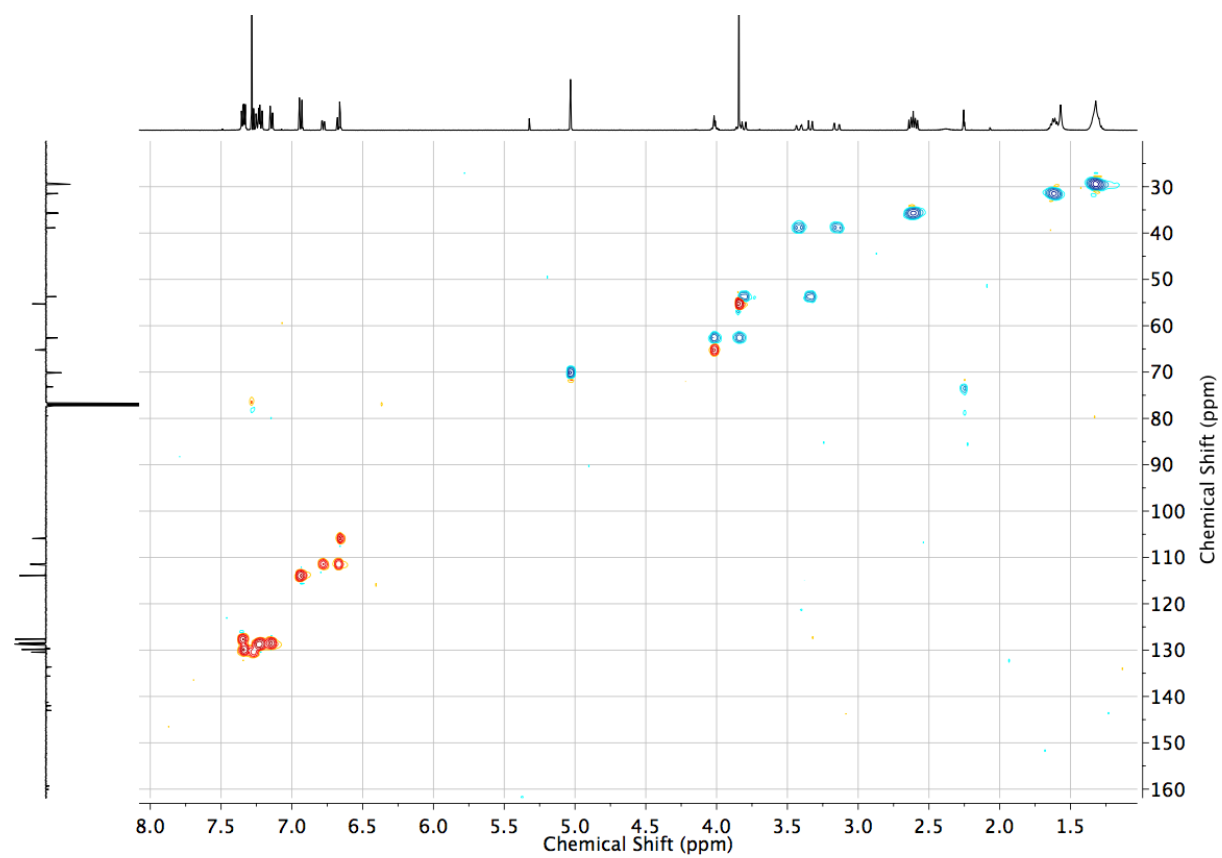


Figure S48 HSQC NMR (CDCl_3) of (*R*)-1.

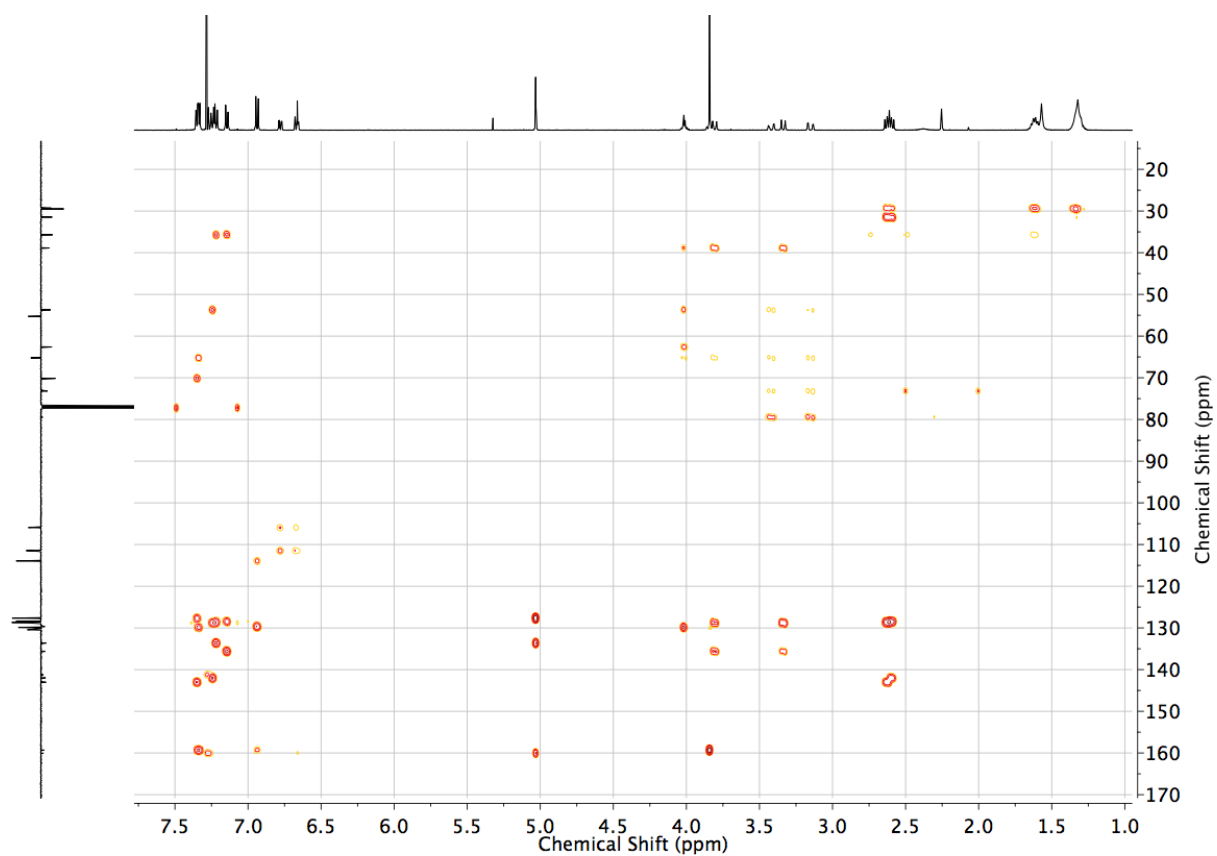


Figure S49 HMBC NMR (CDCl₃) of (R)-1.

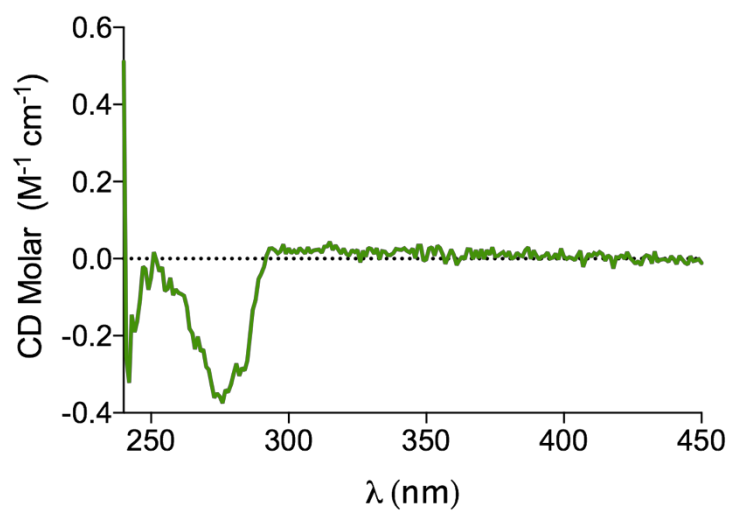
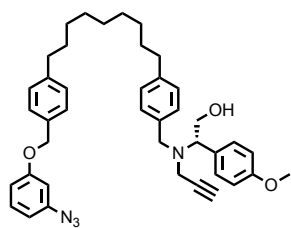


Figure S50 Circular dichroism spectrum of (R)-1 (100.0 μ M in CHCl₃, 293 K).



(*S*)-1

S10 (630 mg, 1.21 mmol, 1 eq.), (*S*)-**S9** (308 mg, 1.50 mmol, 1.2 eq.) and K_2CO_3 (829 mg, 6.00 mmol, 5 eq.) were stirred at 80 °C in MeCN (50 mL) under air in a sealed vial for 20 h. The cooled reaction mixture was filtered through celite and purified by column chromatography (Petrol/ CH_2Cl_2 1/1 with a gradient from 0 to 10% EtOAc) to give the product as a colorless oil (700 mg, 90%). Spectroscopic data were identical to those reported for (*R*)-1.

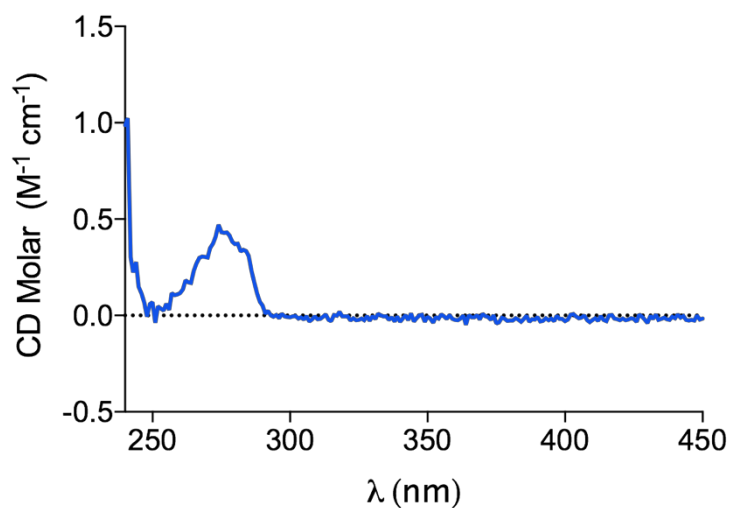
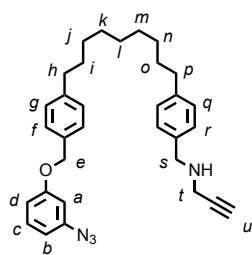


Figure S51 Circular dichroism spectrum of (*S*)-1 (100.0 μ M in $CHCl_3$, 293 K).



S11

S10 (253 mg, 0.50 mmol, 1 eq.), propargylamine (83 mg, 1.5 mmol, 3.0 eq.) and K_2CO_3 (83 mg, 0.60 mmol, 1.2 eq.) were stirred at 80 °C in MeCN (3 mL) under air in a sealed vial for 24 h. The cooled reaction mixture was filtered through celite and purified by column chromatography (CH_2Cl_2 with a gradient from 0 to 5% EtOAc) to give the product as a colorless oil (40 mg, 17%). 1H NMR (400 MHz, $CDCl_3$) δ : 7.34 (d, J = 8.2, 2H, H_i), 7.28-7.23 (m, 3H, H_r , H_d), 7.21 (d, J = 8.2, 2H, H_g), 7.15 (d, J = 8.2, 2H, H_q), 6.79-6.75 (m, 1H, H_b or H_d), 6.68-6.63 (m, 2H, H_a , H_b or H_d), 5.02 (s, 2H, H_e), 3.86 (s, 2H, H_s), 3.44 (d, J = 2.4, 2H, H_t), 2.61 (td, J = 9.5, 7.5, 4H, H_h , H_p), 2.26 (t, J = 2.4, 1H, H_u), 1.69-1.54 (m, 4H, H_i , H_o), 1.39-1.23 (m, 10H, H_j , H_k , H_l , H_m , H_n). ^{13}C NMR (101 MHz, $CDCl_3$) δ : 160.2, 143.2, 142.0, 141.4, 136.7, 133.8, 130.6, 128.8, 128.6, 128.5, 127.8, 111.7 ($\times 2$), 106.1, 82.3, 71.6, 70.3, 52.2, 37.5, 35.8, 35.8, 31.6 ($\times 2$), 29.6 ($\times 3$), 29.4 ($\times 2$). HR-ESI-MS m/z 495.3121 $[M+H]^+$ (calc. for $C_{32}H_{39}N_4O$ 495.3118).

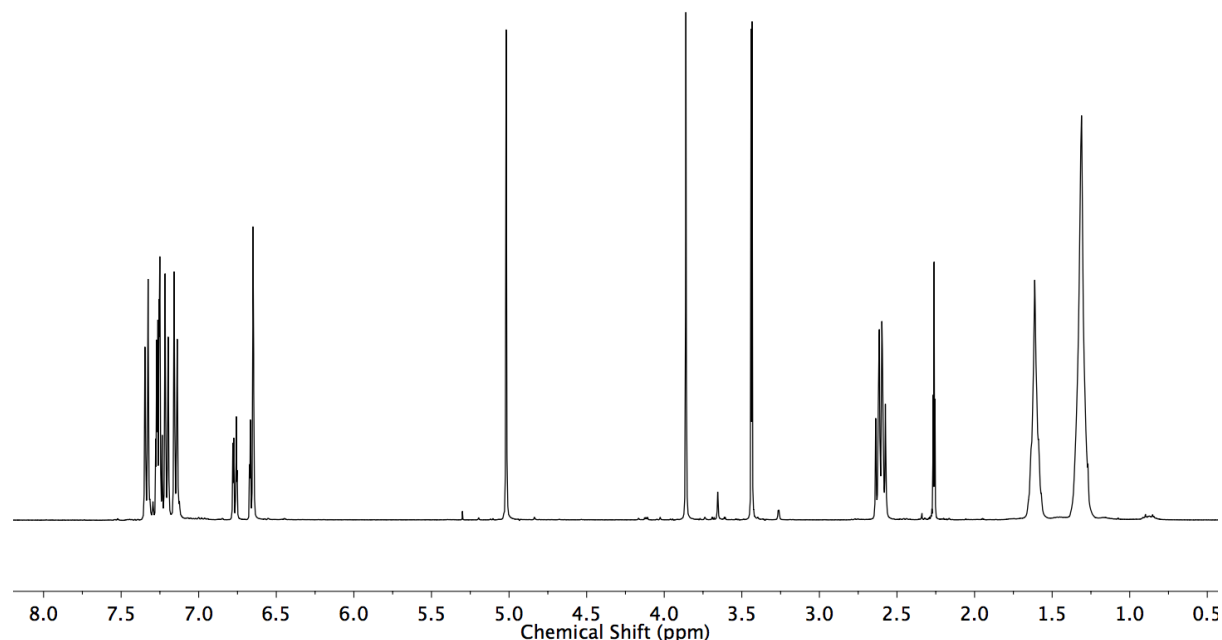


Figure S52 1H NMR (400 MHz, $CDCl_3$) of **S11**.

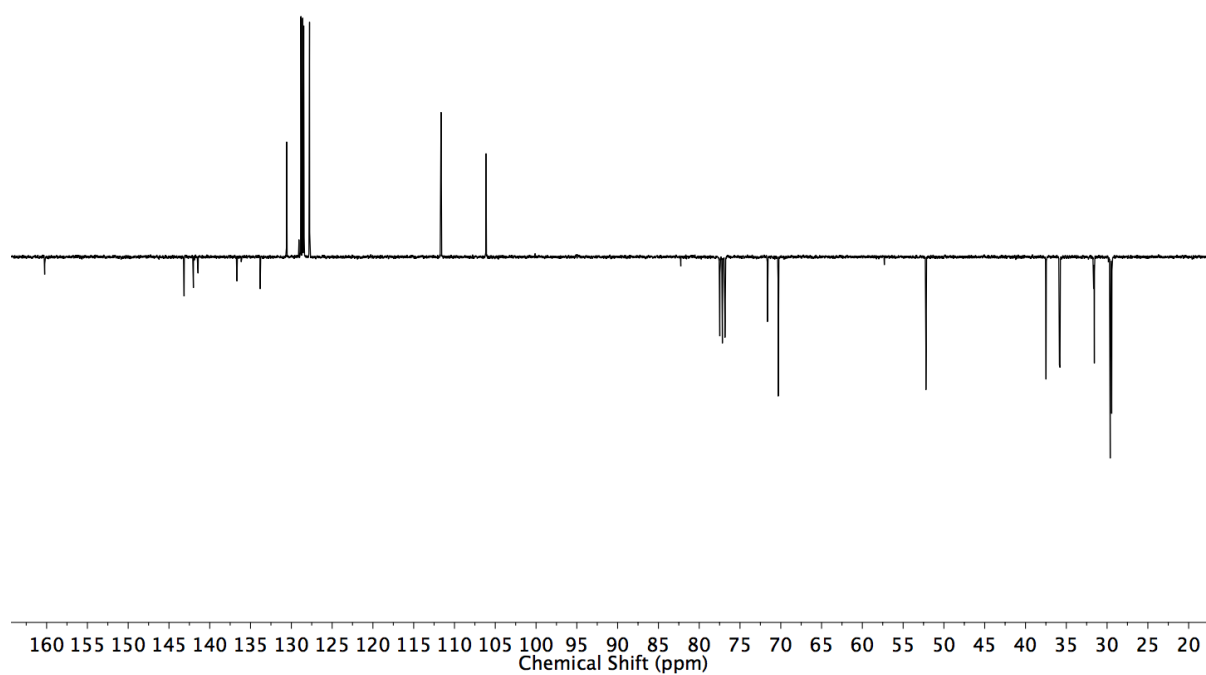


Figure S53 JMOD NMR (101 MHz, CDCl_3) of S11.

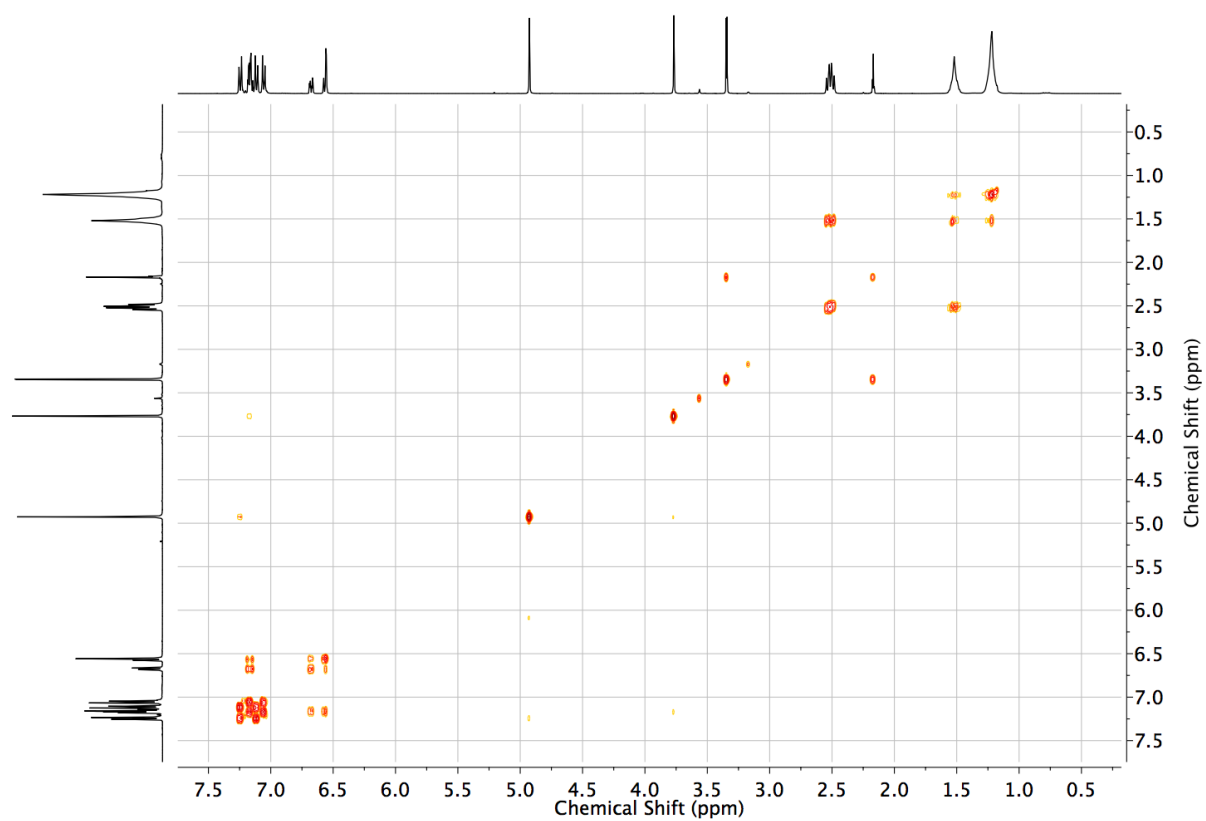


Figure S54 COSY NMR (CDCl_3) of S11.

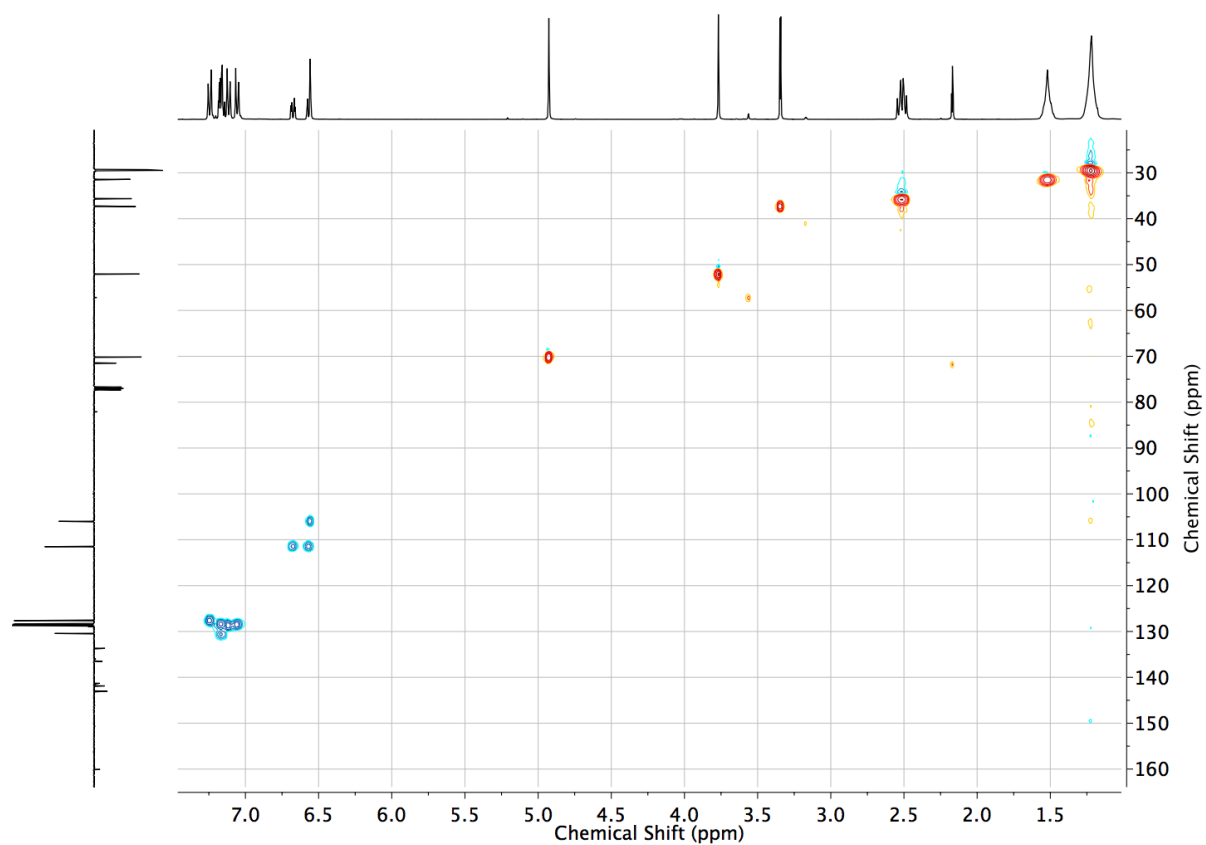


Figure S55 HSQC NMR (CDCl_3) of S11.

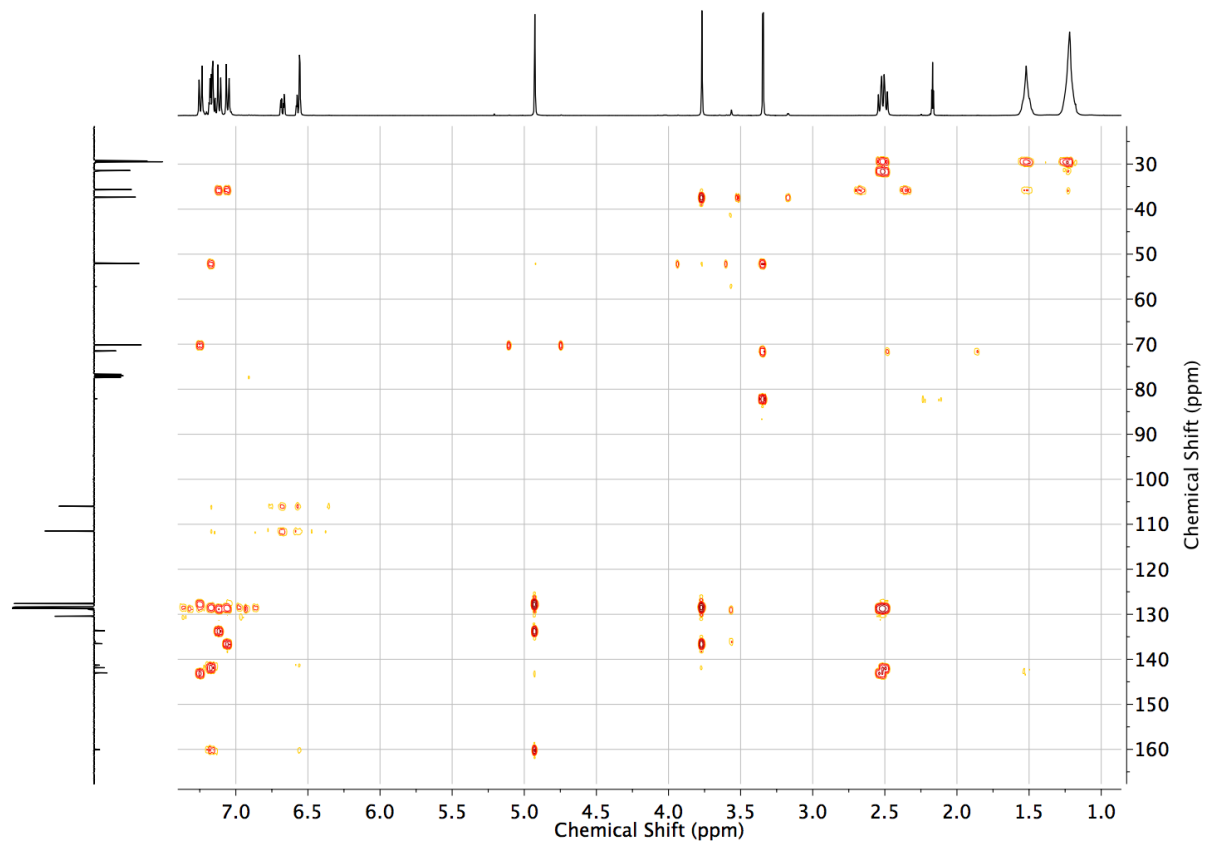
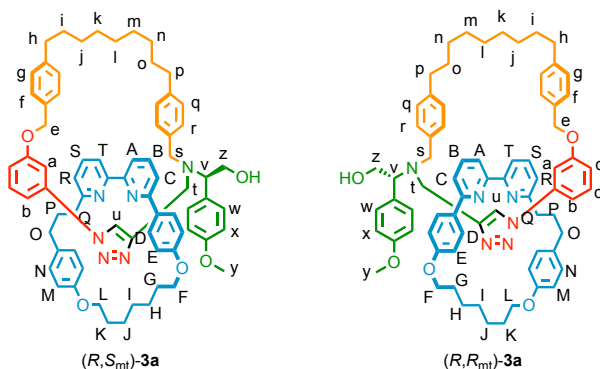


Figure S56 HMBC NMR (CDCl_3) of S11.

4. Syntheses of catenanes **3** and **6**



(R,R/S_{mt})-**3a**

To a solution of **2a** (24.1 mg, 0.050 mmol, 1 eq.), [Cu(CH₃CN)₄]PF₆ (18.5 mg, 0.0495 mmol, 0.99 eq.), ⁱPr₂NEt (18 μL, 0.10 mmol, 2 eq.) in 1:1 CHCl₃/EtOH (5.0 mL) at 60 °C was added (*R*)-**1** (40.0 mg, 0.060 mmol, 1.2 eq.) in 1:1 CHCl₃/EtOH (2.4 mL) over 4 h. After removal of the solvent *in vacuo*, the residue was dissolved in 1:1 CH₂Cl₂/MeOH (2.5 mL) and KCN (16 mg, 0.25 mmol, 5 eq.) added as a solid. After stirring at r.t. for 30 minutes the solvent was removed under a flow of air. The residue was dissolved in CH₂Cl₂ (5 mL) and washed with H₂O (4 × 5 mL), dried (MgSO₄) and the solvent removed *in vacuo*. After purification by column chromatography on silica (Petrol with a gradient of 0 to 100% Et₂O over 10 CVs) (*R,R/S_{mt}*)-**3a** was obtained as a white foam (40.1 mg, 72%, 1 : 1 diastereoisomeric ratio determined by ¹H NMR). ¹H NMR (400 MHz, CDCl₃) **δ**: 9.24 (s, 1H H_u), 9.19 (s, 1H H_u), 7.82 (t, *J* = 7.8, 1H, H_S), 7.79 (t, *J* = 7.8, 1H, H_S), 7.74 (t, *J* = 7.8, 1H, H_B), 7.71-7.63 (m, 3H, H_{B'}, H_T, H_T), 7.57 (dd, *J* = 7.8, 0.9, 1H, H_A), 7.49 (dd, *J* = 7.8, 0.9, 1H, H_{A'}), 7.40-7.32 (m, 3H, H_a or H_{a'} or H_b or H_{b'} or H_c or H_{c'} or H_d or H_{d'}), 7.28-7.02 (m, 24H, H_C, H_{C'}, H_R, H_{R'}, H_r, H_{r'}, H_w, H_f, H_q, H_{q'}, H_a or H_{a'} or H_b or H_{b'} or H_c or H_{c'} or H_d or H_{d'}), 7.01-6.95 (m, 3H, H_g, H_a or H_{a'} or H_b or H_{b'} or H_c or H_{c'} or H_d or H_{d'}), 6.95-6.87 (m, 3H, H_{w'}, H_a or H_{a'} or H_b or H_{b'} or H_c or H_{c'} or H_d or H_{d'}), 6.82 (d, *J* = 8.7, 2H, H_x), 6.76 (s, 4H, H_F, H_g), 6.71 (d, *J* = 8.7, 2H, H_D or H_{D'} or H_N or H_N), 6.28 (d, *J* = 8.5, 2H, H_D or H_{D'} or H_N or H_N), 6.21 (d, *J* = 8.7, 2H, H_E or H_{E'} or H_M or H_M), 6.17 (d, *J* = 8.3 Hz, 2H, H_q or H_{q'} or H_r or H_r), 6.02 (d, *J* = 8.7, 4H, H_E or H_{E'} or H_M or H_M), 5.93 (d, *J* = 8.3 Hz, 2H, H_q or H_{q'} or H_r or H_r), 5.53 (d, *J* = 8.7, 4H, H_E or H_{E'} or H_M or H_M), 5.12-4.96 (m, 2H, H_e), 4.80 (d, *J* = 14.4, 1H, H_e), 4.57 (d, *J* = 14.4, 1H, H_e), 4.21-3.82 (m, 8H, H_v, H_{v'}, H_z, H_{z'}, H_F or H_{F'} or H_L or H_L), 3.79 (s, 3H, H_y), 3.76 (s, 3H, H_y), 3.75-3.50 (m, 6H, 1 of H_s, 1 of H_{s'}, H_F or H_{F'} or H_L or H_L), 3.41 (d, *J* = 14.4, 1H, 1 of H_t), 3.18 (d, *J* = 14.4, 1H, 1 of H_t), 3.01 (d, *J* = 14.4, 1H, 1 of H_t), 2.99 (d, *J* = 14.4, 1H, 1 of H_t), 2.86 (d, *J* = 14.4, 1H, 1 of H_s), 2.70-2.38 (m, 5H, H_h, H_{h'}, 1 of H_s), 1.96-1.78 (m, 8H, H_G, H_{G'}, H_K, H_{K'}), 1.76-1.48 (m, 12H, H_H, H_{H'}, H_J, H_{J'}, H_i, H_{i'}), 1.29-1.20 (m, 2H, H_i), 1.13-0.95 (m, 8H, H_i, H_{i'}, H_j, H_{j'}), 0.78-0.68 (m, 4H, H_i, H_i). ¹³C NMR (101 MHz, CDCl₃) **δ** 163.6, 163.5, 159.5, 159.3, 159.1, 159.0, 158.6, 158.2, 157.9, 157.8, 157.6, 157.1, 156.7, 156.6, 144.0, 143.7, 142.3, 142.1, 141.6, 141.5, 138.4, 138.3, 137.3, 137.2, 137.0, 136.9, 136.8, 136.7, 134.5, 134.4, 131.6, 131.4, 131.3, 130.2, 130.1, 129.3, 129.1, 128.9, 128.8, 128.7, 128.6, 128.5, 128.4, 128.2, 128.1 (×2), 127.5, 126.7, 126.1, 122.7 (×2), 122.6, 122.4, 120.1, 119.9, 119.8 (×2), 119.7, 119.6, 115.1, 114.7, 114.5, 114.3, 113.8, 113.7, 113.6, 113.5, 112.7, 112.0, 106.1, 105.7, 68.8, 68.0, 67.6, 67.4, 65.2, 65.1, 62.9, 62.7, 61.4, 60.9, 55.4, 55.3, 53.5, 53.4, 44.9, 44.3, 41.0, 37.3, 36.1, 36.0, 35.7 (×2), 35.2, 35.1, 33.4, 33.2, 31.7 (×2), 31.6 (×2), 30.4, 30.3, 30.2, 29.4, 29.3, 29.2, 29.1, 29.0 (×2), 28.9, 28.7, 28.6, 28.2, 28.1, 26.1, 26.0 (×2), 25.9. LR-ESI-MS *m/z* = 1123.6 [M+H]⁺ (calc. for C₇₃H₈₃N₆O₅ 1123.6).

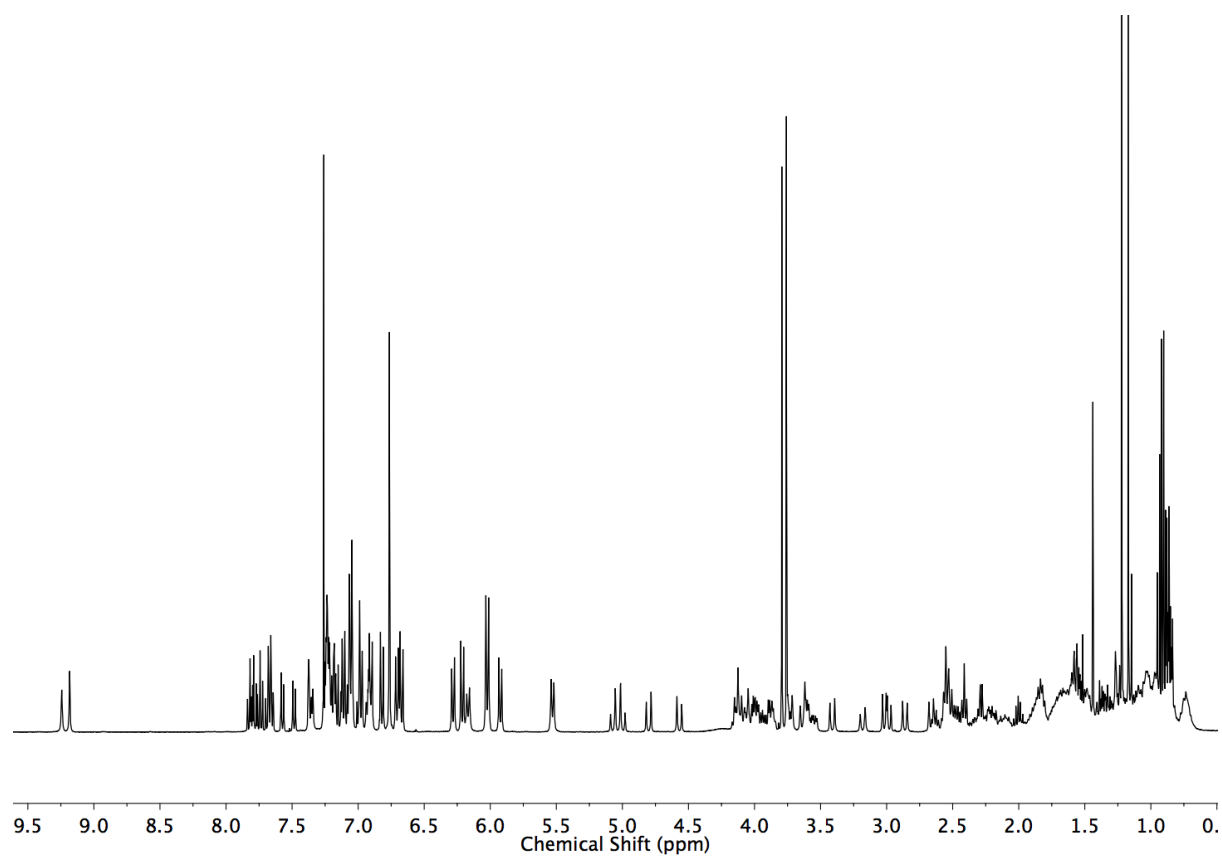


Figure S57 ¹H NMR (400 MHz, CDCl₃) of (R,S/R_{mt})-3a.

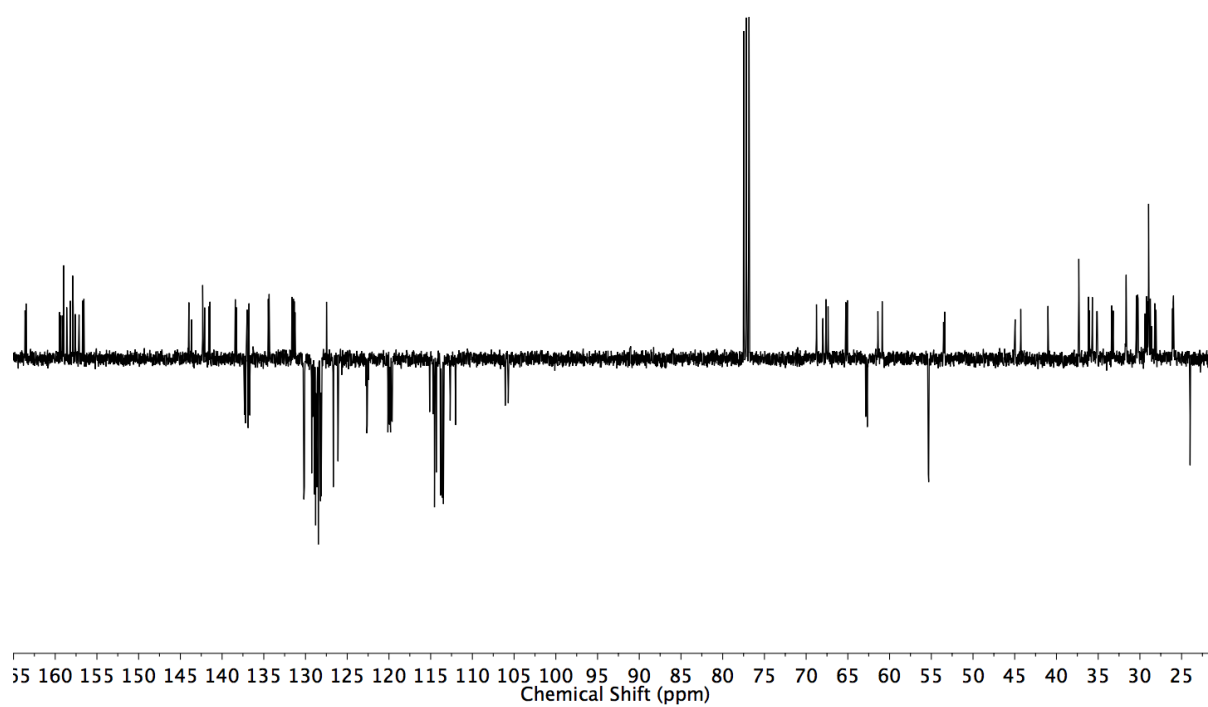


Figure S58 JMOD NMR (101 MHz, CDCl₃) of (R,S/R_{mt})-3a.

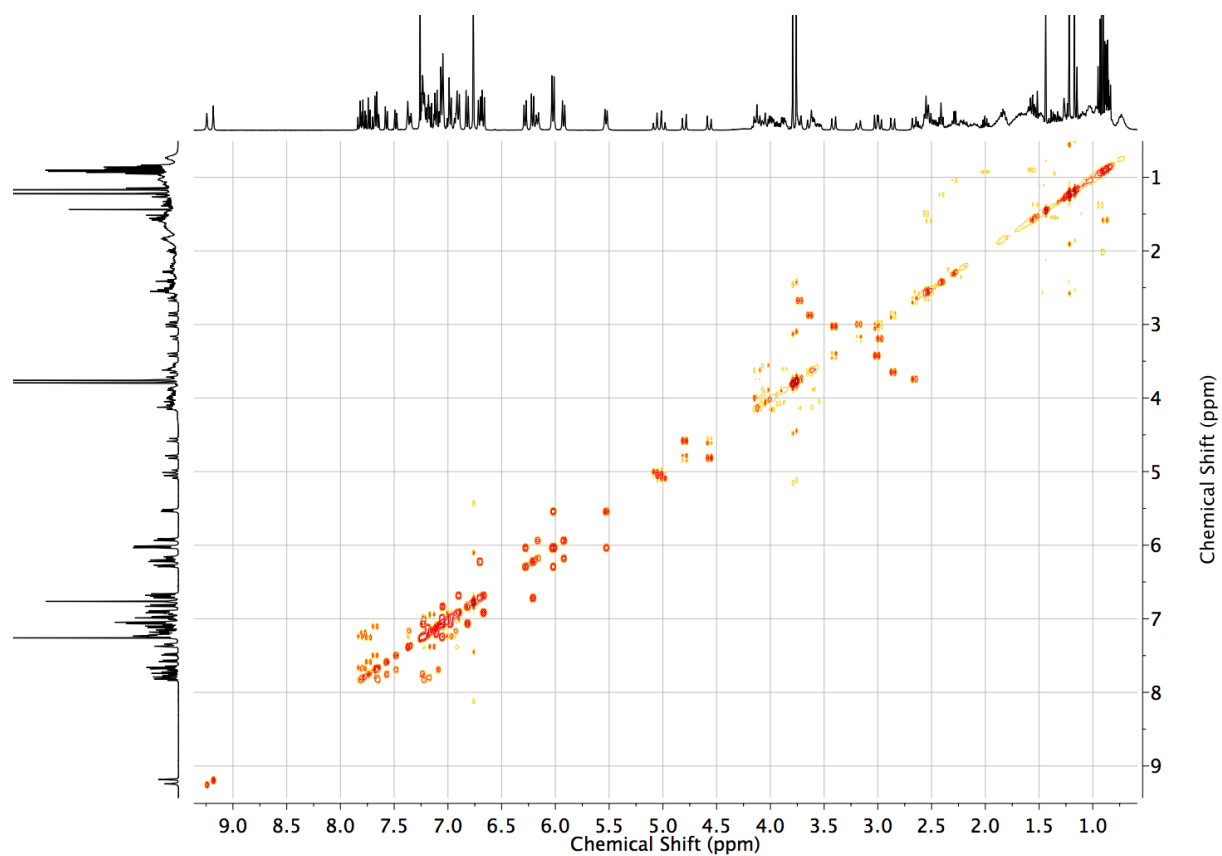


Figure S59 COSY NMR (CDCl_3) of $(R,S/R_{\text{mt}})$ -3a.

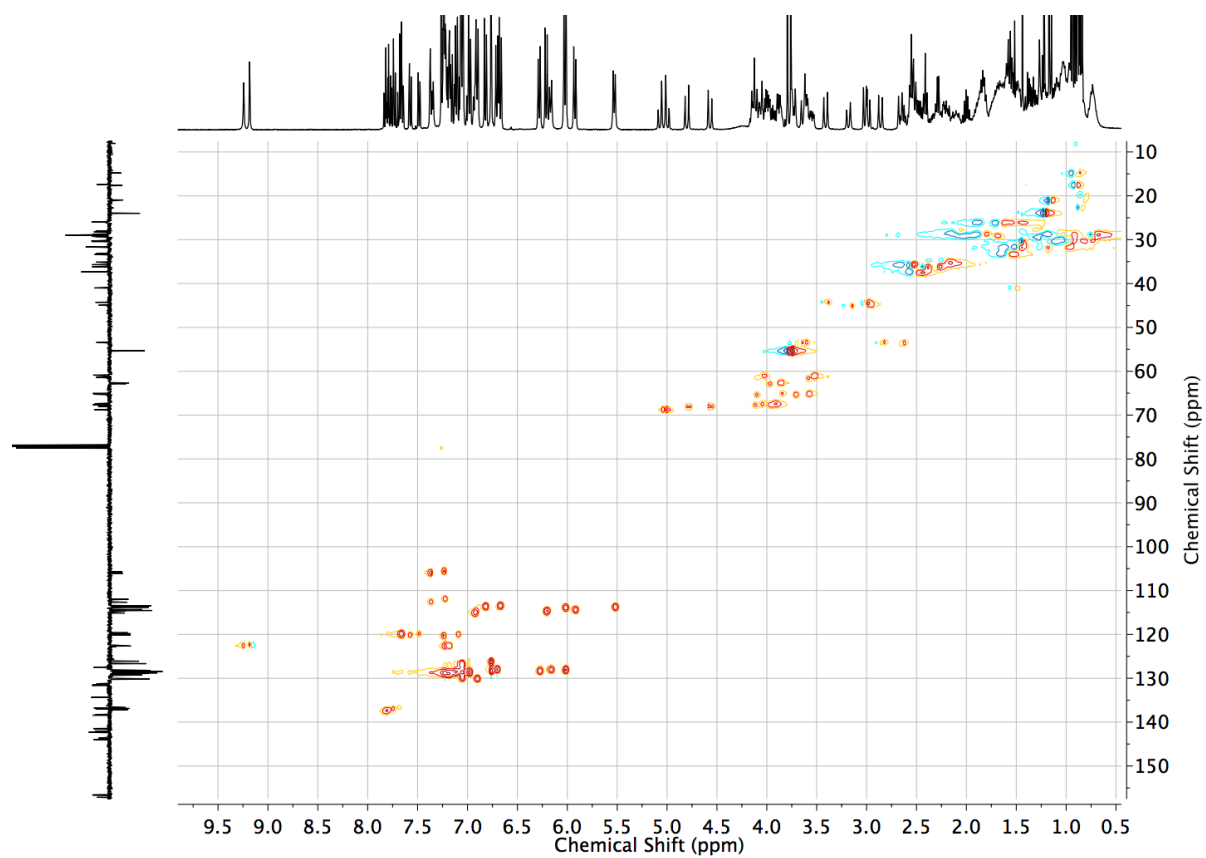


Figure S60 HSQC NMR (CDCl_3) of $(R,S/R_{\text{mt}})$ -3a.

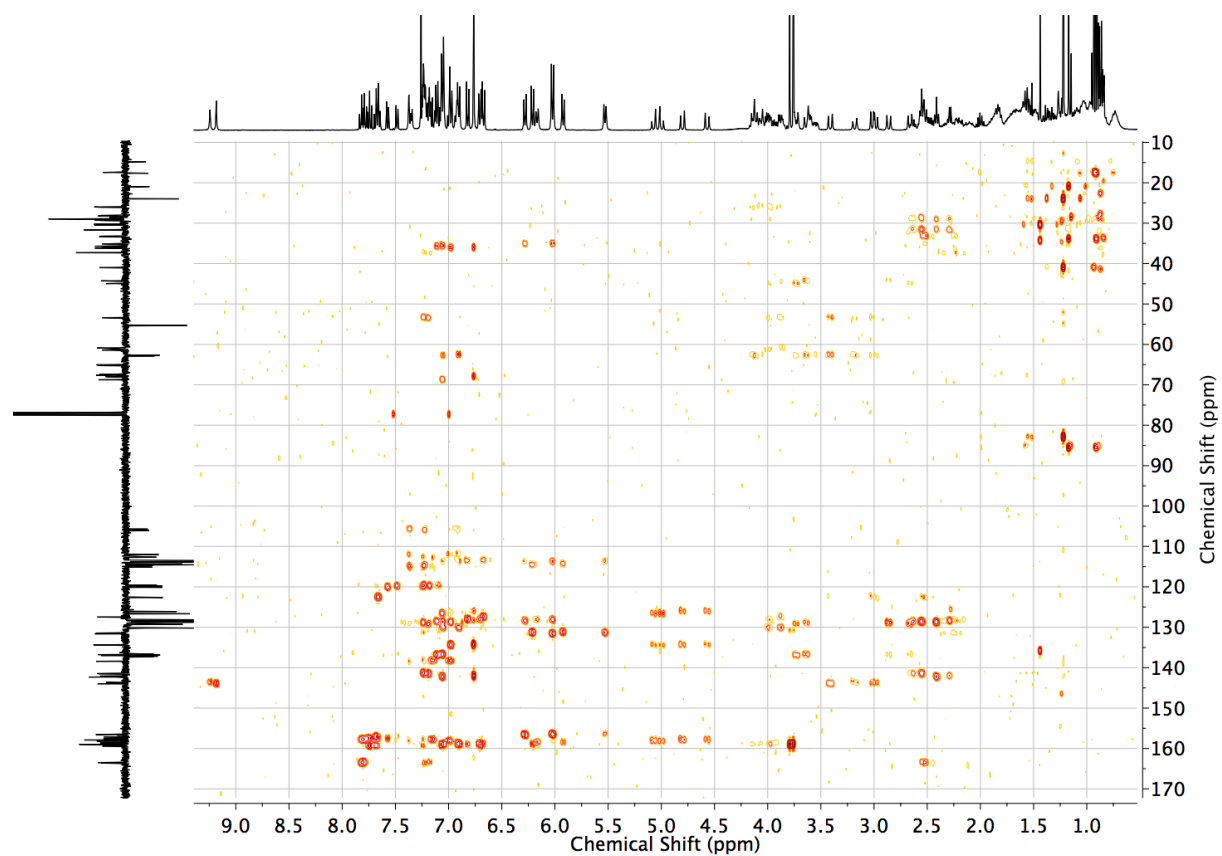


Figure S61 HMBC NMR (CDCl_3) of (*R,S/R_{mt}*)-**3a**.

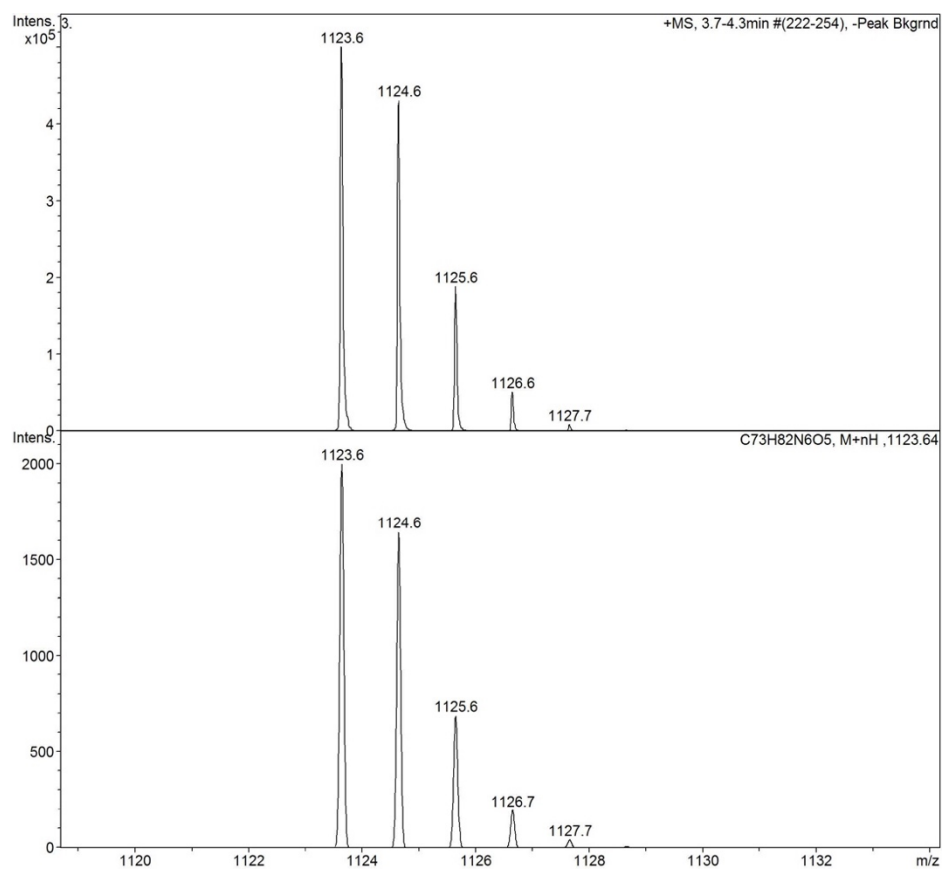
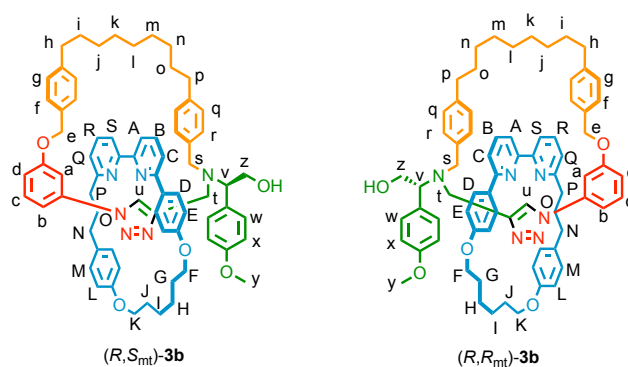


Figure S62 Observed (top) and calculated (bottom) isotopic patterns for (*R,S/R_{mt}*)-**3a**.



(R,S_{mt})-**3b** and (R,R_{mt})-**3b**

To a solution of **2b** (116.2 mg, 0.25 mmol, 1.0 eq.), [Cu(CH₃CN)₄]PF₆ (92.8 mg, 0.249 mmol, 1.0 eq.), ⁱPr₂NEt (87 μL, 0.50 mmol, 2 eq.) in 1:1 CHCl₃/EtOH (10 mL) at 60 °C was added (*R*)-**1** (194.0 mg, 0.60 mmol, 1.2 eq.) in 1:1 CHCl₃/EtOH (15 mL) over 4 h. After removal of the solvent *in vacuo*, the residue was dissolved in 1:1 CH₂Cl₂/MeOH (10 mL) and KCN (160 mg, 2.5 mmol, 10 eq.) added as a solid. After stirring at r.t. for 30 minutes the solvent was removed under a flow of air. The residue was dissolved in CH₂Cl₂ (50 mL) and washed with H₂O (4 × 10 mL), dried (MgSO₄) and the solvent removed *in vacuo*. The residue containing catenane (R,R/S_{mt})-**3b** (in a 0.67:0.33 diastereoisomeric ratio, **Figure S41**) was purified by column chromatography on silica (Petrol/CH₂Cl₂/EtOAc/Et₂O 140/30/15/15), to yield (R,S_{mt})-**3b** (160 mg, 57%) and (R,R_{mt})-**3b** (90 mg, with 5% of (R,S_{mt})-**3b**, 32%) as white foams.

Catenane (R,S_{mt})-**3b**. ¹H NMR (500 MHz, CDCl₃) δ : 9.59 (br. s, 1H, H_u), 7.81 (t, J = 7.8, 1H, H_R), 7.74 (t, J = 7.8, 1H, H_B), 7.69 (dd, J = 7.8, 1.0, 1H, H_S), 7.57 (dd, J = 7.8, 1.0, 1H, H_A), 7.35-7.29 (m, 3H, H_c, H_r), 7.27 (dd, J = 7.8, 0.9, 1H, H_c), 7.21 (dd, J = 7.8, 0.9, 1H, H_o), 7.13-7.07 (m, 5H, H_q, H_f, H_a), 7.04 (d, J = 8.4, 2H, H_g), 6.90 (d, J = 8.7, 2H, H_w), 6.88-6.81 (m, 2H, H_b, H_d), 6.74 (d, J = 8.7, 2H, H_D), 6.58 (d, J = 8.7, 2H, H_x), 6.42 (d, J = 8.7, 2H, H_E), 5.94 (d, J = 7.8, 2H, H_M), 5.35 (d, J = 7.5, 2H, H_L), 5.22-5.15 (m, 2H, H_e), 4.30-4.21 (m, 1H, one of H_F), 4.19-4.04 (m, 2H, one of H_z, one of H_F), 3.95 (dd, J = 11.2, 4.5, 1H, H_v), 3.85 (d, J = 13.6, 1H, one of H_s), 3.75-3.72 (m, 4H, 1 of H_K, H_y), 3.70-3.63 (m, 1H, one of H_K), 3.63-6.56 (m, 1H, 1 of H_z), 3.37 (d, J = 14.4, 1H, one of H_i), 3.08 (d, J = 14.4, 1H, one of H_i), 2.79 (d, J = 13.7, 1H, one of H_s), 2.67-2.59 (m, 1H, one of H_P), 2.56 (t, J = 6.9, 2H, H_h), 2.54- 2.38 (m, 1H, one of H_P), 2.32- 2.24 (m, 1H, one of H_N), 2.13- 2.04 (m, 1H, one of H_N), 2.04-1.97 (m, 1H, one of H_G), 1.97- 1.90 (m, 1H, one of H_G), 1.90-1.73 (m, 6H, H_J, H_H, H_I), 1.67-1.55 (m, 4H, H_i, H_j), 1.49 (q, J = 6.9, 2H, H_o), 1.39-1.22 (m, 4H, H_n, H_o), 1.19-1.10 (m, 2H, H_k), 1.10-1.00 (m, 2H, H_m), 0.81-0.68 (m, 2H, H_i). ¹³C NMR (126 MHz, CDCl₃) δ : 163.3, 159.9, 159.5, 159.0, 158.1, 157.9, 157.6, 156.8, 143.2, 142.2, 141.6, 138.5, 137.3, 136.9, 136.8, 134.5, 132.0, 131.4, 130.2, 129.1, 128.9, 128.8 (×2), 128.0, 127.9, 127.2, 126.1, 123.4, 122.8, 120.4, 120.1, 119.8, 116.2, 114.9, 114.2, 113.4, 111.8, 105.2, 69.9, 68.7, 65.3, 62.5, 60.6, 55.3, 52.7, 44.7, 37.2, 36.2, 35.8, 35.1, 33.2, 31.7, 31.6, 30.5, 30.4, 29.7, 29.3, 29.2, 28.8 (×2), 25.3, 24.8. LR-ESI-MS *m/z* = 1109.64 [M+H]⁺ (calc. for C₇₂H₈₁N₆O₅ 1109.63).

Catenane (*R,R_{mt}*)-**3b**. ^1H NMR (500 MHz, CDCl_3) δ : 9.66 (s, 1H, H_u), 7.80 (t, $J = 7.7$, 1H, H_R), 7.68 (t, $J = 7.7$, 1H, H_B), 7.64 (d, $J = 7.8$, 1H, H_S), 7.47 (dd, $J = 7.8$, 0.9, 1H, H_A), 7.42 (br. s, 1H, H_a), 7.37 (dd, $J = 7.8$, 0.9, 1H, H_d), 7.24 (d, $J = 7.7$, 0.9, 1H, H_O), 7.17 (d, $J = 7.7$, 2H, H_I), 7.14-7.03 (m, 7H, H_C , H_c , H_g , H_q), 6.94-6.86 (m, 1H, H_b), 6.87-6.76 (m, 6H, H_f , H_w , H_x), 6.25 (d, $J = 7.8$, 2H, H_M), 6.13 (d, $J = 8.2$, 4H, H_D or H_E , H_L), 5.94 (d, $J = 8.1$, 2H, H_D or H_E), 4.82 (d, $J = 14.4$, 1H, one of H_e), 4.62 (d, $J = 14.4$, 1H, one of H_e), 4.28-4.18 (m, 1H, one of H_K), 4.15 (app. t, $J = 10.8$, 1H, H_F), 4.10-4.00 (m, 2H, one of H_z , H_V), 4.00-3.93 (m, 2H, 1 of H_K , one of H_z), 3.80 (s, 3H, H_Y), 3.75 (d, $J = 13.8$, 1H, H_S), 3.61 (dd, $J = 10.5$, 4.3, 1H, H_F), 3.25 (d, $J = 15.0$, 1H, H_I), 3.12 (d, $J = 15.0$, 1H, H_I), 2.68-2.48 (m, 5H, H_P , H_h , one of H_S), 2.39-2.21 (m, 2H, H_N), 2.05-1.75 (m, 8H, H_G , H_H , H_I , H_J), 1.66-1.45 (m, 6H, H_O , H_i , H_o), 1.25-0.95 (m, 8H, H_j , H_k , H_m , H_n), 0.90-0.75 (m, 2H, H_i). ^{13}C NMR (126 MHz, CDCl_3) δ 163.3, 159.6, 159.2, 159.0, 157.8, 157.5, 156.9, 156.7, 143.3, 141.9, 141.5, 138.3, 137.3, 136.7, 136.6, 134.3, 131.8, 131.7, 130.1, 129.3, 128.7, 128.5, 128.3 ($\times 2$), 127.9, 127.8, 125.8, 123.4, 122.7, 120.1, 119.7, 119.6, 115.9, 114.9, 114.3, 113.5, 112.8, 106.0, 69.9, 67.8, 66.0, 62.4, 61.1, 55.2, 53.3, 45.2, 37.2, 35.9, 35.7, 35.0, 33.0, 31.6 ($\times 2$), 30.2, 30.1, 29.4, 29.2, 29.0, 28.8 ($\times 2$), 25.2, 24.6. LR-ESI-MS $m/z = 1109.64$ $[\text{M}+\text{H}]^+$ (calc. for $\text{C}_{72}\text{H}_{81}\text{N}_6\text{O}_5$ 1109.63).

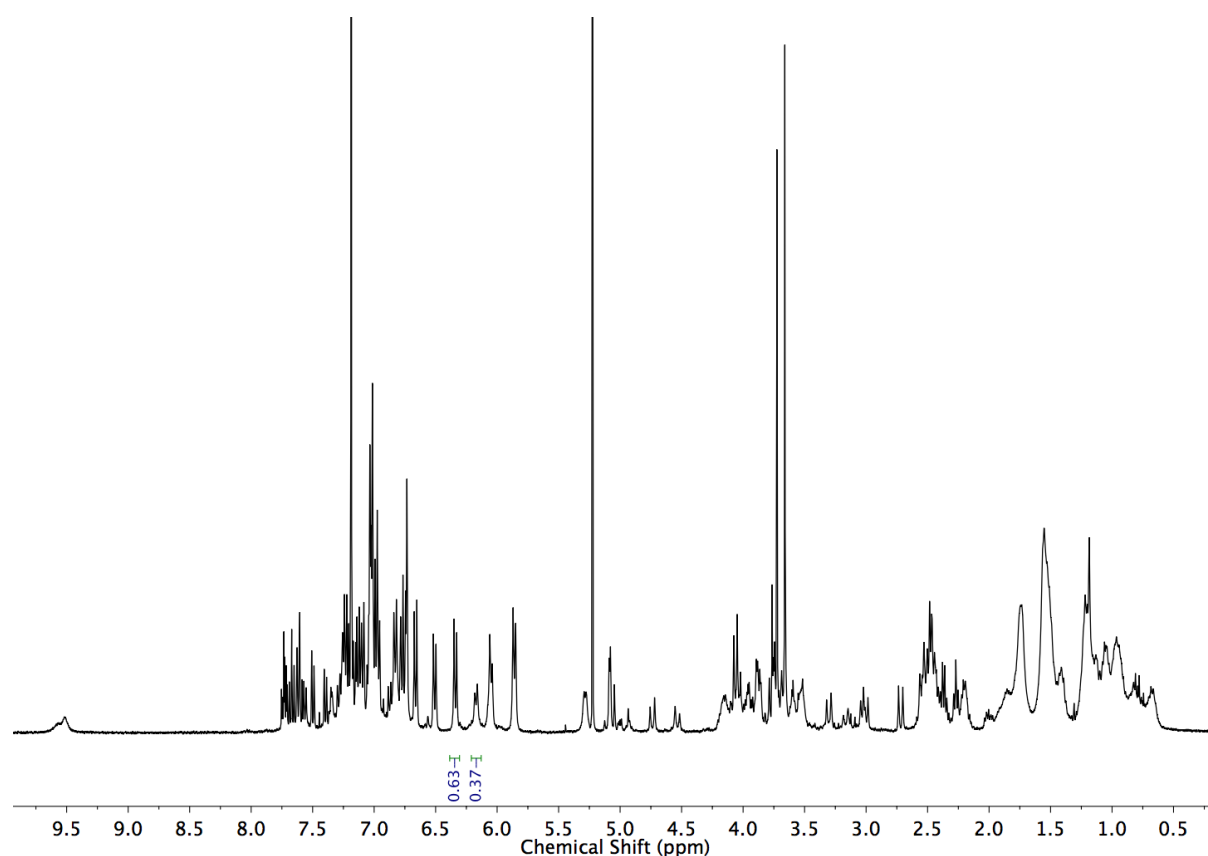


Figure S63 ^1H NMR (400 MHz, CDCl_3) of (*R,R/S_{mt}*)-**3b** prior to purification by chromatography.

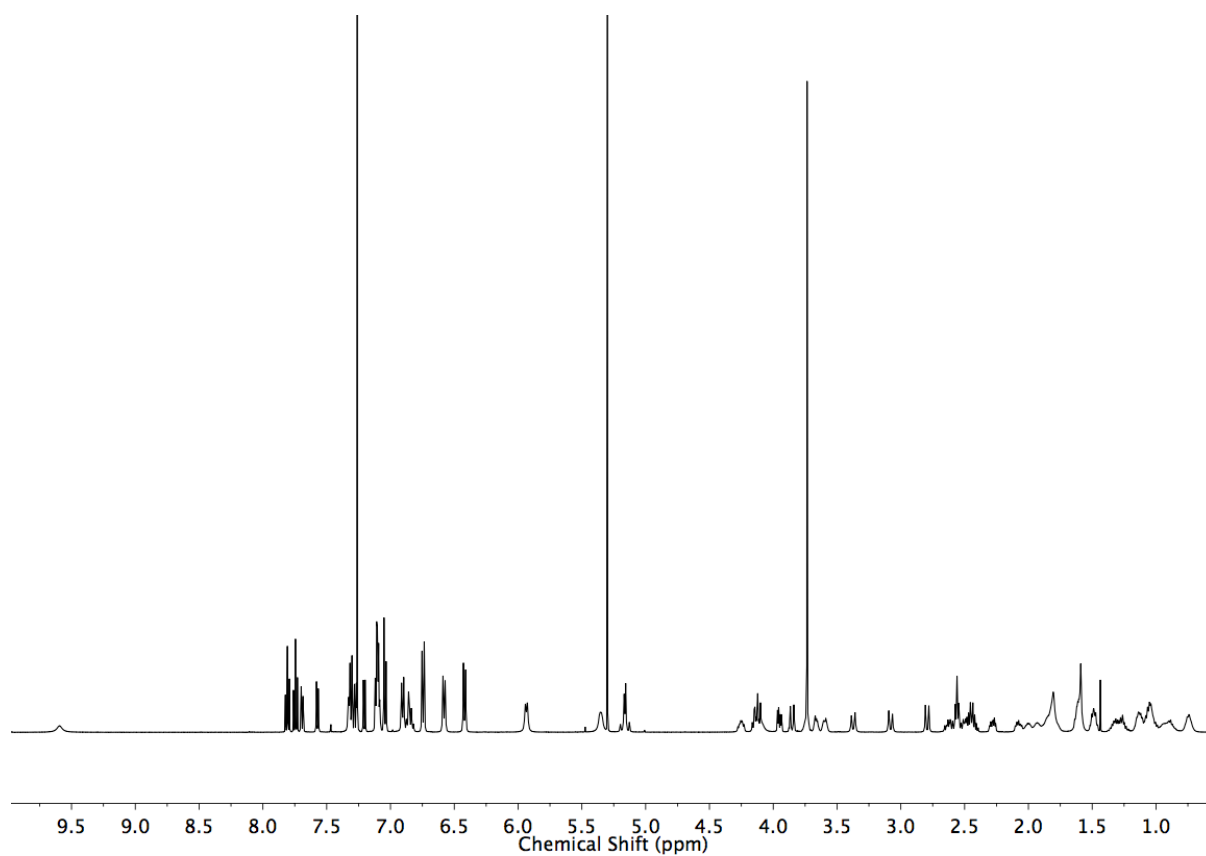


Figure S64 ^1H NMR (500 MHz, CDCl_3) of (R,S_{mt}) -**3b**.

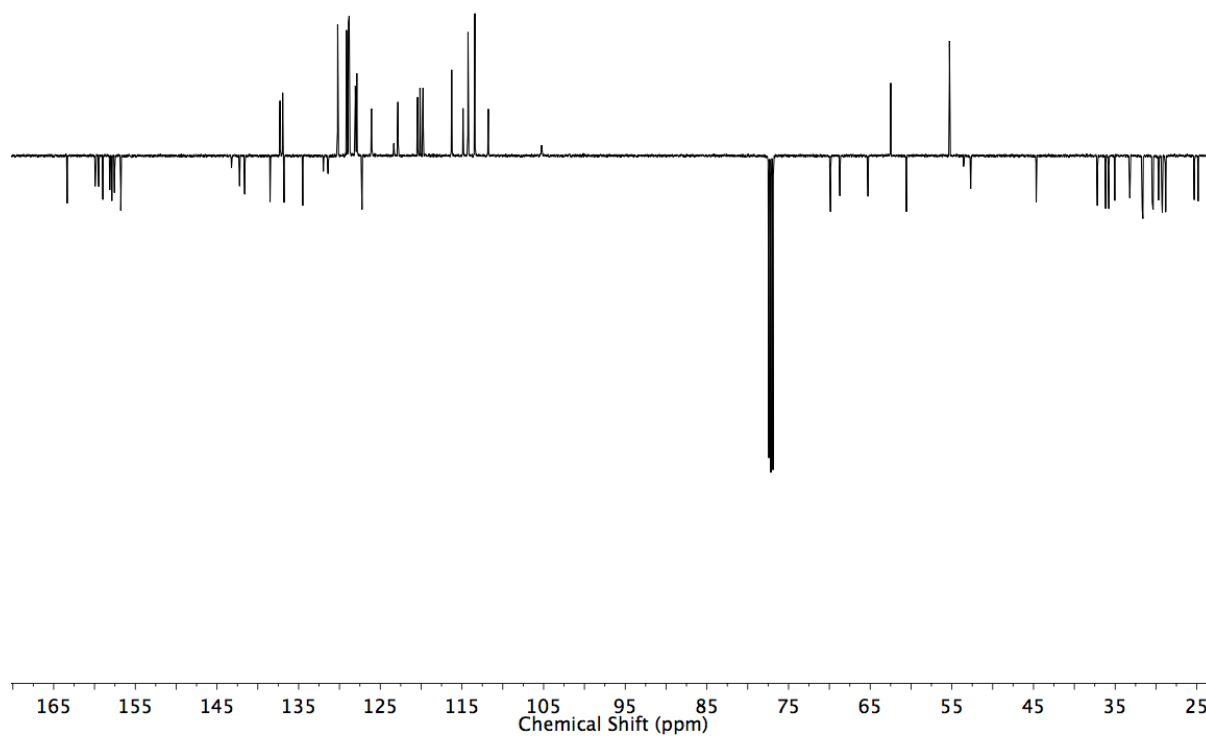


Figure S65 JMOD NMR (126 MHz, CDCl_3) of (R,S_{mt}) -**3b**.

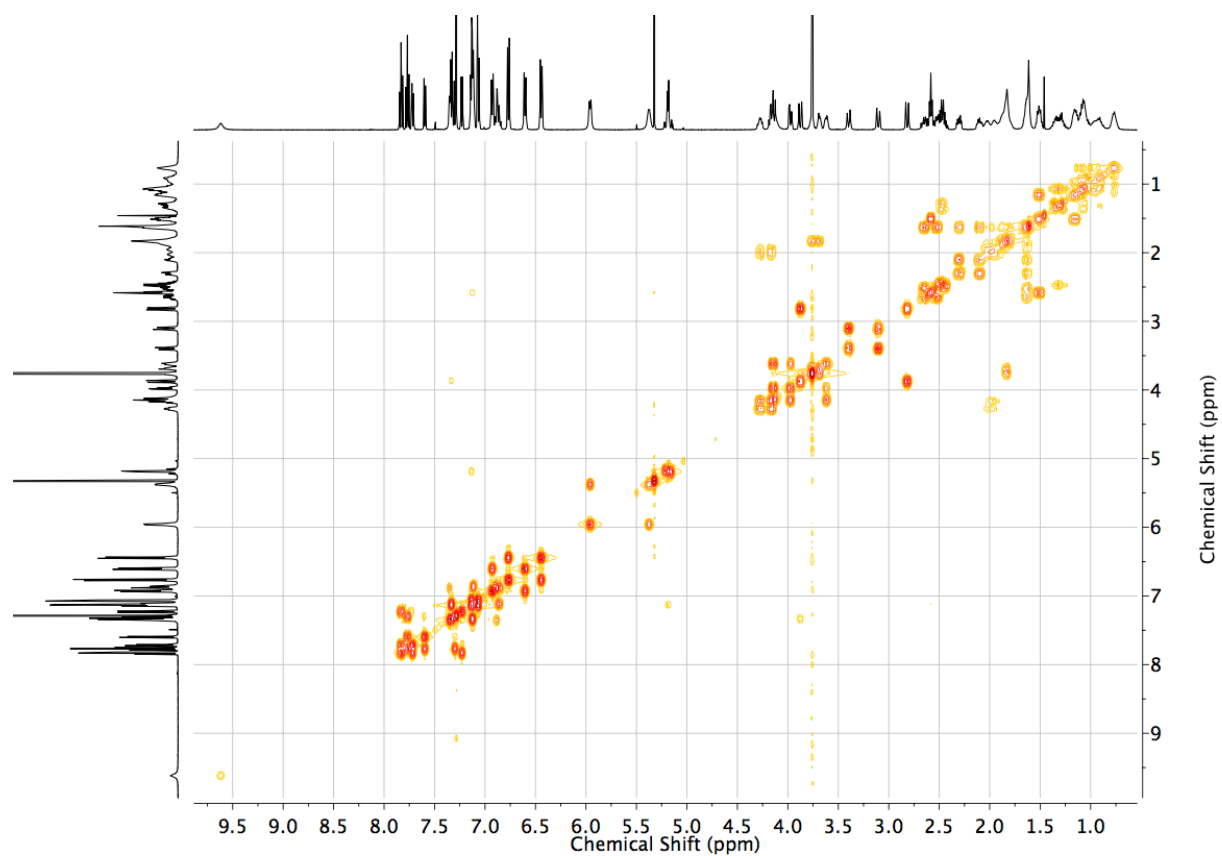


Figure S66 COSY NMR (CDCl₃) of (R,S_{mt})-3b.

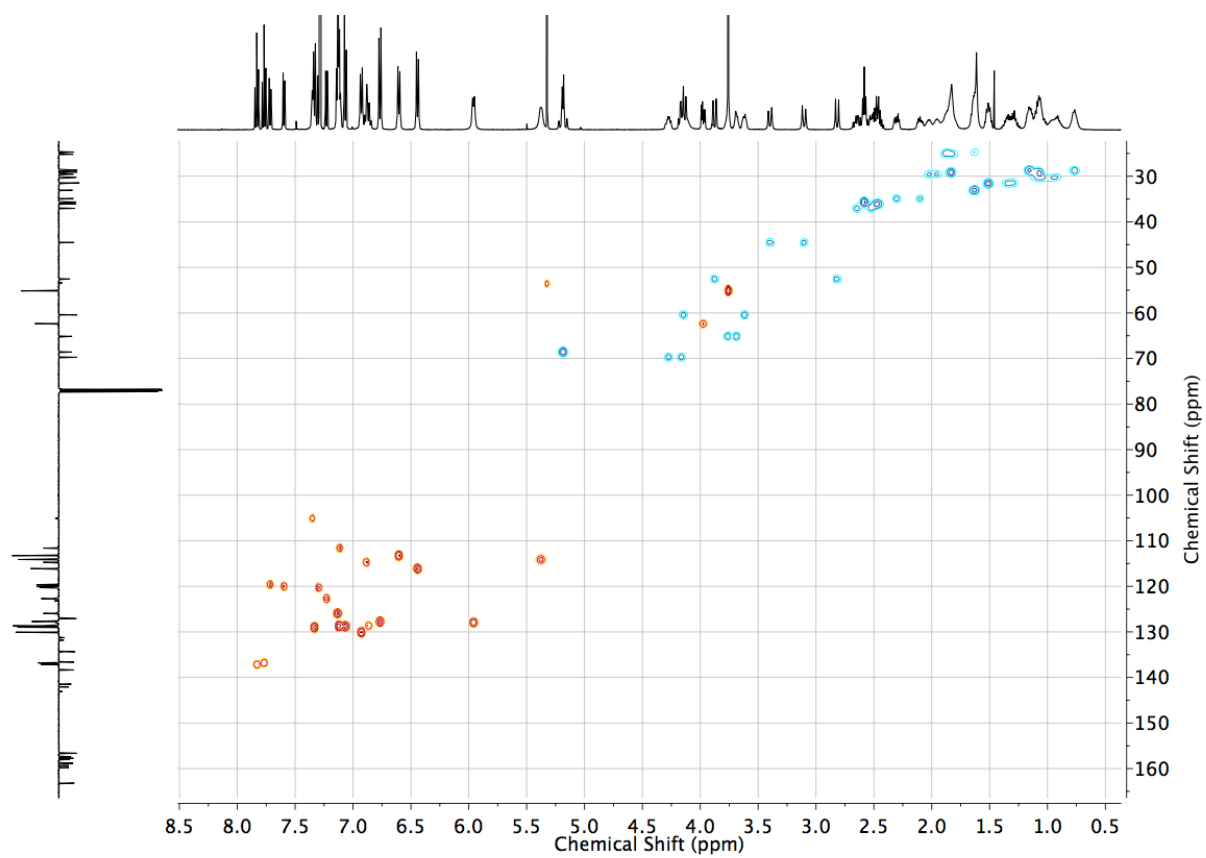


Figure S67 HSQC NMR (CDCl₃) of (R,S_{mt})-3b.

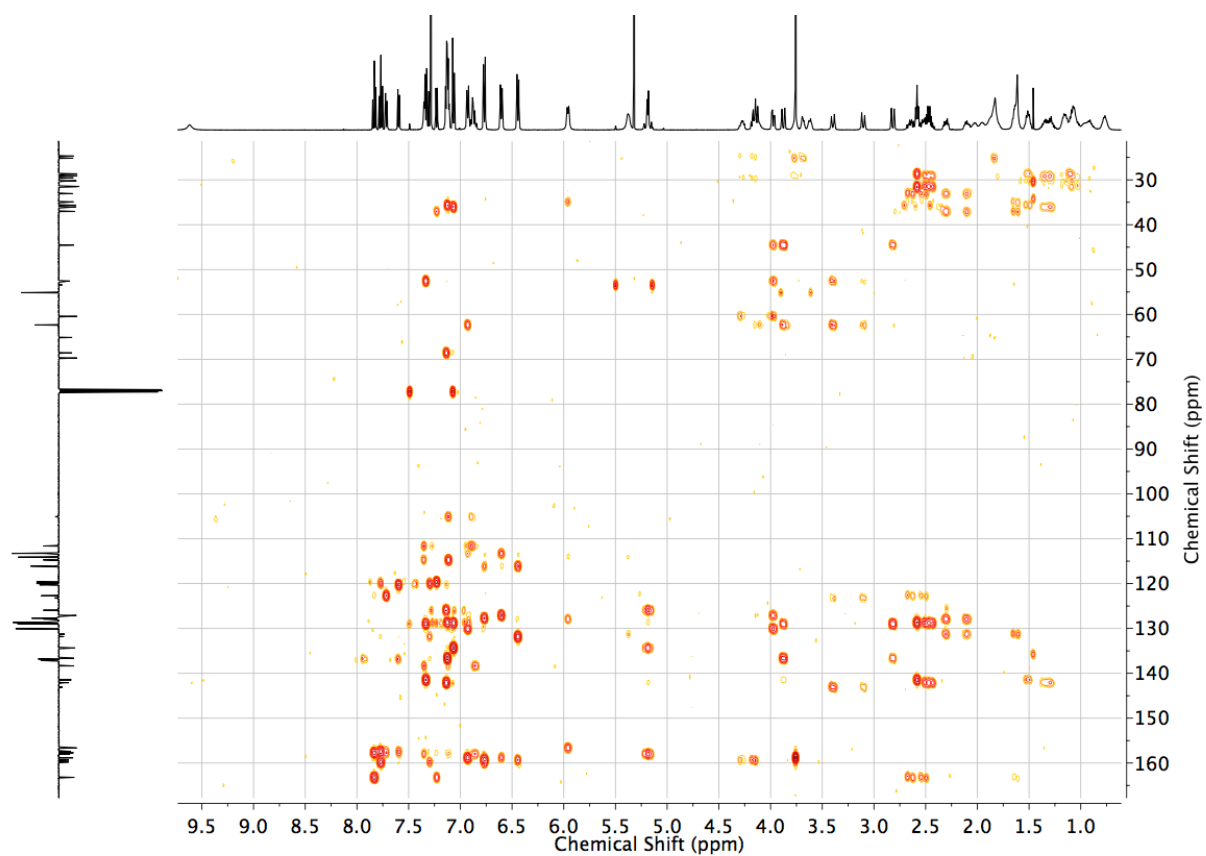


Figure S68 HMBC NMR (CDCl_3) of (R,S_{mt}) -**3b**.

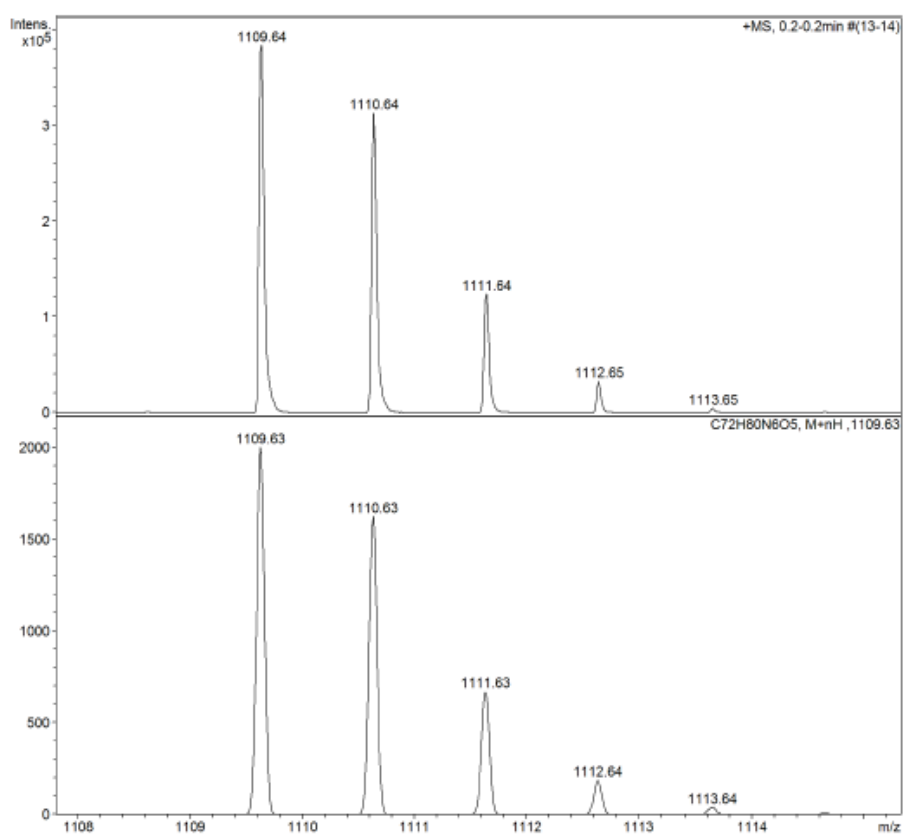


Figure S69 Observed (top) and calculated (bottom) isotopic patterns for (R,S_{mt}) -**3b**.

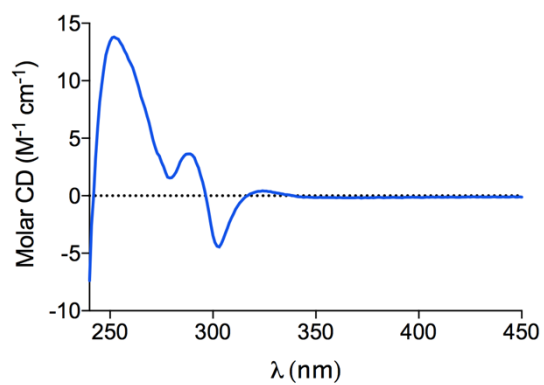


Figure S70 Circular dichroism spectrum of (*R,S_{mt}*)-**3b** (35.0 μ M in CHCl_3 , 293 K).

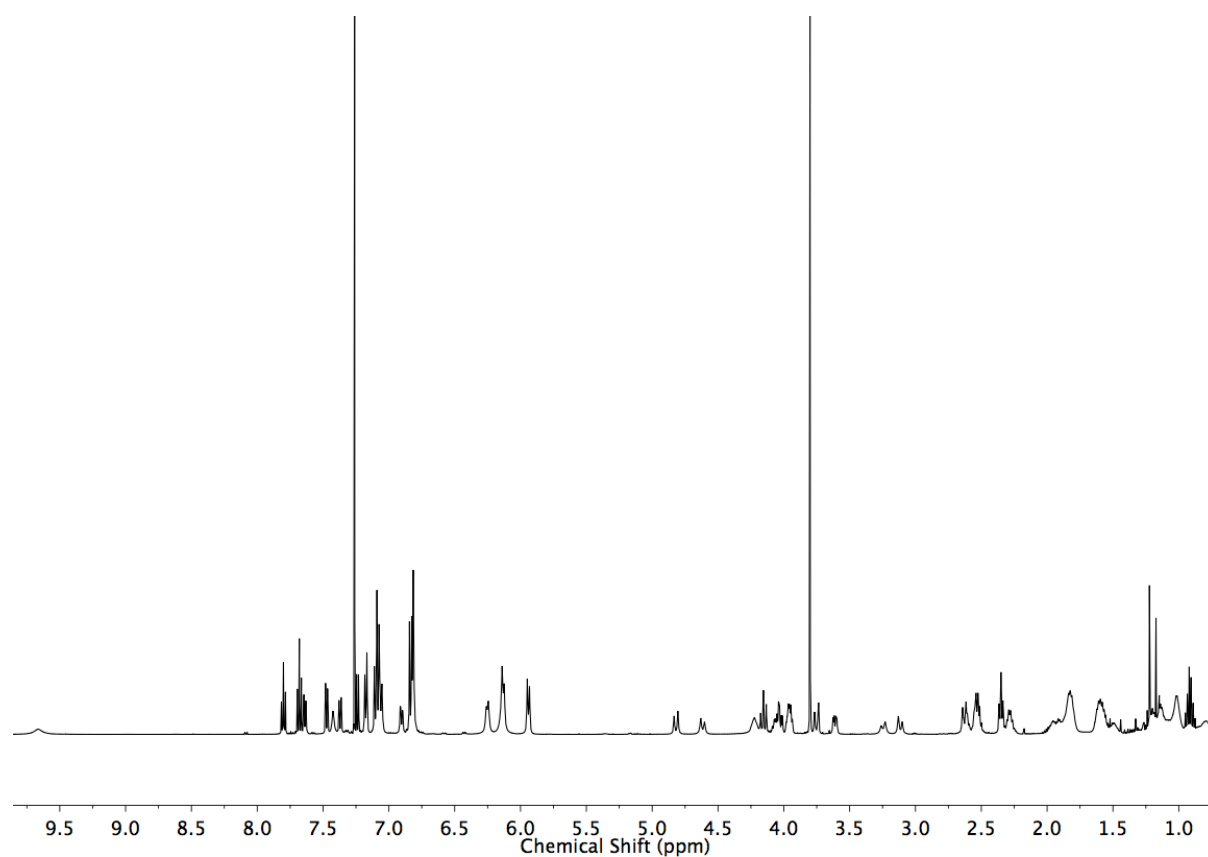


Figure S71 ^1H NMR (500 MHz, CDCl_3) of (*R,R_{mt}*)-**3b**.

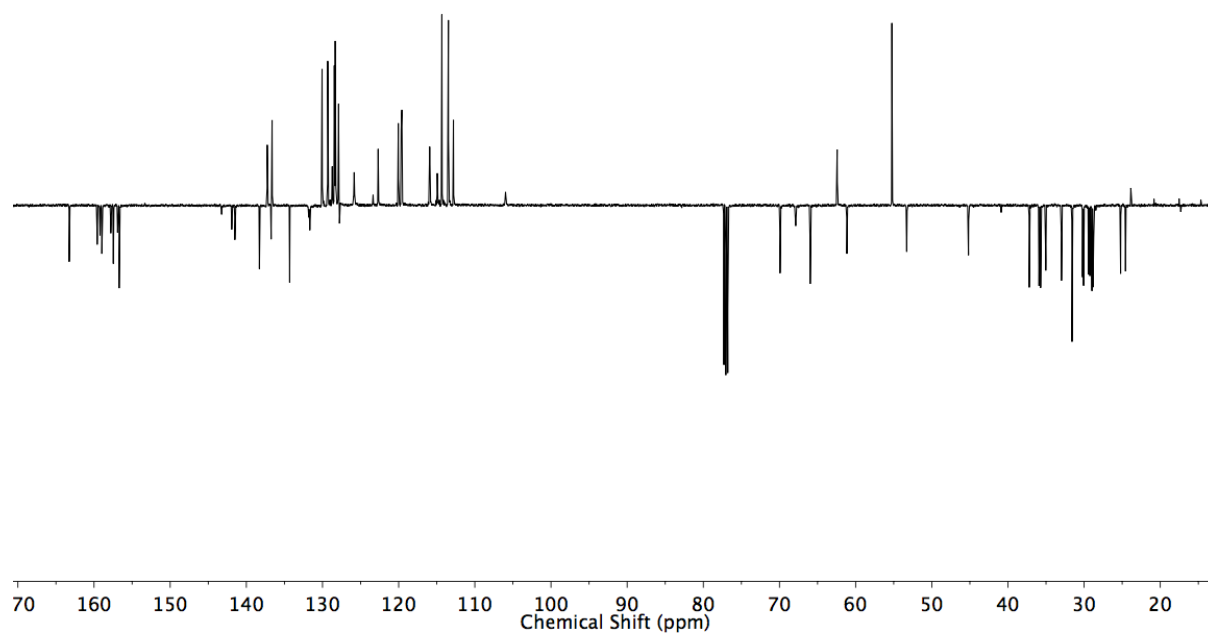


Figure 72 JMOD NMR (126 MHz, CDCl_3) of (R,R_{mt}) -**3b**.

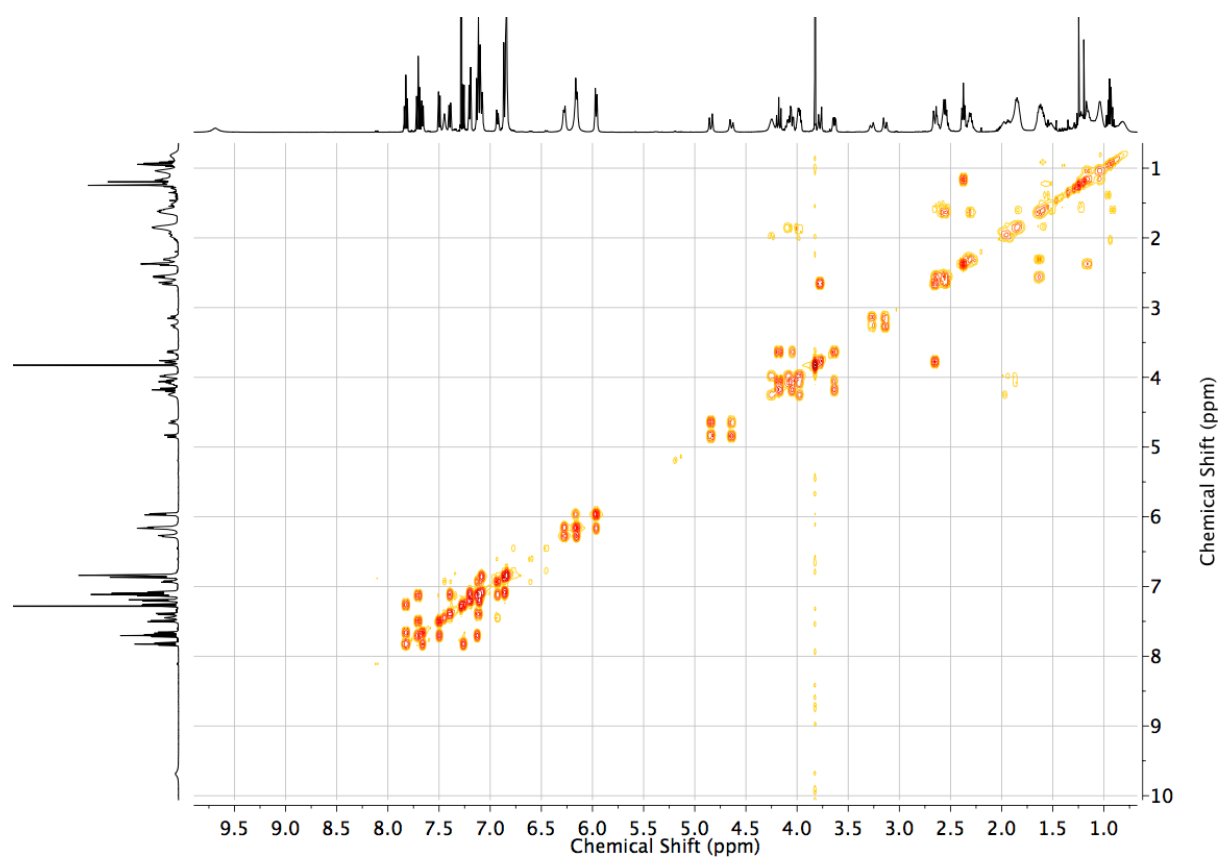


Figure S73 COSY NMR (CDCl_3) of (R,R_{mt}) -**3b**.

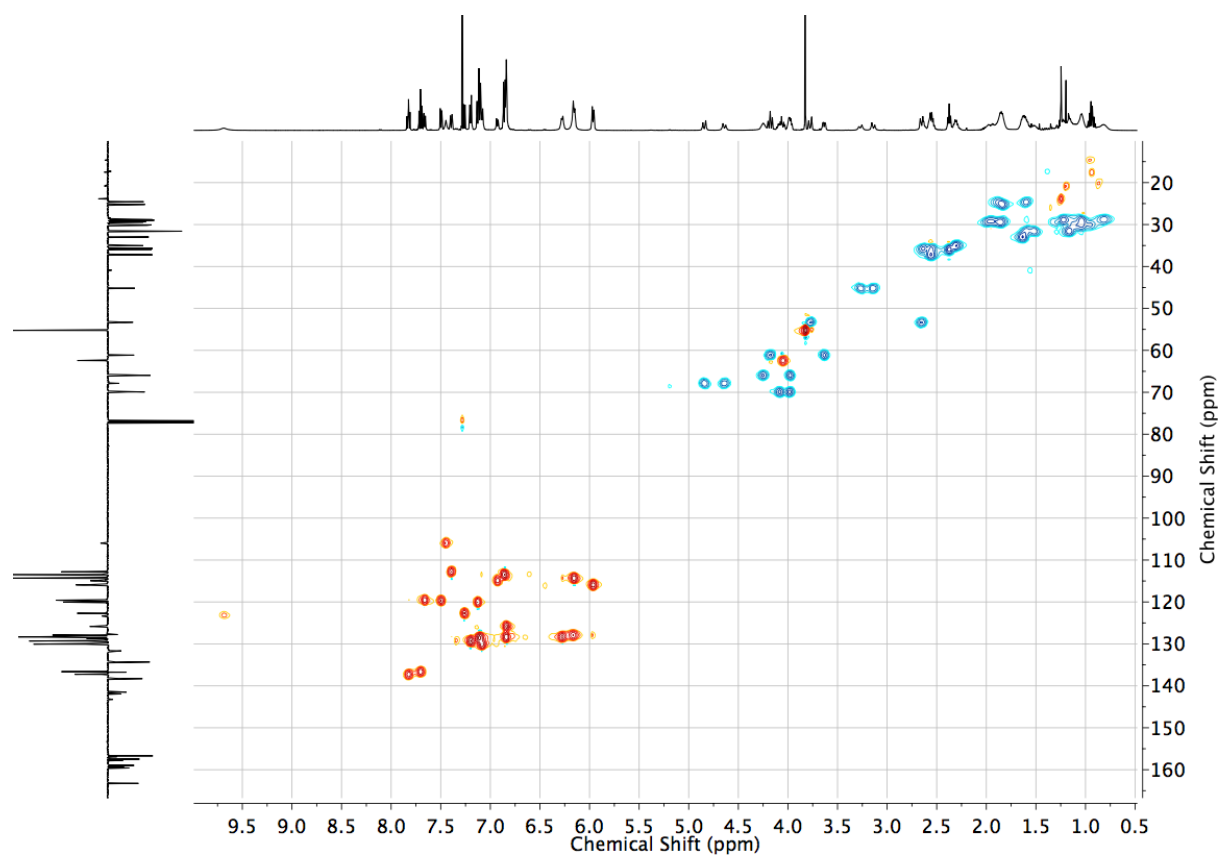


Figure S74 HSQC NMR (CDCl₃) of (*R,R_{mt}*)-**3b**.

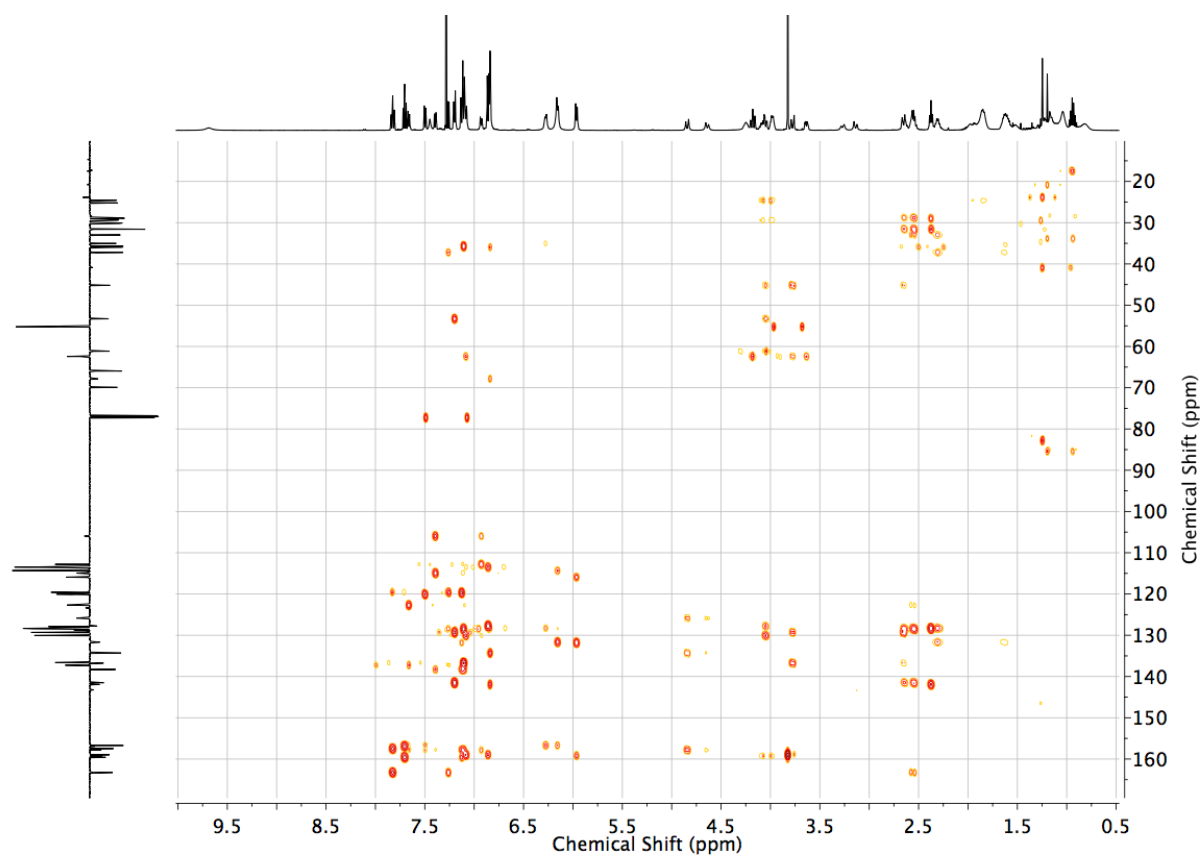


Figure S75 HMBC NMR (CDCl₃) of (*R,R_{mt}*)-**3b**.

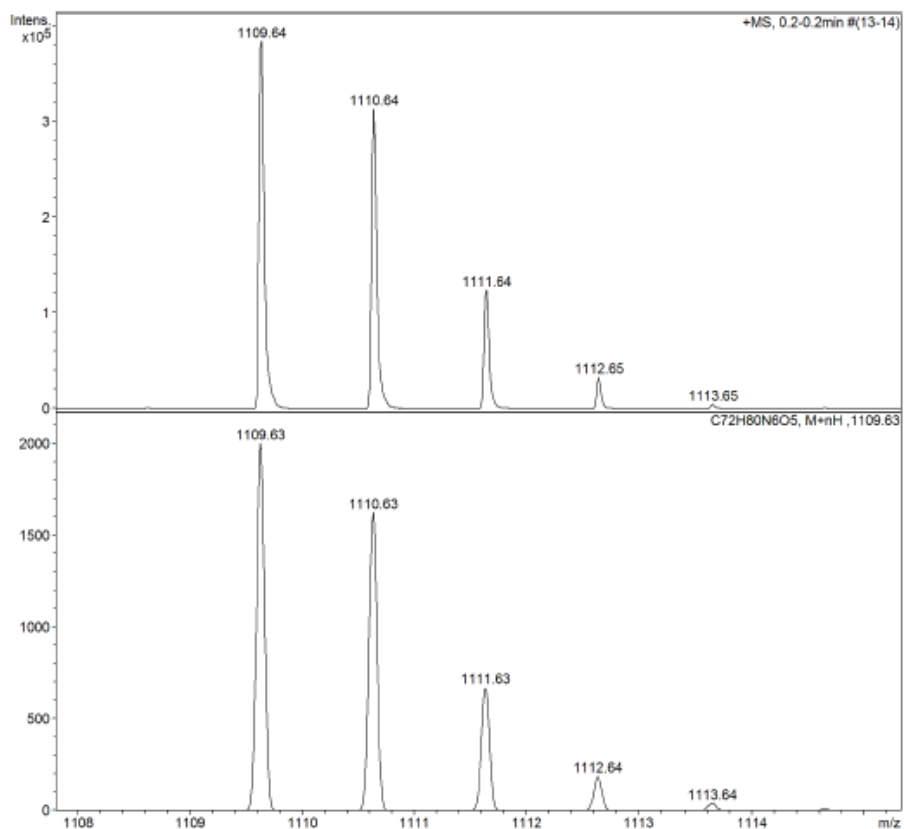


Figure S76 Observed (top) and calculated (bottom) isotopic patterns for (R,R_{mt}) -**3b**.

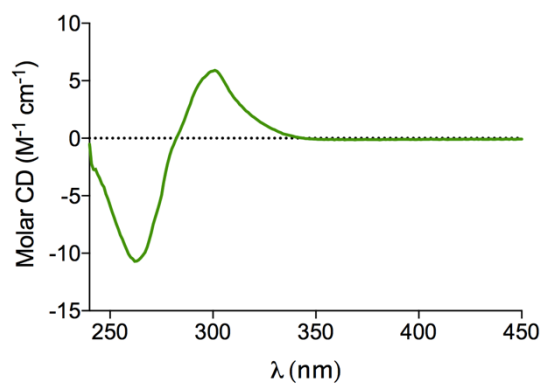
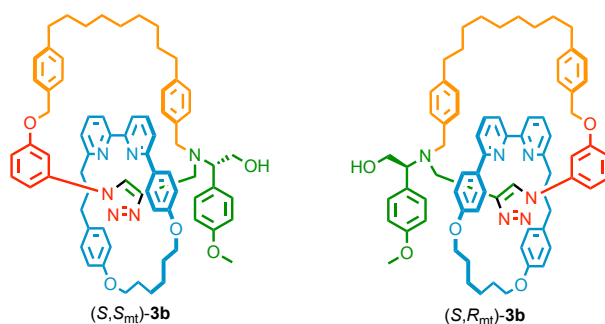


Figure S77 Circular dichroism spectrum of (R,R_{mt}) -**3b** (35.0 μ M in CHCl₃, 293 K).



(S,S_{mt})-**3b** and (S,R_{mt})-**3b**

To a solution of **2b** (288 mg, 0.62 mmol, 1.0 eq.), [Cu(CH₃CN)₄]PF₆ (231 mg, 0.62 mmol, 1.0 eq.), *i*Pr₂NEt (218 μ L, 1.24 mmol, 2 eq.) in 1:1 CHCl₃/EtOH (25 mL) at 60 °C was added (S)-**1** (400 mg, 0.62 mmol, 1.2 eq.) in 1:1 CHCl₃/EtOH (24 mL) over 4 h. After removal of the solvent *in vacuo*, the residue was dissolved in 1:1 CH₂Cl₂/MeOH (20 mL) and KCN (320 mg, 5 mmol, 8 eq.) added as a solid. After stirring at r.t. for 30 minutes the solvent was removed under a flow of air. The residue was dissolved in CH₂Cl₂ (100 mL) and washed with H₂O (4 \times 20 mL), dried (MgSO₄) and the solvent removed *in vacuo*. The residue containing catenane (S,R/S_{mt})-**3b** (in a 0.67:0.33 diastereoisomeric ratio) was purified by column chromatography on silica (Petrol/CH₂Cl₂/EtOAc/Et₂O 140/30/15/15), to yield (S,R_{mt})-**3b** (300 mg, 44%) and (S,S_{mt})-**3b** (200 mg, with 3% of (S,R_{mt})-**3b**, 30%) as a white foams. Spectroscopic data were identical to those reported for (R,S_{mt})-**3b** and (R,R_{mt})-**3b** respectively with the exception of the circular dichroism spectra.

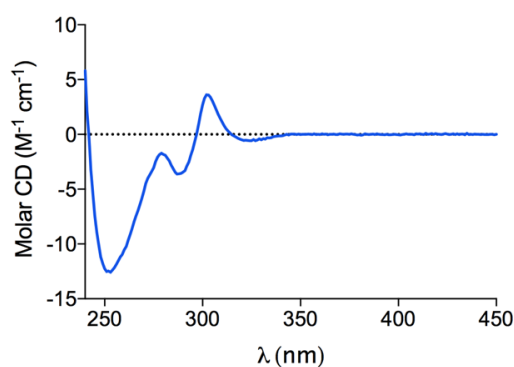


Figure S78 Circular dichroism spectrum of (S,R_{mt})-**3b** (35.0 μ M in CHCl₃, 293K).

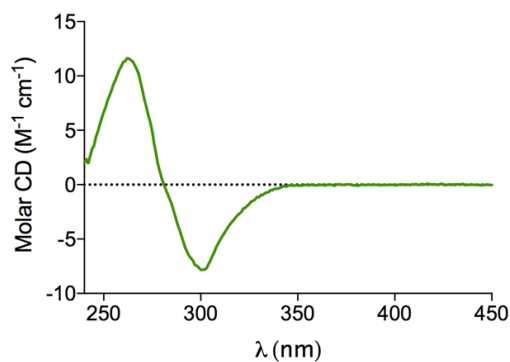
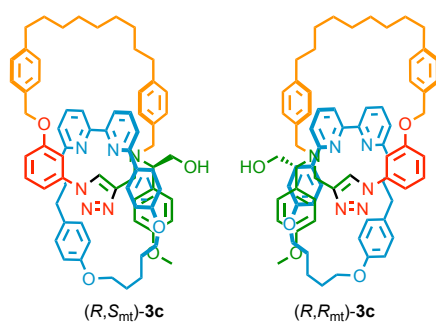


Figure S79 Circular dichroism spectrum of (S,S_{mt})-**3b** (35.0 μ M in CHCl₃, 293 K).



(R,R/S_{mt})-**3c**

To a solution of **2c** (11.3 mg, 0.025 mmol, 1 eq.), [Cu(CH₃CN)₄]PF₆ (8.9 mg, 0.024 mmol, 0.96 eq.), ⁱPr₂NEt (9 μL, 0.050 mmol, 2 eq.) in 1:1 CHCl₃/EtOH (2.5 mL) at 60 °C was added (*R*)-**1** (16.1 mg, 0.025 mmol, 1 eq.) in 1:1 CHCl₃/EtOH (1.0 mL) over 4 h. After removal of the solvent *in vacuo*, the residue was dissolved in 1:1 CH₂Cl₂/MeOH (2.5 mL) and KCN (16 mg, 0.25 mmol, 10 eq.) added as a solid. After stirring at r.t. for 30 minutes the solvent was removed under a flow of air. The residue was dissolved in CH₂Cl₂ (5 mL) and washed with H₂O (4 × 5 mL), dried (MgSO₄) and the solvent removed *in vacuo*. Low conversion of **2c** was observed (~23%). The residue containing catenane (R,R/S_{mt})-**3c** in a 1:1 diastereoisomeric ratio (Figure S80) was not purified.

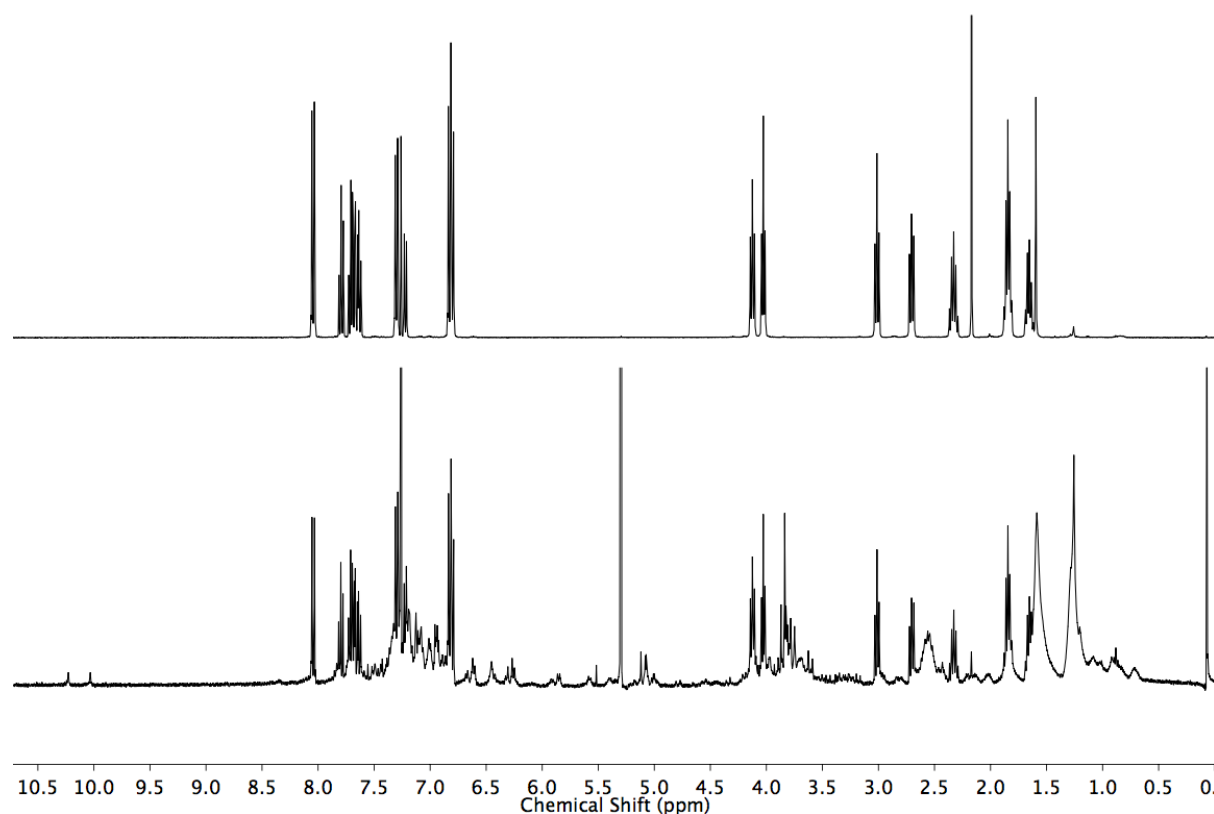
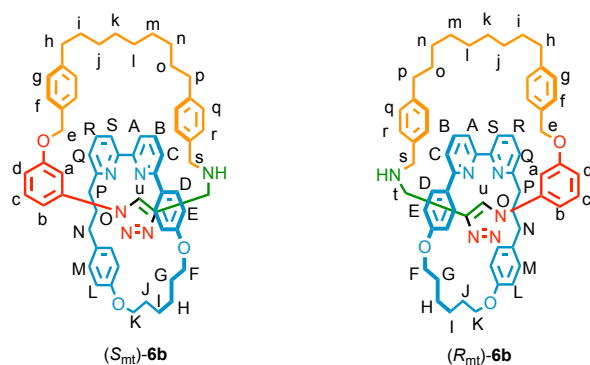


Figure S80 Stacked partial ¹H NMR (400 MHz, CDCl₃) spectra of **2c** (top) and crude **3c** reaction mixture.



rac-**6b**

To a solution of **2b** (23.2 mg, 0.050 mmol, 1 eq.), [Cu(CH₃CN)₄]PF₆ (18.5 mg, 0.0495 mmol, 0.99 eq.), iPr₂N₂Et (18 μL, 0.10 mmol, 2 eq.) in 1:1 CHCl₃/EtOH (5.0 mL) at 60 °C was added **S11** (24.0 mg, 0.060 mmol, 1.2 eq.) in 1:1 CHCl₃/EtOH (2.4 mL) over 4 h. After removal of the solvent *in vacuo*, the residue was dissolved in 1:1 CH₂Cl₂/MeOH (2.5 mL) and KCN (16 mg, 0.25 mmol, 10 eq.) added as a solid. After stirring at r.t. for 30 minutes the solvent was removed under a flow of air. The residue was dissolved in CH₂Cl₂ (5 mL) and washed with H₂O (4 × 5 mL), dried (MgSO₄) and the solvent removed *in vacuo*. After purification by column chromatography on silica (CH₂Cl₂ with a gradient of 0 to 50% EtOAc) *rac*-**6b** was obtained as a white foam (33.0 mg, 70%). ¹H NMR (500 MHz, CDCl₃) **δ**: 9.29 (s, 1H, H_u), 7.56 (t, *J* = 7.8 Hz, 1H, H_R), 7.43-7.36 (m, 2H, H_B, H_a or H_b or H_c or H_d), 7.30 (m, 1H, H_a or H_b or H_c or H_d), 7.23 (dd, *J* = 5.1, 3.5 Hz, 1H, H_A), 7.21-7.12 (m, 3H, H_C, H_O, H_S), 7.03-6.96 (m, 5H, H_q, H_r, H_a or H_b or H_c or H_d), 6.90 (d, *J* = 7.6 Hz, 2H, H_i), 6.88-6.83 (m, 2H, H_a or H_b or H_c or H_d), 6.79 (d, *J* = 8.0 Hz, 2H, H_g), 6.68 (d, *J* = 6.6 Hz, 2H, H_D), 6.44 (d, *J* = 7.9 Hz, 2H, H_M), 6.40 (d, *J* = 8.7 Hz, 2H, H_E), 6.33 (d, *J* = 8.7 Hz, 2H, H_I), 4.71 (m, 2H, H_e), 4.21-4.02 (m, 4H, H_F, H_K), 3.45 (d, *J* = 11.6 Hz, 1H, 1 of H_s), 3.36 (d, *J* = 12.1 Hz, 1H, 1 of H_s), 3.30 (d, *J* = 11.3 Hz, 1H, 1 of H_t), 3.13 (d, *J* = 11.8 Hz, 1H, 1 of H_t), 2.64 (td, *J* = 13.6, 4.9 Hz, 1H, 1 of H_p or H_N), 2.52 (t, *J* = 7.1 Hz, 2H, H_h or H_p), 2.50-2.42 (m, 3H, H_h or H_p), 2.40-2.28 (m, 3H, H_p or H_N), 1.94-1.87 (m, 2H, H_G or H_J), 1.86-1.78 (m, 2H, H_G or H_J), 1.76-1.51 (m, 6H, H_H, H_I, H_O), 1.48-1.31 (m, 4H, H_i, H_O), 1.21-1.04 (m, 8H, H_j, H_k, H_m, H_n), 1.04-0.80 (m, 2H, H_l). ¹³C NMR (126 MHz, CDCl₃) **δ** 163.0, 159.4, 158.8 (×2), 157.3, 156.8, 156.7, 142.3, 140.7 [assigned by HMBC analysis], 138.3, 137.0, 136.6, 134.2, 132.5 (×2), 129.5, 128.9, 128.7 [assigned by HMBC analysis] 128.5 (×2), 128.4 (×2), 127.9, 127.1, 122.2, 120.3, 120.0, 119.3, 116.1, 114.2, 113.4, 112.1, 106.7, 105.4, 69.4, 69.3, 66.1, 53.7, 44.9, 36.9, 35.7, 35.5, 35.1, 32.3, 31.7, 31.4, 30.3, 30.2, 29.4, 29.3, 29.2, 28.9, 28.7, 25.3, 24.9. HR-ESI-MS *m/z* = 959.5591 [M+H]⁺ (calc. for C₆₃H₇₁N₆O₃ 959.5582).

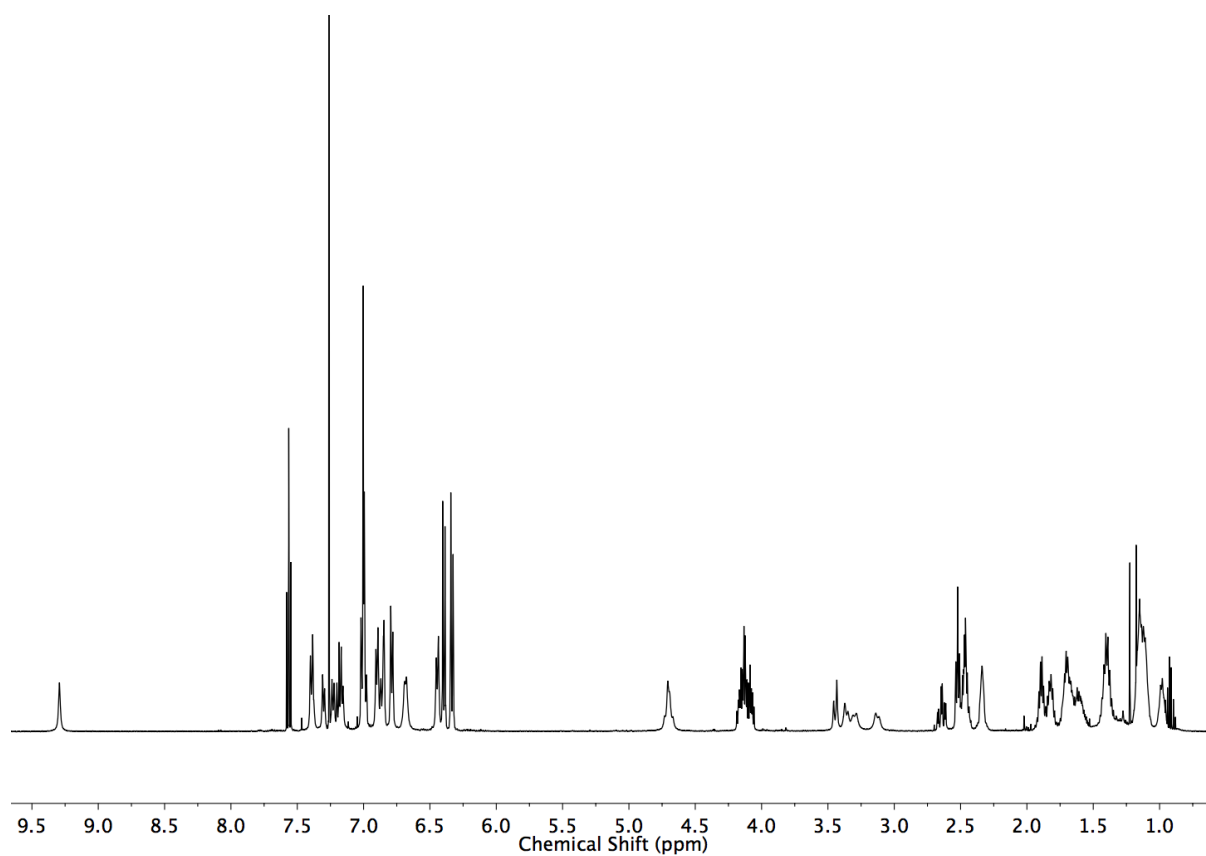


Figure S81 ^1H NMR (500 MHz, CDCl_3) of **6b**.

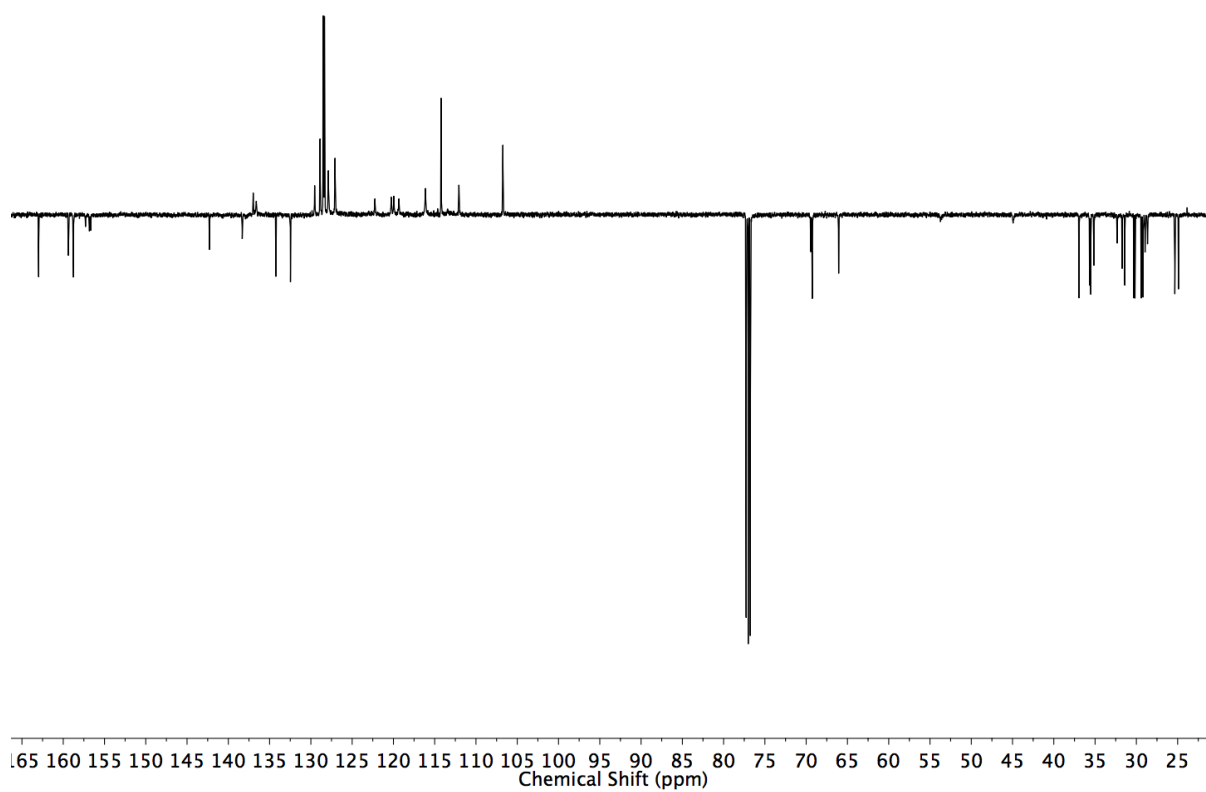


Figure S82 JMOD NMR (126 MHz, CDCl_3) of **6b**.

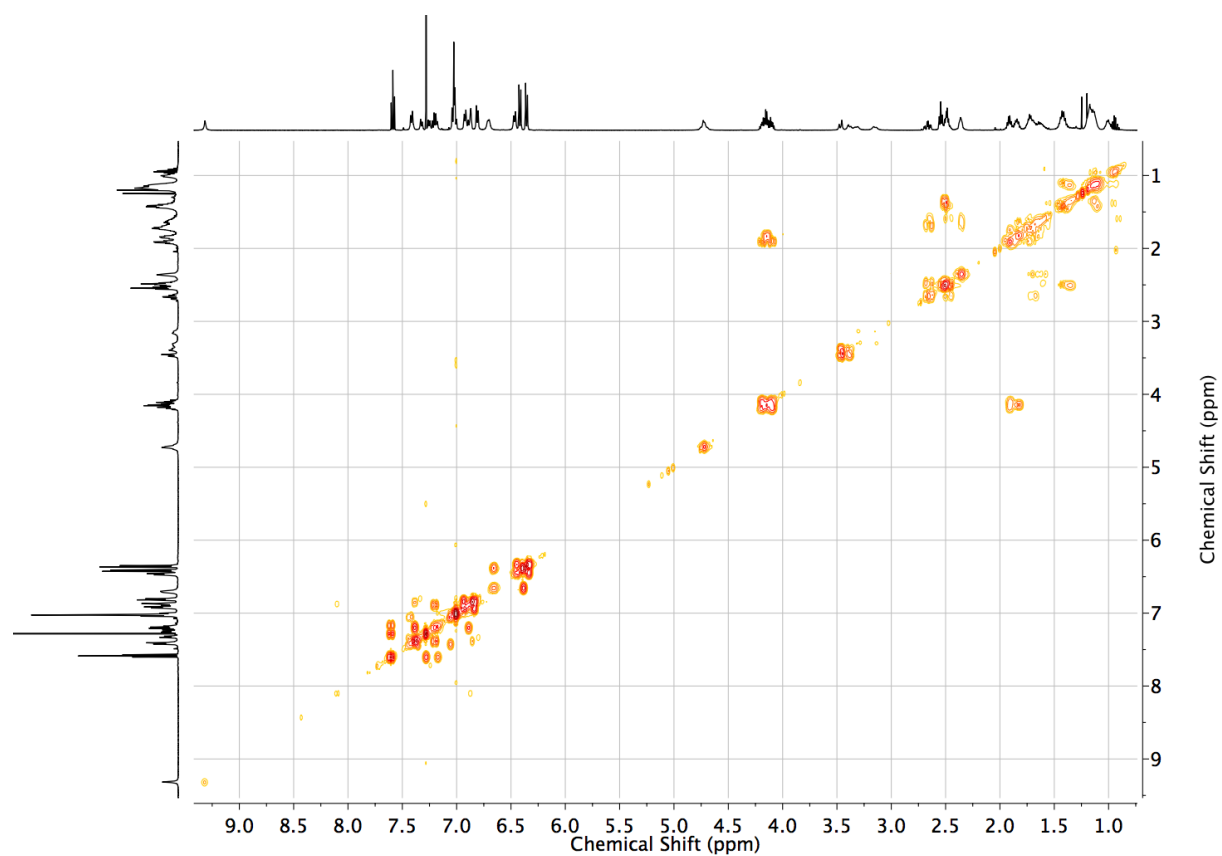


Figure S83 COSY NMR (CDCl₃) of **6b**.

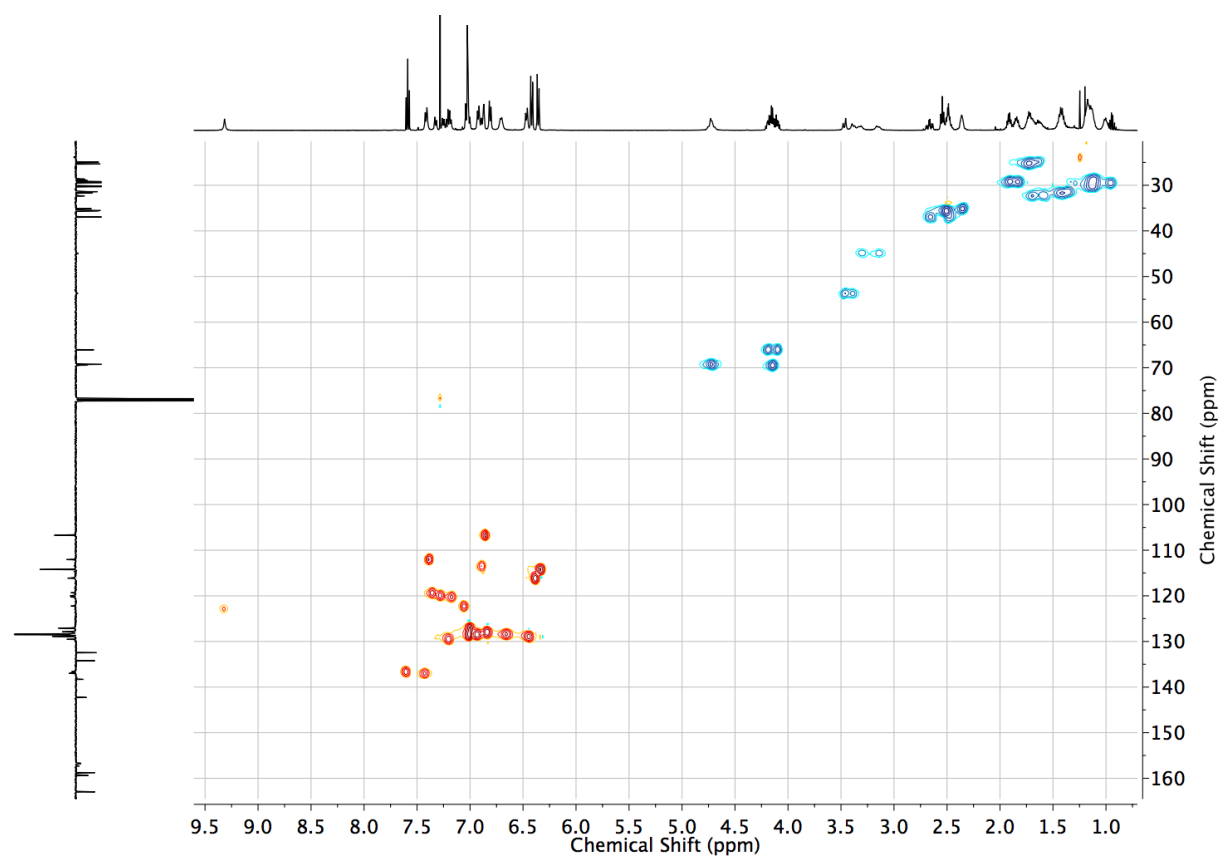


Figure S84 HSQC NMR (CDCl₃) of **6b**.

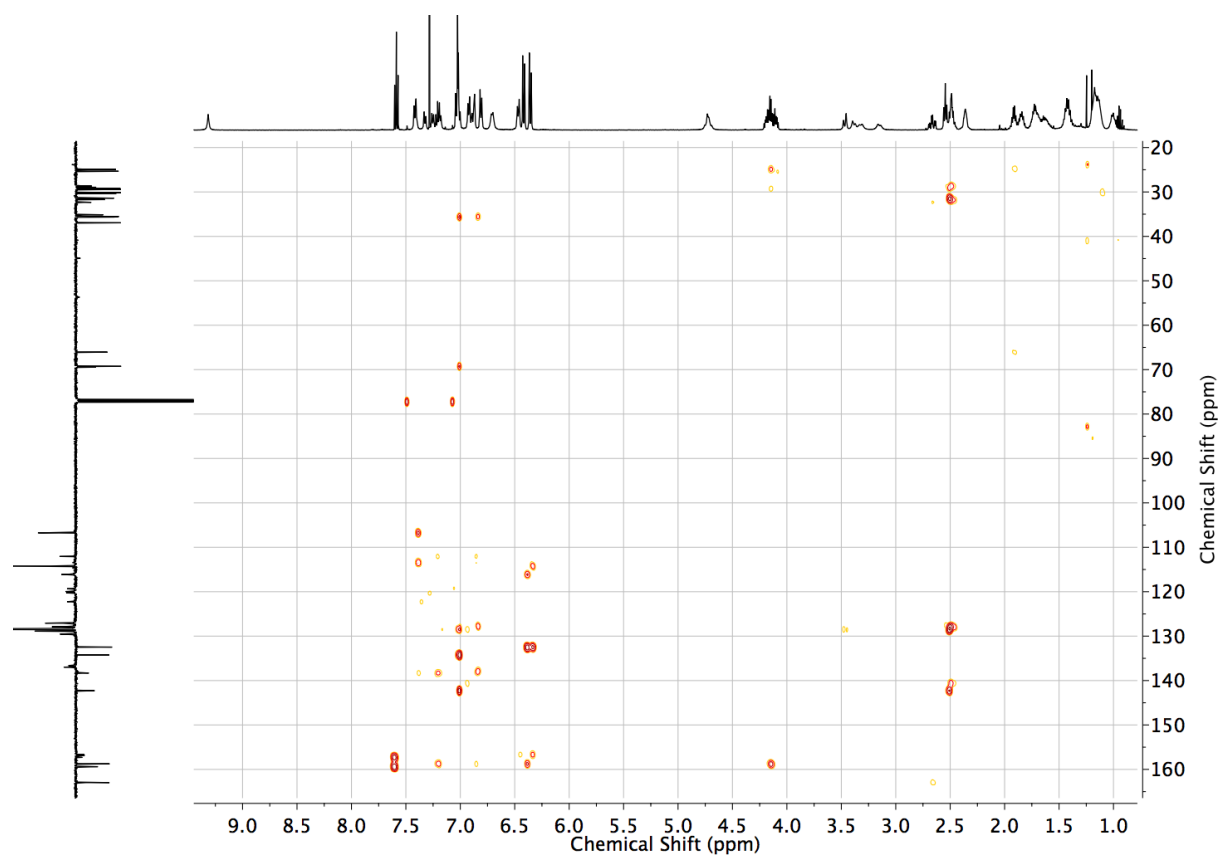


Figure S85 HMBC NMR (CDCl_3) of **6b**.

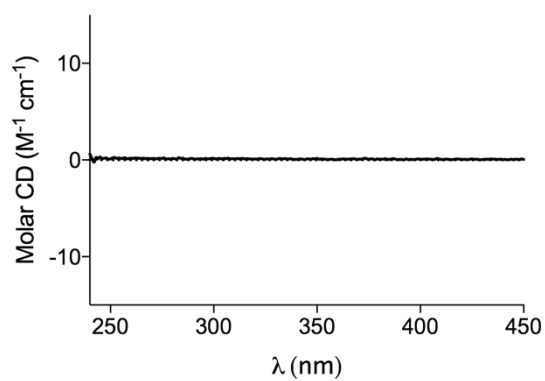
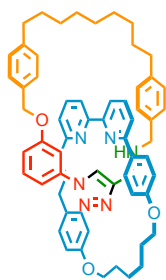


Figure S86 Circular dichroism spectrum of *rac*-**6b** (43.0 μM in CHCl_3 , 293 K).



(*S_{mt}*)-**6b**

To a solution of oxalyl chloride (140 μ L, 1.60 mmol, 1.2 eq.) in dry CH_2Cl_2 (3 mL) at -78°C was added DMSO (230 μ L, 3.25 mmol, 2.4 eq.). The mixture was stirred for 10 minutes at -78°C before 0.67 mL of the activated DMSO solution was added to (*R,S_{mt}*)-**3b** (150 mg, 0.135 mmol, 1 eq.) in dry CH_2Cl_2 (5 mL) at -78°C . NEt_3 (91 μ L, 0.65 mmol, 4.8 eq.) was added at -78°C . The mixture was warmed to r.t. and stirred at r.t. for 1 h. The reaction mixture was diluted with CH_2Cl_2 (50 mL) and washed with a saturated solution of NaHCO_3 (aq) (20 mL), dried (MgSO_4) and the solvent removed *in vacuo*. The residue was dissolved in CHCl_3 (5 mL), AcOH (1 mL) was added and the mixture was stirred for 3 h at r.t. The solvent was removed *in vacuo*. The residue was dissolved in CH_2Cl_2 (100 mL) and washed with NaHCO_3 (20 mL), dried (MgSO_4) and the solvent removed *in vacuo*. After purification by column chromatography on silica (CH_2Cl_2 with a gradient of 0 to 50% EtOAc) (*S_{mt}*)-**6b** was obtained as a white foam (89.0 mg, 68% over 2 steps). HPLC: RegisCell (hexane/*i*-PrOH, 98:2), flow rate $0.5\text{ mL}\cdot\text{min}^{-1}$, $t_{\text{major}} = 26.5$, ee = 98.5%. Spectroscopic data were identical to those reported for *rac*-**6b** with the exception of the circular dichroism spectra.

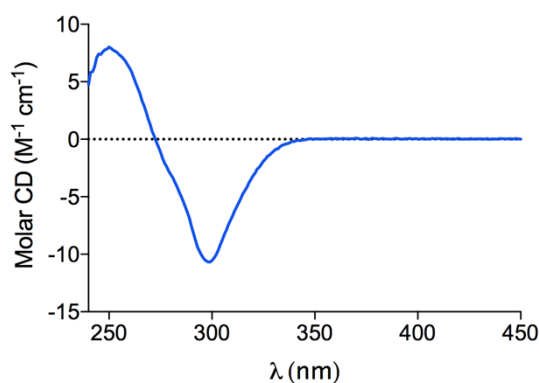
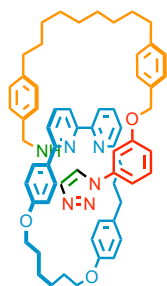


Figure S87 Circular dichroism spectrum of (*S_{mt}*)-**6b** (43.0 μM in CHCl_3 , 293 K).



(*R_{mt}*)-**6b**

An identical procedure to that for (*S_{mt}*)-**6b** but employing (*S,R_{mt}*)-**3b** (290 mg, 0.27 mmol), oxalyl chloride (50 μ L, 0.60 mmol, 2.2 eq.), DMSO (85 μ L, 1.20 mmol, 4.4 eq.) and NEt₃ (167 μ L, 1.20 mmol, 4.4 eq.) afforded (*R_{mt}*)-**6b** as a white foam (120 mg, 50% over 2 steps). HPLC: RegisCell (hexane/*i*-PrOH, 98:2), flow rate 0.5 mL.min⁻¹, t_{major} = 20.0, ee > 99%). Spectroscopic data were identical to those reported for *rac*-**6b** with the exception of the circular dichroism spectra.

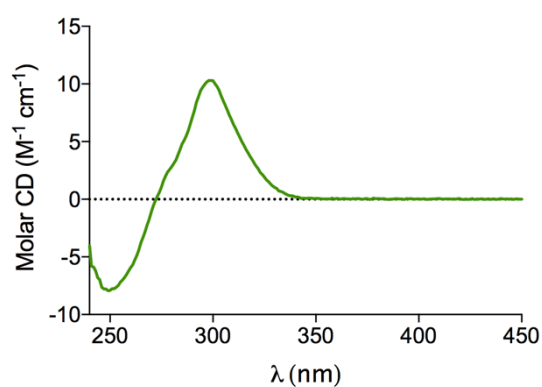
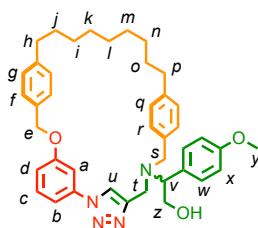


Figure S88 Circular dichroism spectrum of (*R_{mt}*)-**6b** (43.0 μ M in CHCl₃, 293 K).

5. Syntheses of triazole-functionalised macrocycles **S12** and **S13**



S12

To a solution of $[\text{Cu}(\text{CH}_3\text{CN})_4]\text{PF}_6$ (23.1 mg, 0.062 mmol, 0.98 eq.), $i\text{Pr}_2\text{NEt}$ (27 μL , 0.15 mmol, 2.4 eq.) in 1:1 $\text{CHCl}_3/\text{EtOH}$ (6.2 mL) at 60 °C was added **1** (40.0 mg, 0.062 mmol, 1.0 eq.) in 1:1 $\text{CHCl}_3/\text{EtOH}$ (2.4 mL) over 4 h. After removal of the solvent *in vacuo*, the residue was dissolved in CH_2Cl_2 (20 mL) and washed with EDTA-NH_3 (2 \times 10 mL), dried (MgSO_4) and the solvent removed *in vacuo*. After purification by column chromatography on silica (Petrol/ CH_2Cl_2 1/1 with a gradient from 0 to 20% EtOAc) **S12** was obtained as a white foam (30.0 mg, 75%). ^1H NMR (500 MHz, CDCl_3) **S12**: 7.69 (s, 1H, H_u), 7.54-7.41 (m, 2H, H_c , H_b or H_d), 7.32 (d, $J = 8.2$, 2H, H_i), 7.27 (d, $J = 8.8$, 2H, H_w), 7.21 (d, $J = 8.0$, 2H, H_r), 7.17 (d, $J = 8.4$, 2H, H_g), 7.12 (d, $J = 8.2$, 2H, H_q), 7.08 (dt, $J = 2.4$, 1.0, 1H, H_a), 7.07-7.04 (m, 1H, H_b or H_d), 6.95 (d, $J = 8.8$, 2H, H_x), 5.12 (s, 2H, H_e), 4.12 (t, $J = 10.6$, 1H, 1 of H_2), 4.04 (dd, $J = 10.4$, 4.8, 1H, H_v), 3.95 (d, $J = 15.2$, 1H, 1 of H_t), 3.88 (d, $J = 13.4$, 1H, 1 of H_3), 3.84 (s, 3H, H_y), 3.68 (dd, $J = 10.8$, 4.7, 1H, 1 of H_2), 3.61 (d, $J = 14.6$, 1H, 1 of H_t), 3.18 (d, $J = 13.6$, 1H, 1 of H_3), 2.62 (td, $J = 6.7$, 2.4, 2H, H_h or H_p), 2.54 (t, $J = 7.7$, 2H, H_h or H_p), 1.64-1.50 (m, 4H, H_i , H_o), 1.22 (m, 10H, H_j , H_k , H_l , H_m , H_n). ^{13}C NMR (126 MHz, CDCl_3) **S12** 159.5 ($\times 2$), 147.5, 143.0, 142.1, 136.2, 133.5, 130.8, 130.5, 129.2, 128.8, 128.7, 128.1, 127.2, 120.4, 114.2, 113.9, 113.2, 108.3, 70.4, 63.6, 61.0, 55.4, 53.9, 44.7, 35.6, 35.5, 31.2, 30.9, 29.6, 29.2, 29.0, 28.9, 28.3. HR-ESI-MS $m/z = 645.3813$ [$\text{M}+\text{H}$] $^+$ (calc. for $\text{C}_{41}\text{H}_{49}\text{N}_4\text{O}_3$ 645.3799).

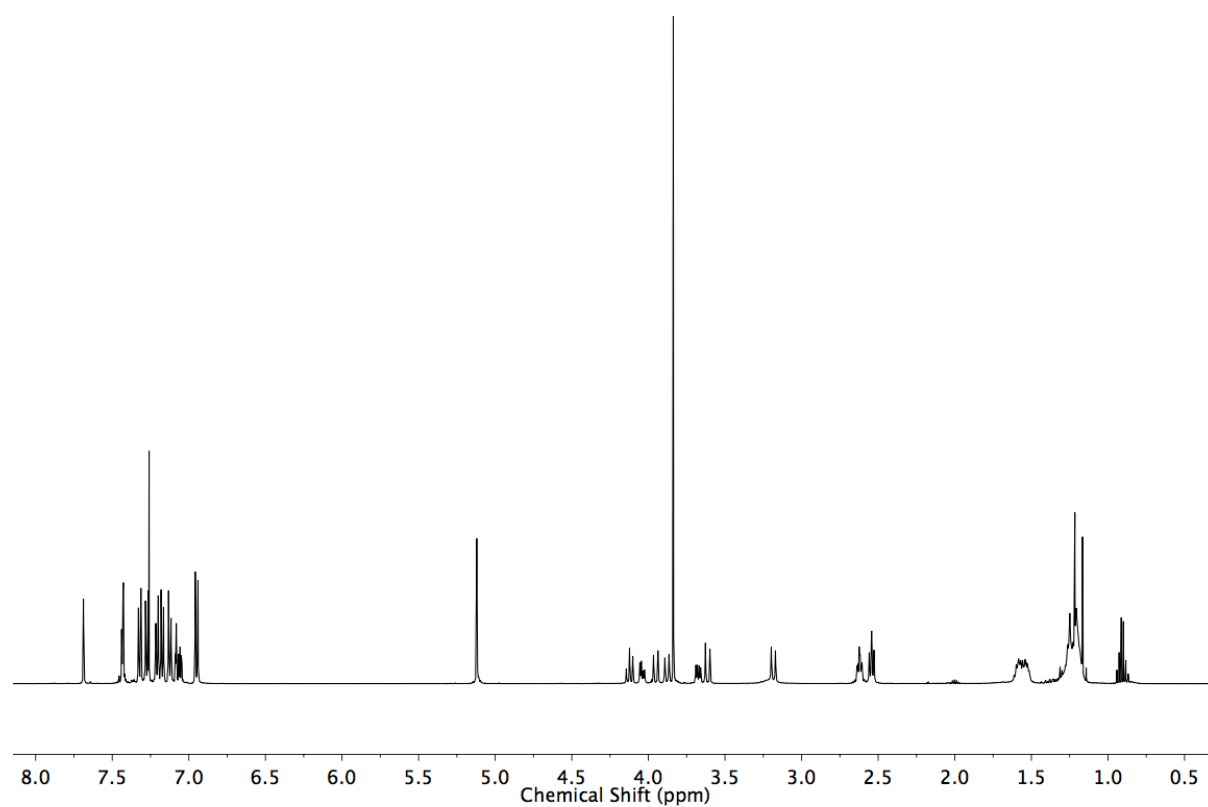


Figure S89 ^1H NMR (500 MHz, CDCl_3) of **S12**.

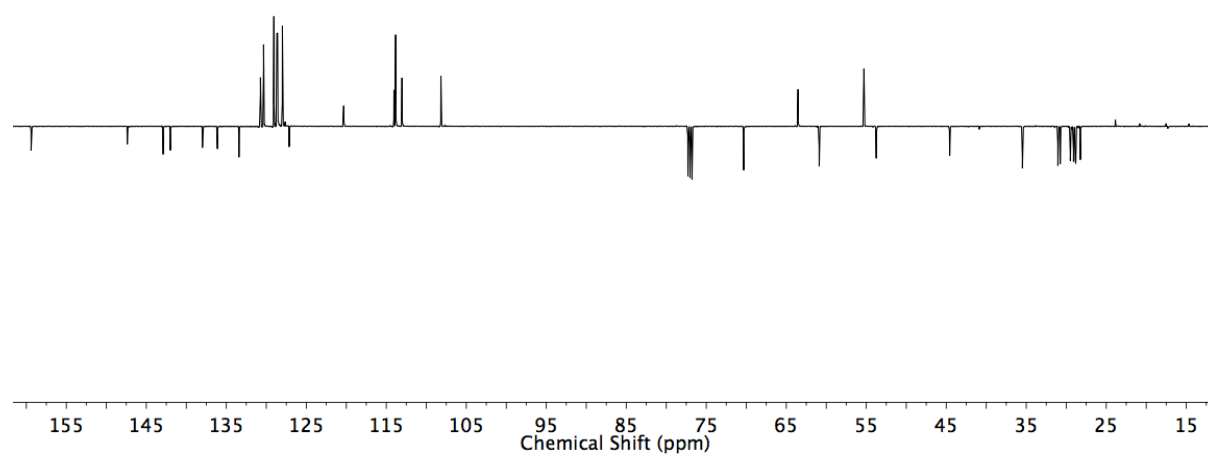


Figure S90 JMOD NMR (126 MHz, CDCl_3) of **S12**.

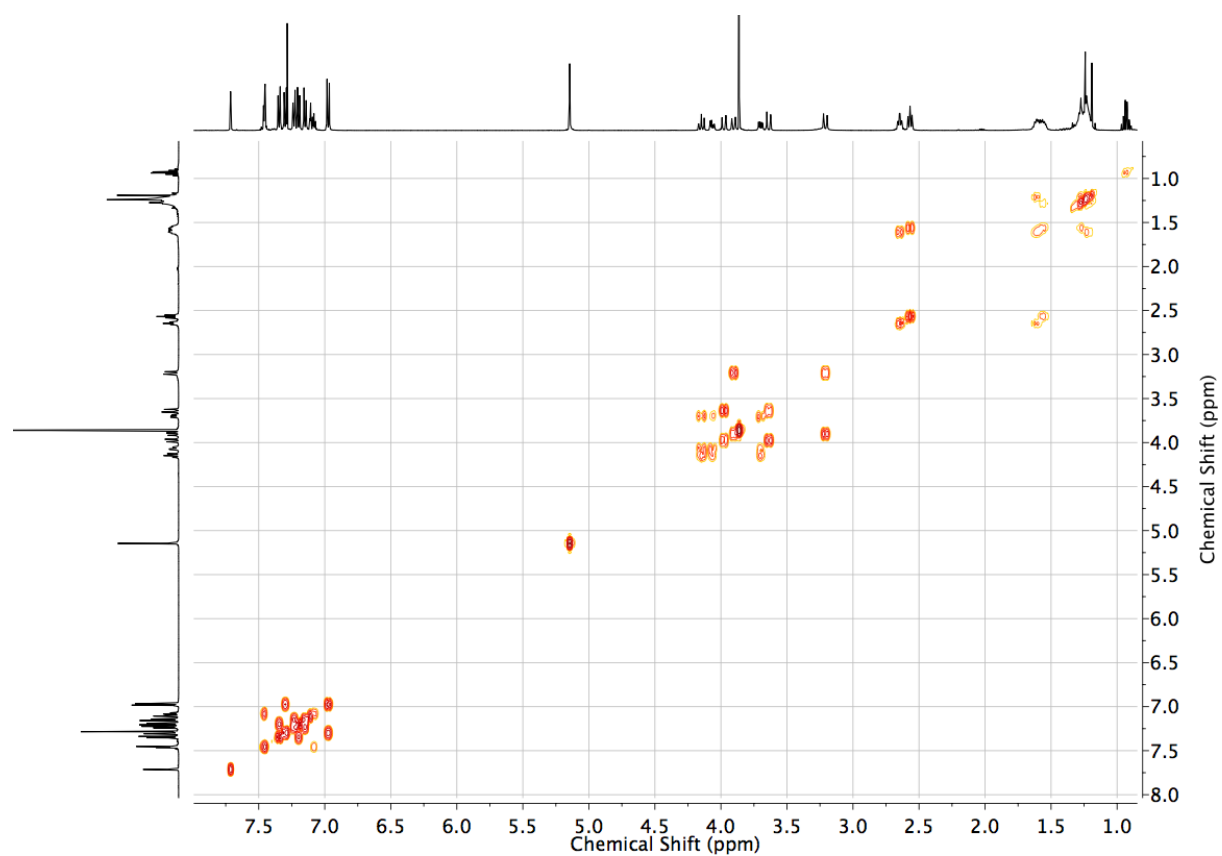


Figure S91 COSY NMR (CDCl_3) of **S12**.

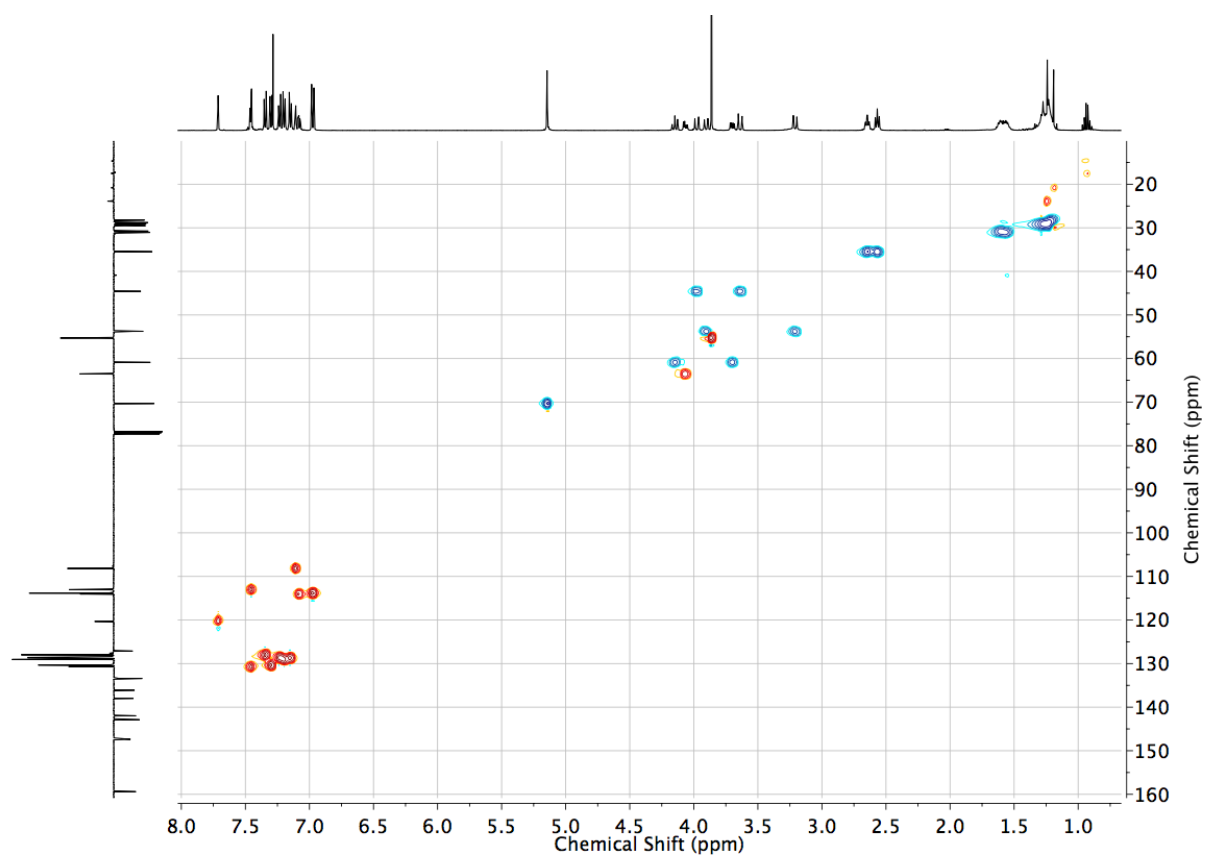


Figure S92 HSQC NMR (CDCl_3) of **S12**.

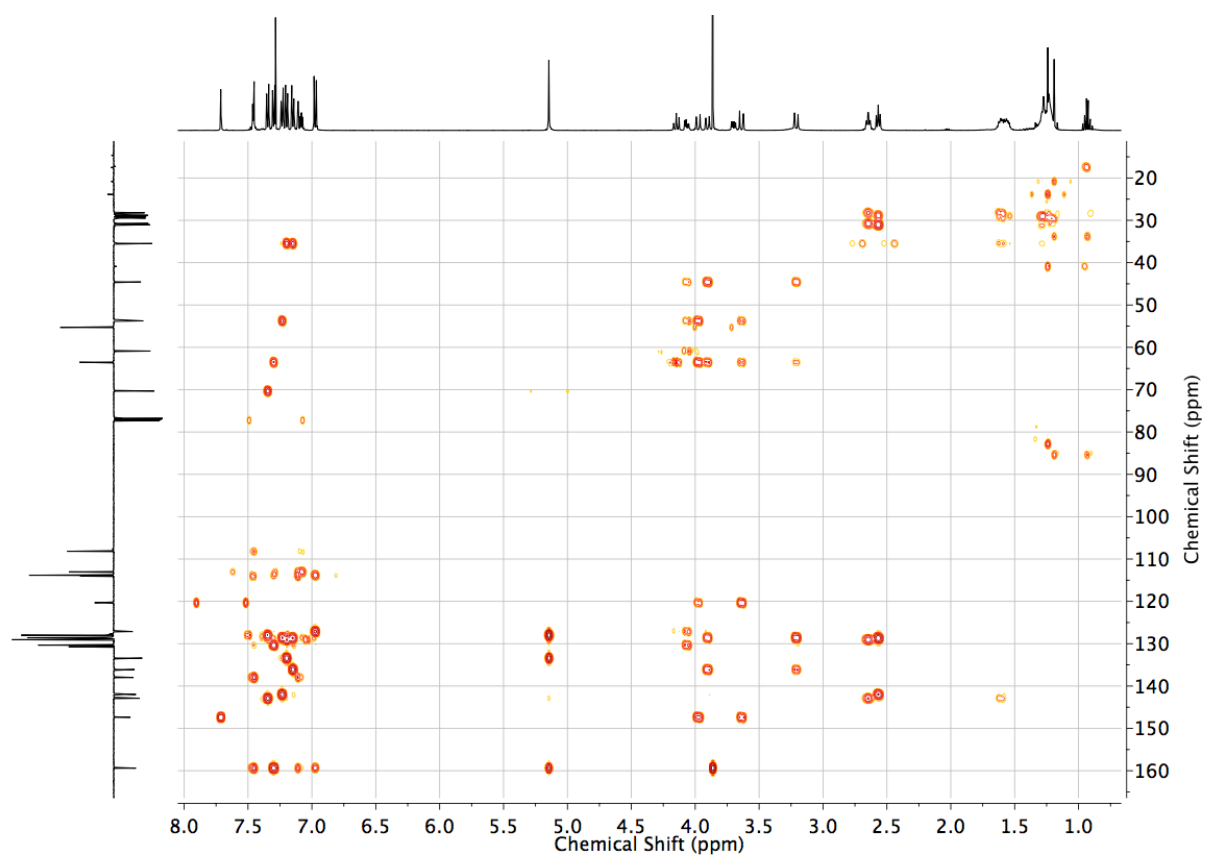
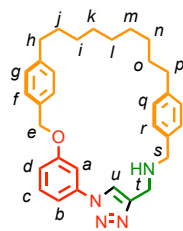


Figure S93 HMBC NMR (CDCl_3) of **S12**.



S13

To a solution of $[\text{Cu}(\text{CH}_3\text{CN})_4]\text{PF}_6$ (27.9 mg, 0.075 mmol, 0.98 eq.), $i\text{Pr}_2\text{NEt}$ (27 μL , 0.15 mmol, 2.0 eq.) in 1:1 $\text{CHCl}_3/\text{EtOH}$ (7.5 mL) at 60 $^\circ\text{C}$ was added **S11** (38.0 mg, 0.077 mmol, 1.0 eq.) in 1:1 $\text{CHCl}_3/\text{EtOH}$ (3.0 mL) over 4 h. After removal of the solvent *in vacuo*, the residue was dissolved in CH_2Cl_2 (20 mL) and washed with EDTA-NH_3 (2×10 mL), dried (MgSO_4) and the solvent removed *in vacuo*. After purification by column chromatography on silica (Petrol/ CH_2Cl_2 1/1 with a gradient from 0 to 50% EtOAc) **S13** was obtained as a white foam (12.0 mg, 32%). ^1H NMR (500 MHz, CDCl_3) **S13**: 7.73 (s, 1H, H_u), 7.44-7.41 (m, 2H, H_c , H_b or H_d), 7.27 (d, $J = 8.4$, 2H, H_l), 7.22 (d, $J = 8.4$, 2H, H_r), 7.14 (d, $J = 8.4$, 2H, H_g), 7.10 (d, $J = 8.4$, 2H, H_q), 7.08-7.04 (m, 1H, H_b or H_d), 7.00-6.97 (m, 1H, H_a), 5.13 (s, 2H, H_e), 4.04 (s, 2H, H_v), 3.82 (s, 2H, H_s), 2.57 (t, $J = 7.3$, 4H, H_h , H_p), 1.62-1.50 (m, 4H, H_i , H_o), 1.40-1.05 (m, 10H, H_j , H_k , H_l , H_m , H_n). ^{13}C NMR (126 MHz, CDCl_3) **S13**: 159.7, 148.1, 143.0, 141.7, 138.2, 137.2, 133.7, 130.8, 129.1, 128.8, 128.3, 127.6, 120.3, 115.1, 113.2, 107.8, 70.6, 53.4, 44.6, 35.7, 35.4, 31.2 ($\times 2$), 29.6 ($\times 2$), 29.2, 28.9, 28.4. HR-ESI-MS m/z 495.3123 $[\text{M}+\text{H}]^+$ (calc. for $\text{C}_{32}\text{H}_{39}\text{N}_4\text{O}$ 495.3118).

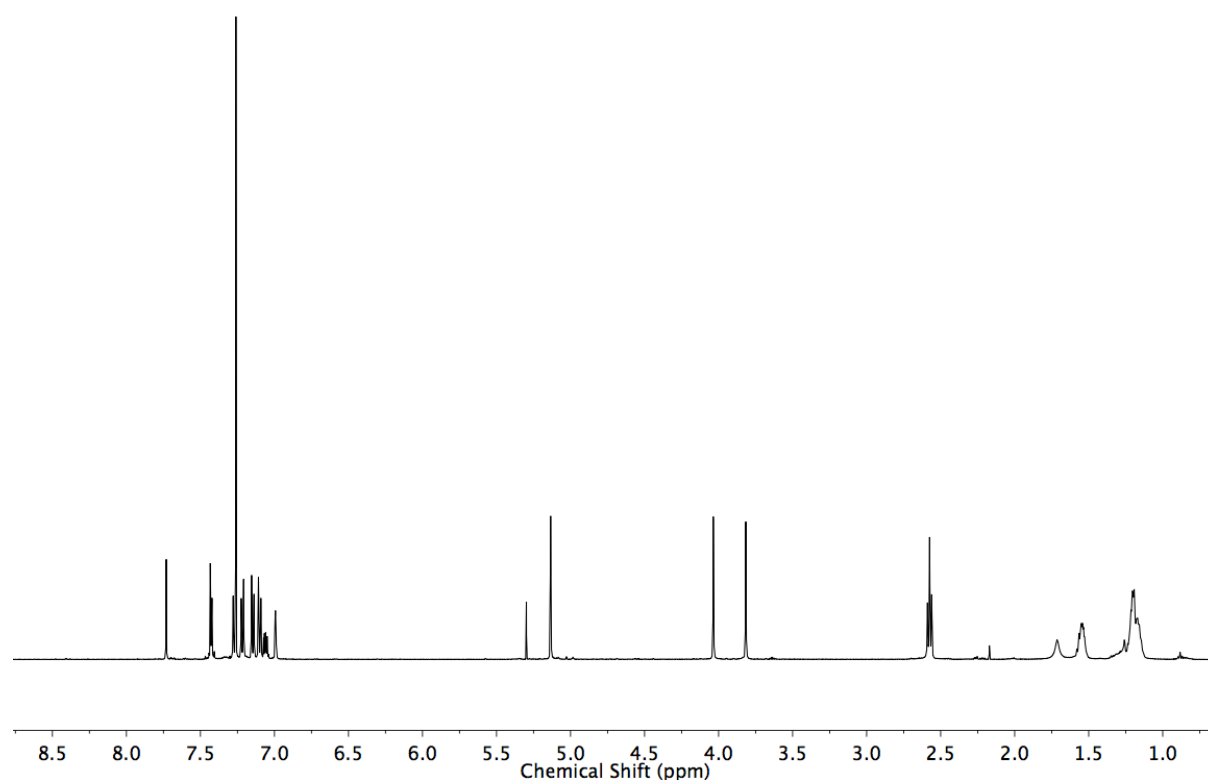


Figure S94 ^1H NMR (500 MHz, CDCl_3) of **S13**.

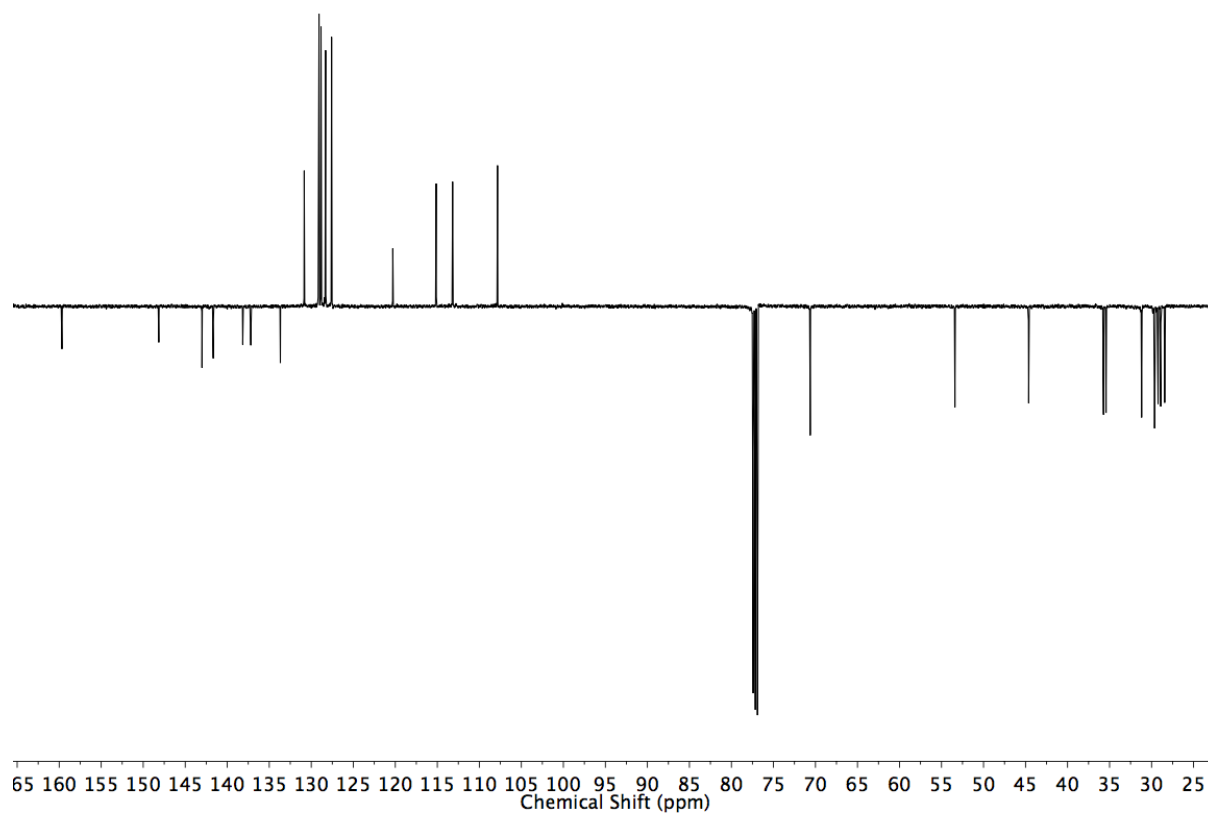


Figure S95 JMOD NMR (126 MHz, CDCl_3) of **S13**.

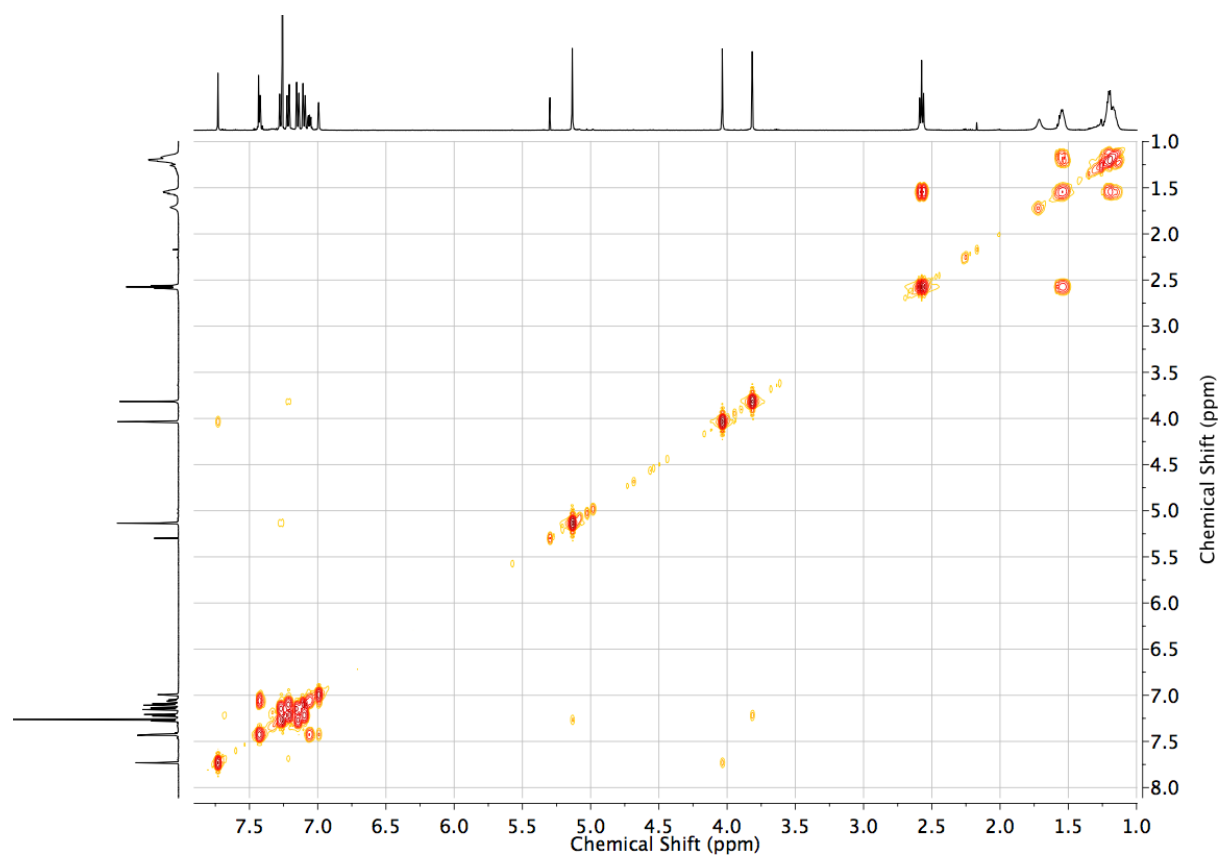


Figure S96 JMOD NMR (CDCl_3) of **S13**.

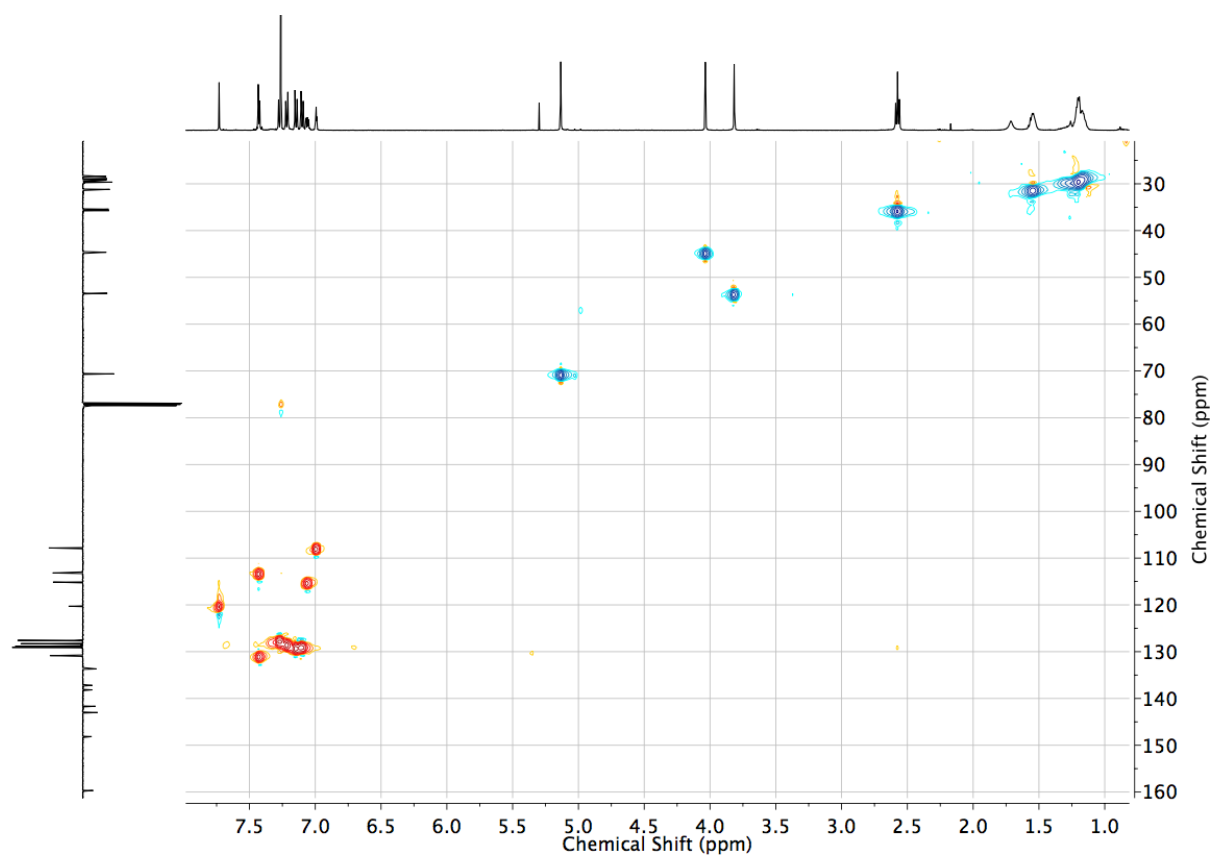


Figure S97 HSQC NMR (CDCl_3) of **S13**.

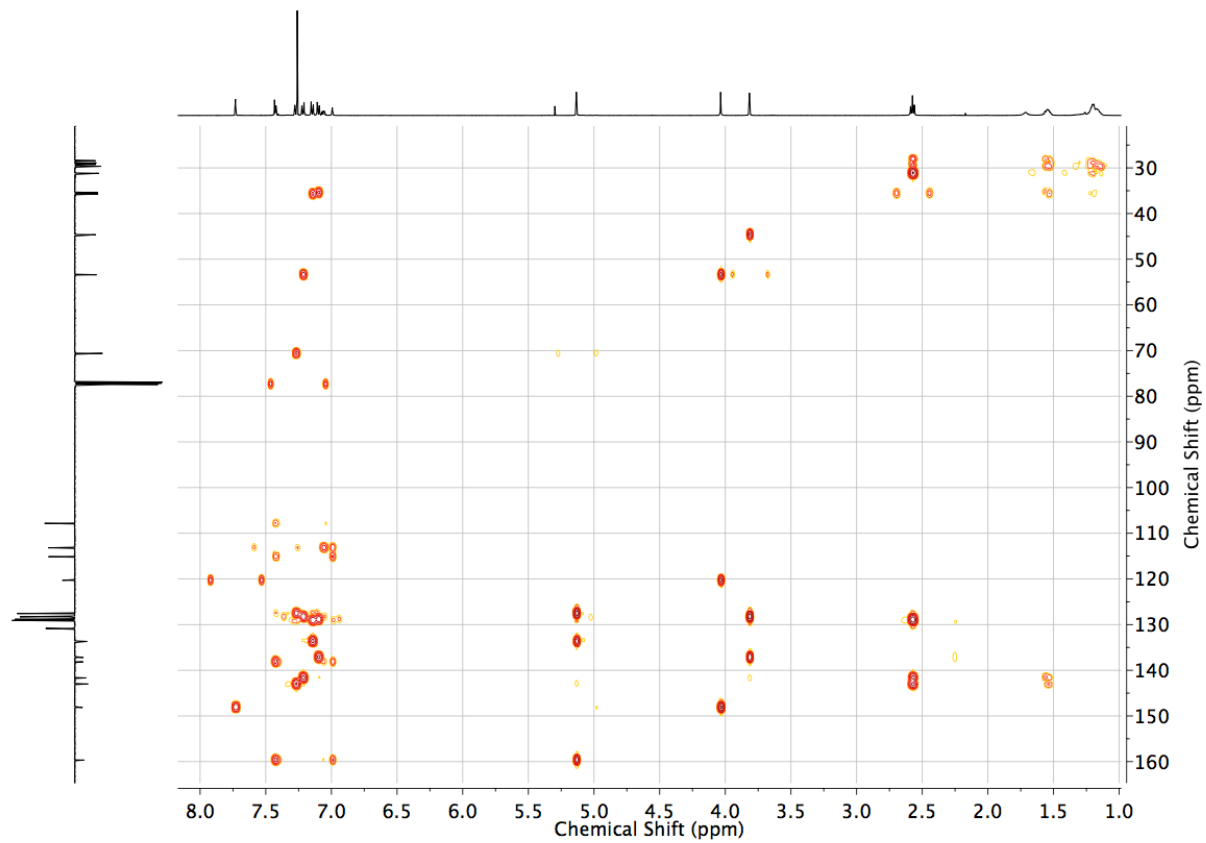


Figure S98 HMBC NMR (CDCl_3) of **S13**.

6. Chiral Stationary Phase HPLC analysis of catenane **6b**, **S8** and **S9**

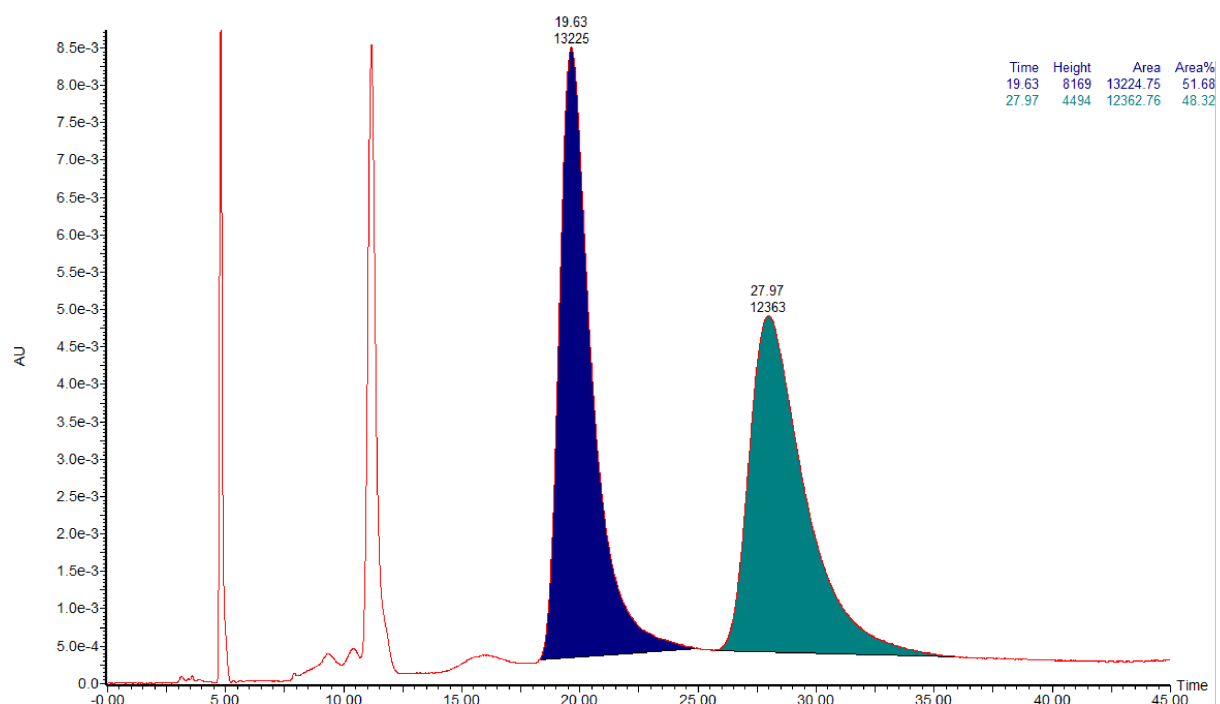


Figure S99 CSP-HPLC for the Racemic catenane **6b**. RegisCell (hexane/*i*-PrOH, 98:2), flow rate 0.5 mL.min⁻¹, diode array detection.

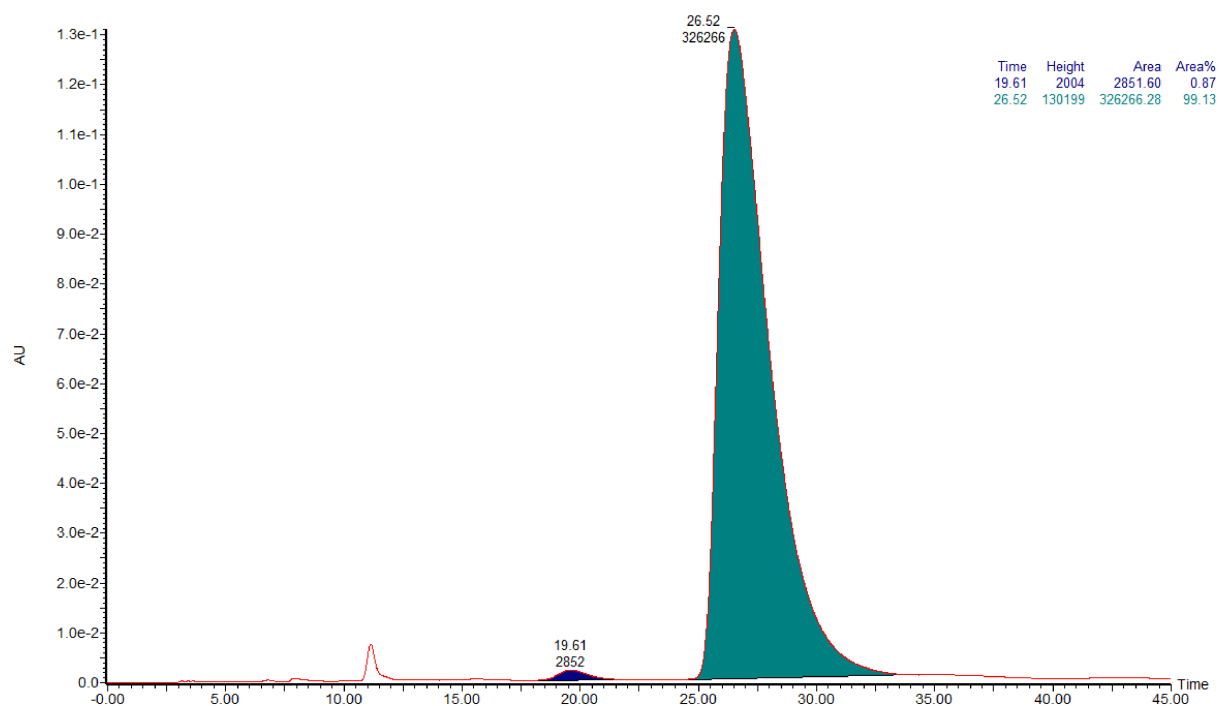


Figure S100 CSP-HPLC for the (*R_{mt}*)-**6b**. RegisCell (hexane/*i*-PrOH, 98:2), flow rate 0.5 mL.min⁻¹, diode array detection.

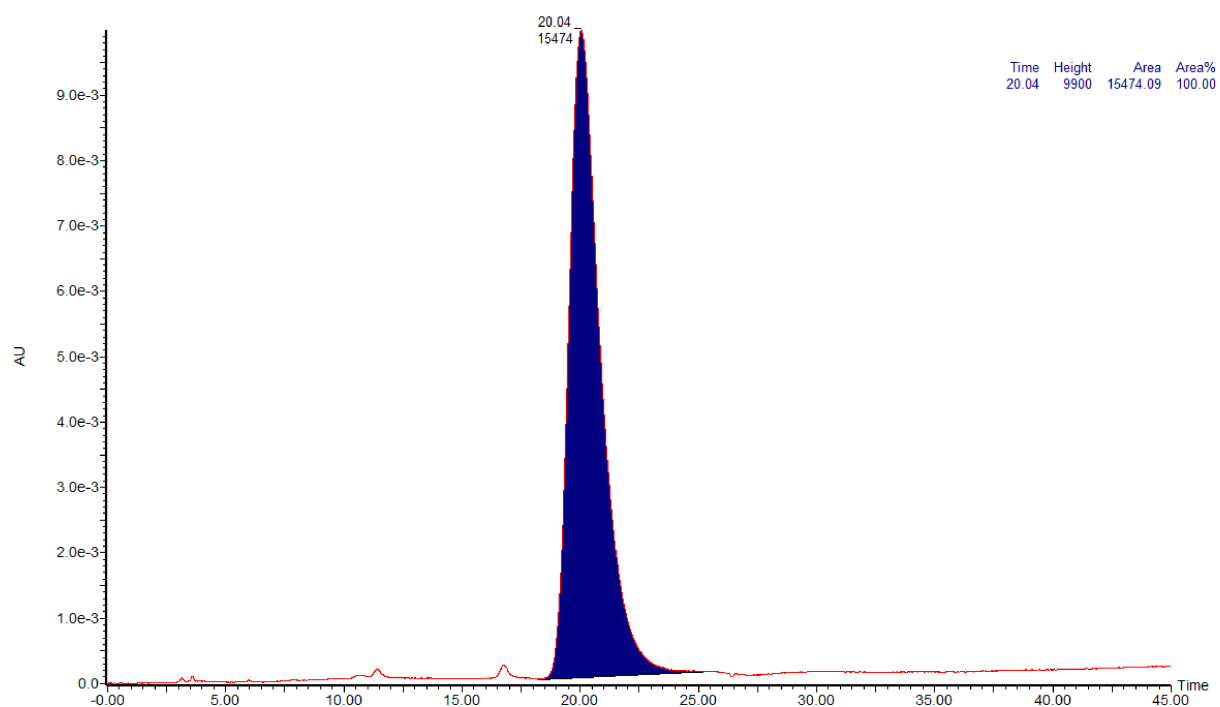


Figure S101 CSP-HPLC for the (*S*_{mt})-**6b**. RegisCell (hexane/*i*-PrOH, 98:2), flow rate 0.5 mL.min⁻¹, diode array detection.

MD-IX-R amino ester - Whelk

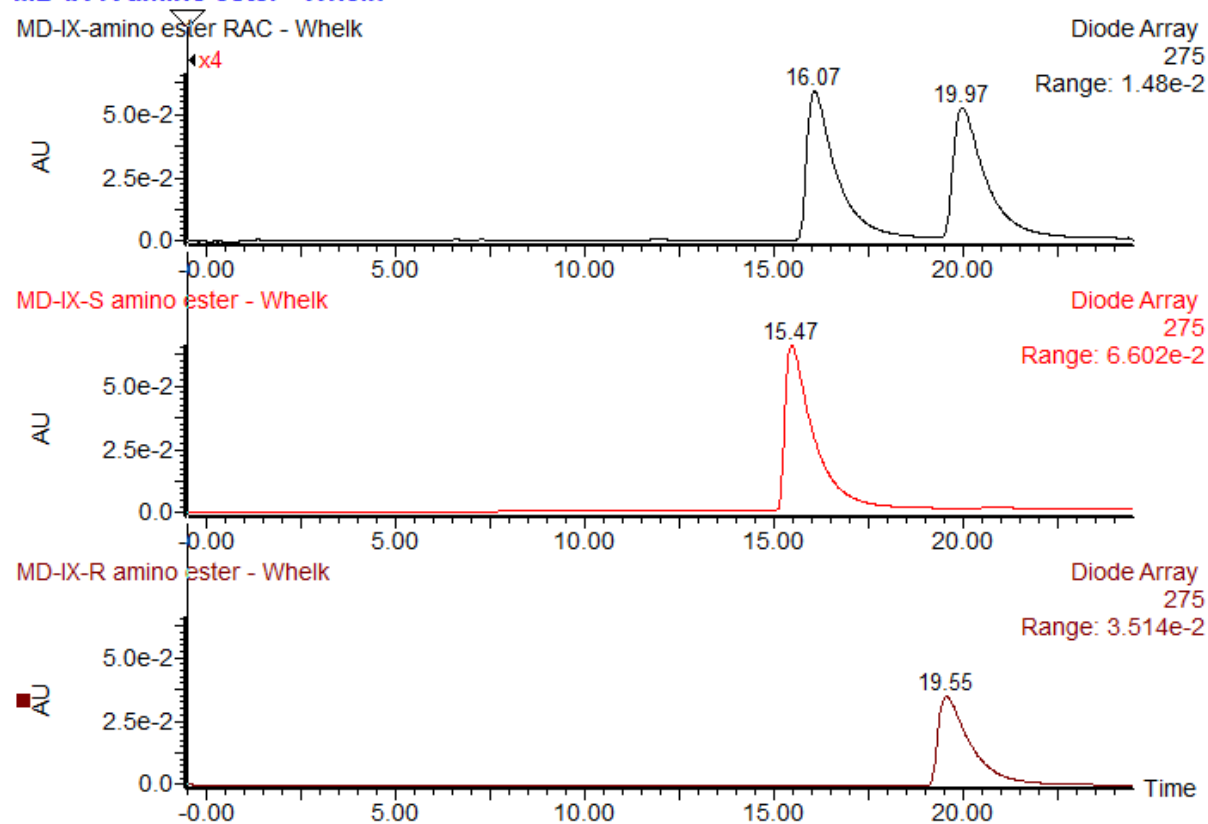
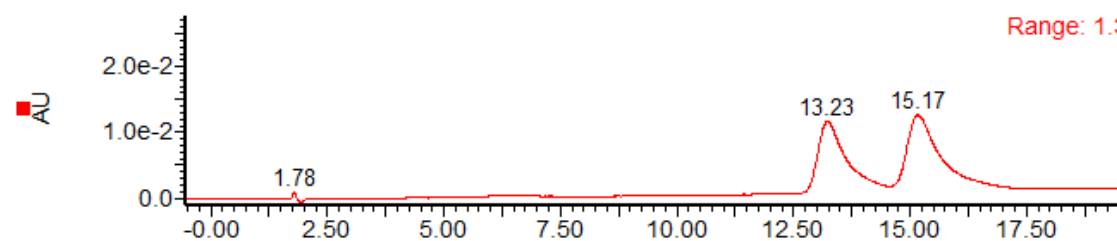


Figure S102 CSP-HPLC of (top) rac-**S8**, (middle) (*S*)-**S8**, and (bottom) (*R*)-**S8**. Whelk-O 1 (hexane/*i*-PrOH, 90:10), flow rate 2.0 mL.min⁻¹, λ = 275 nm.

MD-IX-Rac hydroxy propargylamine - RegisPack

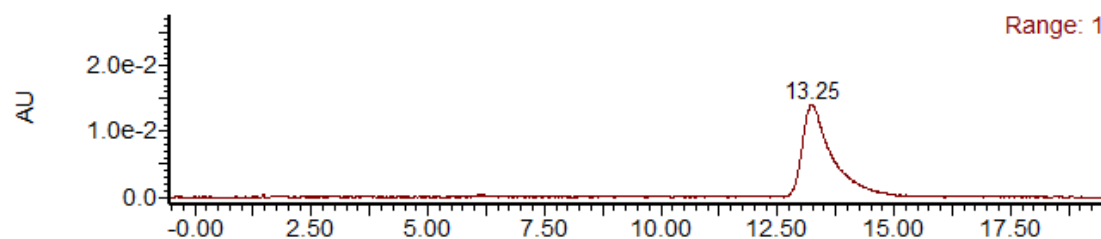
MD-IX-Rac hydroxy propargylamine - RegisPack

Diode Array
275
Range: 1.327e-2



MD-IX-S hydroxy propargylamine C- RegisPack

Diode Array
275
Range: 1.43e-2



MD-IX-R hydroxy propargylamine - RegisPack

Diode Array
275
Range: 2.774e-2

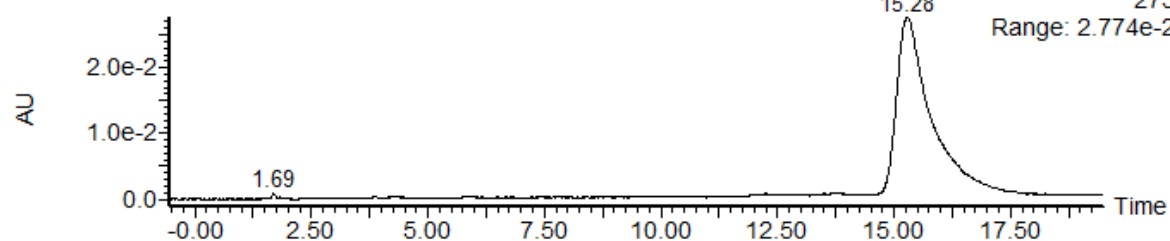


Figure S103 CSP-HPLC of (top) rac-S9, (middle) (S)-S9, and (bottom) (R)-S9. RegisPack (hexane/EtOH, 97:3), flow rate 1.5 mL.min⁻¹, λ = 275 nm.

7. Single Crystal X-ray Analysis of Catenane (S^*,R_{mt}^*)-**3b**

Experimental: Single colourless crystals of catenane (S^*,R_{mt}^*)-**3b** were obtained from vapor diffusion of pentane into a chloroform solution of the product. A suitable crystal was selected ($0.10 \times 0.09 \times 0.08$ mm³) and data were collected at a steady $T = 100(2)$ K using a FRE+ HF diffractometer equipped with a Saturn 724+ enhanced sensitivity detector. Cell determination, data collection, data reduction, cell refinement and absorption correction were performed with CrysAlisPro. During the data processing, the lower resolution limit was set to 0.90 Å because of the low resolution of the material. The structure was solved with the SHELXT⁶ structure solution program using the Intrinsic Phasing solution method and by using Olex2⁷ (Dolomanov et al., 2009) as the graphical interface. The model was refined against F_2 using anisotropic thermal displacement parameters for all non-hydrogen atoms using with version 2018/3 of SHELXL⁶ using Least Squares minimisation. Hydrogen atoms were placed in calculated positions and refined using a riding model. SHELX SADI, SIMU, ISOR, and RIGU restraints were used in the refinement strategy, as listed in the cif file, mostly for one of the aromatic rings and the alkyl chain connected to it in one of the two catenanes present within the unit cell.

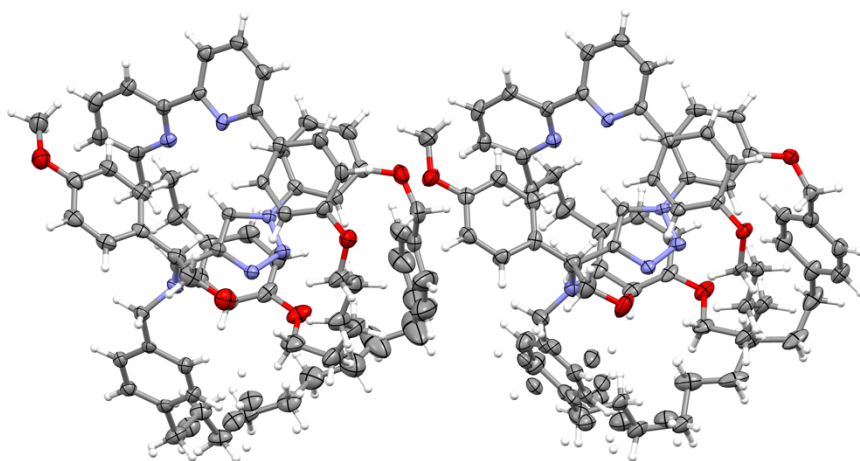


Figure S104 Ellipsoid plot of the asymmetric unit of a racemic mixture (R,S_{mt}) and (S,R_{mt}) of catenane **3b**. Ellipsoids are shown at the 50% probability level.

Compound	**C6MajorDia**	
CCDC No.	1885204	
Empirical formula	$C_{144}H_{158}N_{12}O_{10}$	
Formula weight	2216.81	
Temperature	100(2) K	
Wavelength	0.71073 Å	
Crystal system	Monoclinic	
Space group	$P2_1/n$	
Unit cell dimensions	$a = 26.2879(9)$ Å	$\alpha = 90^\circ$
	$b = 16.1275(5)$ Å	$\beta = 106.741(4)^\circ$
	$c = 29.7838(11)$ Å	$\gamma = 90^\circ$
Volume	$12091.9(8)$ Å ³	
Z	4	
Density (calculated)	1.218 Mg/m ³	
Absorption coefficient	0.077 mm ⁻¹	
F(000)	4744	
Crystal size	$0.095 \times 0.090 \times 0.080$ mm ³	
Theta range for data collection	1.500 to 23.256° .	

Index ranges	-29<=h<=29, -17<=k<=17, -33<=l<=33
Reflections collected	162942
Independent reflections	17362 [R(int) = 0.1998]
Completeness to theta = 23.256°	100.0 %
Absorption correction	Semi-empirical from equivalents
Max. and min. transmission	1.00000 and 0.72382
Refinement method	Full-matrix least-squares on F ²
Data / restraints / parameters	17362 / 0 / 1499
Goodness-of-fit on F ²	1.038
Final R indices [I>2sigma(I)]	R ₁ = 0.0885, wR ₂ = 0.2087
R indices (all data)	R ₁ = 0.1668, wR ₂ = 0.2649
Extinction coefficient	n/a
Largest diff. peak and hole	0.673 and -0.575 e.Å ⁻³

The solid state structure of the racemic (*R,S_{mt}*)-**3b**/*(S,R_{mt})*-**3b** mixture contains two crystallographically independent conformers of the catenane in the asymmetric unit. These pack together to form one-dimensional chains composed of single enantiomers extending along the *a* axis (**Figure S105**). Adjacent to each of the chains pack, on one side, anti-parallel chains of the same enantiomer, and, on the other side, chains of the opposite enantiomer. This results in a two-dimensional lattice with a repeating pattern of (*R,S_{mt}*) (*R,S_{mt}*) (*S,R_{mt}*) (*S,R_{mt}*) one-dimensional chains (**Figure S106**), with adjacent chains of opposite enantiomers packing in an anti-parallel fashion. This packing of chains composed of opposite enantiomers adjacent to each other could help explain the relative ease with which the racemic mixture was able to be crystallised relative to the enantiopure compound.

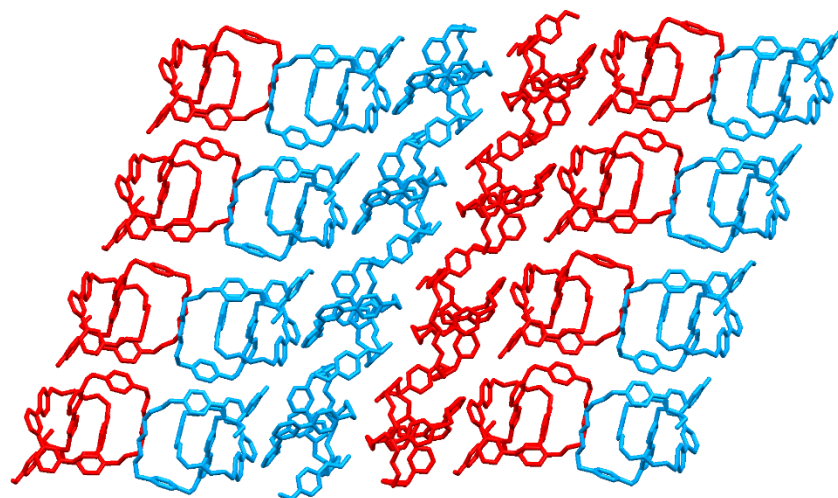


Figure S105 Packing diagram of the solid state structure of (*R,S_{mt}*)-**3b**/*(S,R_{mt})*-**3b** showing the one-dimensional chains that run parallel to the *a* axis. (*R,S_{mt}*)-**3b** is shown in red and (*S,R_{mt}*)-**3b** in blue. Hydrogen atoms have been omitted for clarity

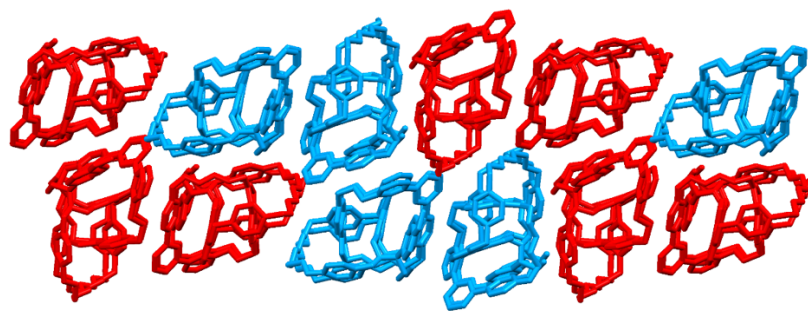
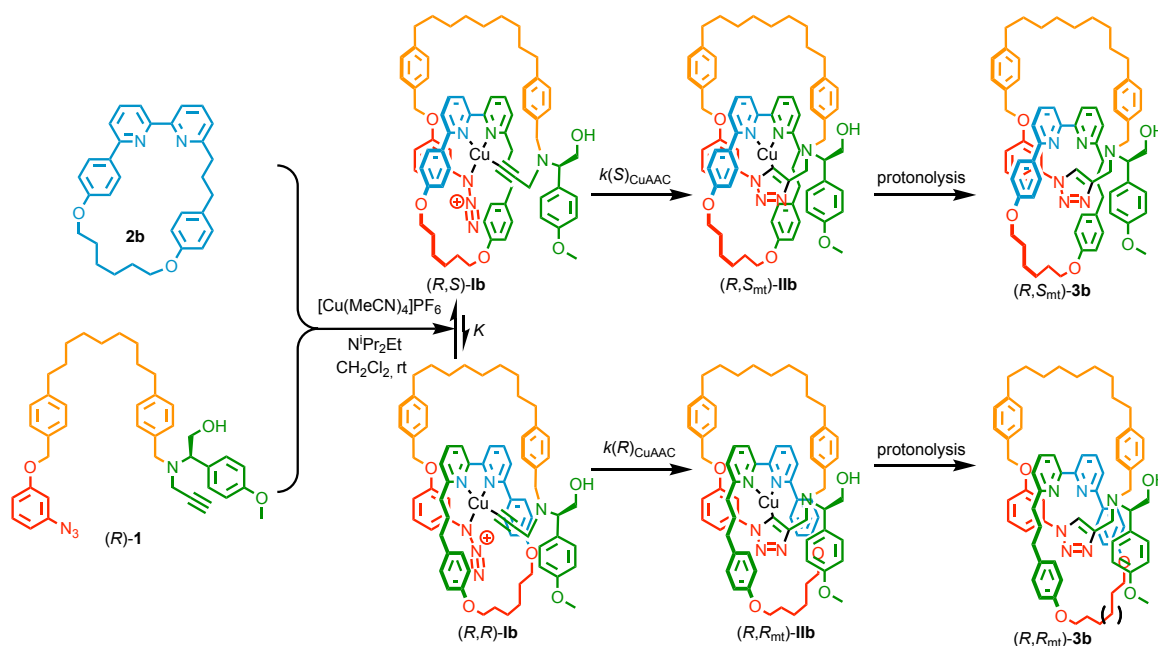


Figure S106 Packing diagram of the solid state structure of $(R,S_m)\text{-3b}/(S,R_m)\text{-3b}$ viewed down the a axis. $(R,S_m)\text{-3b}$ is shown in red and $(S,R_m)\text{-3b}$ in blue. Hydrogen atoms have been omitted for clarity.

8. Preliminary Molecular Modelling of the AT-CuAAC Reaction Between (*R*)-1 and 2b

Based on previous work,⁴ the AT-CuAAC reaction of macrocycle **2b** with (*R*)-1 is thought to proceed via Cu^I-acetylides **1b** which are irreversibly converted to Cu^I-triazolides **11b** and then, after protolytic work-up, to catenanes (*R,S_{mt}*)-**3b** (major) and (*R,R_{mt}*)-**3b** (Scheme S4). Based on this proposed mechanism, two obvious sources of diastereoselectivity can be identified; i) an energy difference between (*R,S*)-**1b** and (*R,R*)-**1b** which results in a biased pre-equilibrium (Cu^I acetylide formation can be expected to be reversible in the presence of NⁱPr₂Et) prior to irreversible covalent bond formation; ii) a difference in reaction rate for the conversion of (*R,S*)-**1b** → (*R,S_{mt}*)-**11b** and (*R,R*)-**1b** → (*R,R_{mt}*)-**11b**.

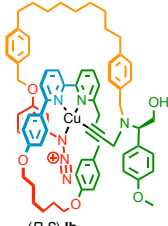
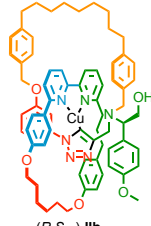
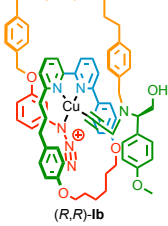
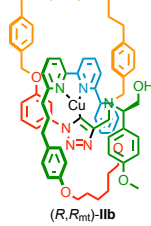


Scheme S4 Schematic mechanism of the AT-CuAAC reaction via acetylides (**1b**) and triazolides (**11b**)

To probe the origin of stereoselectivity in this AT-CuAAC reaction we carried out preliminary calculations (DFT, rB3LYP, 631G) to determine the relative energies of diastereomers **1** and the $\Delta_r G$ of the diastereomeric reactions **1b** → **11b**. It should be noted that, given the controversial nature of the cycloaddition mechanism and the size of the molecules concerned, accurately identifying the transition state energies for the cycloaddition step lies beyond the scope of this preliminary study. However, linear-free energy relationship considerations suggest that reactions proceeding via the same pathway but with a more negative $\Delta_r G$ of reaction can be expected to have a lower reaction barrier, although the difference in reaction energies is likely to be significantly larger than the difference in activation energies as this exoergic reaction is predicted to have an early barrier (Hammond postulate). Thus, although these calculations cannot be used to derive the difference in reaction rates for (*R,S*)-**1b** → (*R,S_{mt}*)-**11b** and (*R,R*)-**1b** → (*R,R_{mt}*)-**11b**, the comparison of the reaction energies gives an indication of whether a difference in reaction rates is to be expected.

Molecular models of intermediates **1b** and **11b** were prepared in Spartan '10 (Wavefunction Ltd) and subjected to a conformer search (MMFF).⁵ The lowest energy conformer of each was selected and the coordinates obtained were transferred to GausView5 (Gaussian, Inc., Wallingford CT, 2009). Each lowest energy conformer was subjected to optimization first using semi-empirical (PM6) then DFT (rB3LYP, 631G, gas phase) using Gaussian '09 (Gaussian, Inc., Wallingford CT, 2009).⁶ The energies obtained (normalized to the lowest energy of the series) are given in Table S1.

Table S1. Computed energies (normalised to 0 kJmol⁻¹ for (*R,S_{mt}*)-**IIb**) of molecular models of the AT-CuAAC reaction intermediates of pre-macrocycle (*R*)-**1** and macrocycle **2b**.

Entry	Acetylide intermediate	Triazolide intermediate
1	 (<i>R,S</i>)- Ib 243.8 kJmol ⁻¹	 (<i>R,S_{mt}</i>)- IIb 0 kJmol ⁻¹
	$\Delta G = -243.8 \text{ kJmol}^{-1}$	
2	 (<i>R,R</i>)- Ib 248.5 kJmol ⁻¹	 (<i>R,R_{mt}</i>)- IIb 1.8 kJmol ⁻¹
	$\Delta G = -246.7 \text{ kJmol}^{-1}$	
$\Delta E =$	4.7 kJmol ⁻¹	-2.9 kJmol ⁻¹
		1.8 kJmol ⁻¹

Based on the results in Table S1 the origin of the stereoselectivity is predicted to be complex as the biased pre-equilibrium, which favours (*R,S*)-**Ib** by approximately 5.3:1 at 337 K, is opposed by the predicted kinetic preference of the cycloaddition step, which the data suggests favours the formation of the (*R,R_{mt}*) product ($\Delta_r G$ for (*R,R*)-**Ib** \rightarrow (*R,R_{mt}*)-**IIb** is $\sim 2.9 \text{ kJmol}^{-1}$ more exoergic than (*R,S*)-**Ib** \rightarrow (*R,S_{mt}*)-**IIb**). It should be noted, however, that the predicted level of selectivity in both cases is low. Furthermore, given that the difference in ΔG^\ddagger for the cycloaddition step is expected to be much lower than the difference in reaction energies (i.e. much less than 2.9 kJmol^{-1}), it seems reasonable that the slight bias in the pre-equilibrium step is sufficient to render the reaction stereoselective.

Perhaps unsurprisingly, given the small energy differences calculated, examining the models obtained does not give any significant clues as to the origin of different stabilities of the intermediates beyond the observation that all of the structures are highly sterically hindered (see space filling models in Figures S107-110) and that, thanks to the nature of the catenane architecture, this steric hindrance is expressed throughout the contact points between the two rings. The most noteworthy feature is that in all cases the large aromatic substituent of the auxiliary is projected away from the rest of the molecule.

In the case of (*R,R*)-**Ib** this appears to force the encircling chain (orange) of the alkyne/azide pre-macrocycle to partially straddle an aromatic ring (green) of the bipyridine macrocycle whereas in all of the other calculated structures the pre-macrocycle chain sits below the aromatic ring and mainly interacts with the alkyl region of the macrocycle. This may help account for the slight predicted destabilization of (*R,R*)-**Ib** vs (*R,S*)-**Ib** but this is clearly speculative.

It is also worth noting that in both triazolide intermediates, a hydrogen bond between the N³ of the triazolide and the hydroxyl group is predicted. This interaction creates a cycle that includes the fixed stereogenic centre of the auxiliary and might be expected to enhance the transfer of chiral information and thus aid diastereoselection. However, given that this interaction is not presented in the predicted lowest energy conformations of the acetylide precursor (the distance N \cdots H-O is too great), it raises the question as to whether intermediates **Ib** and **IIb** are directly connected by a single transition state (i.e. perhaps the initially formed triazolide lacks this interaction and then undergoes conformational

rearrangement to take advantage of this stabilising contact). The favourability of this interaction is also likely to be modulated by competition with solvent, particularly relevant given the reaction is carried out in an EtOH co-solvent. Finally, it is worth noting that this H-bonding interaction is absent in the solid state structure of (*R*^{*},*S*^{*}_{mt})-**3b**, where the OH is engaged in an H-bond with the sp³ nitrogen instead, suggesting multiple H-bonded conformations/co-conformations are accessible.

Thus, although the calculations presented are consistent with the observed stereoselectivity, much more detailed studies are required to give a true explanation of the observed behaviour. In particular, a transition state must be found that connects the acetylide and triazolide intermediates and, given the potential role direct interactions with solvent may play, it is likely that explicit solvent will be required to gain an accurate representation of the process. These calculations lie outside the scope of this report, but we are currently working on generating predictive models that can then be tested and refined experimentally and the results of this study will be reported in due course.

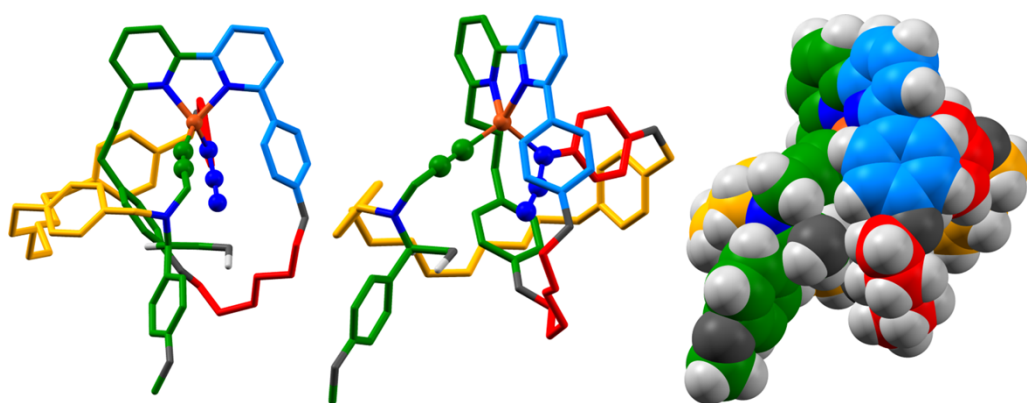


Figure S107. DFT (B3LYP, 631G, gas phase) model of intermediate (*R,R*)-**1a** viewed from the front and side in capped sticks representation, and from the side in space-filling representation.

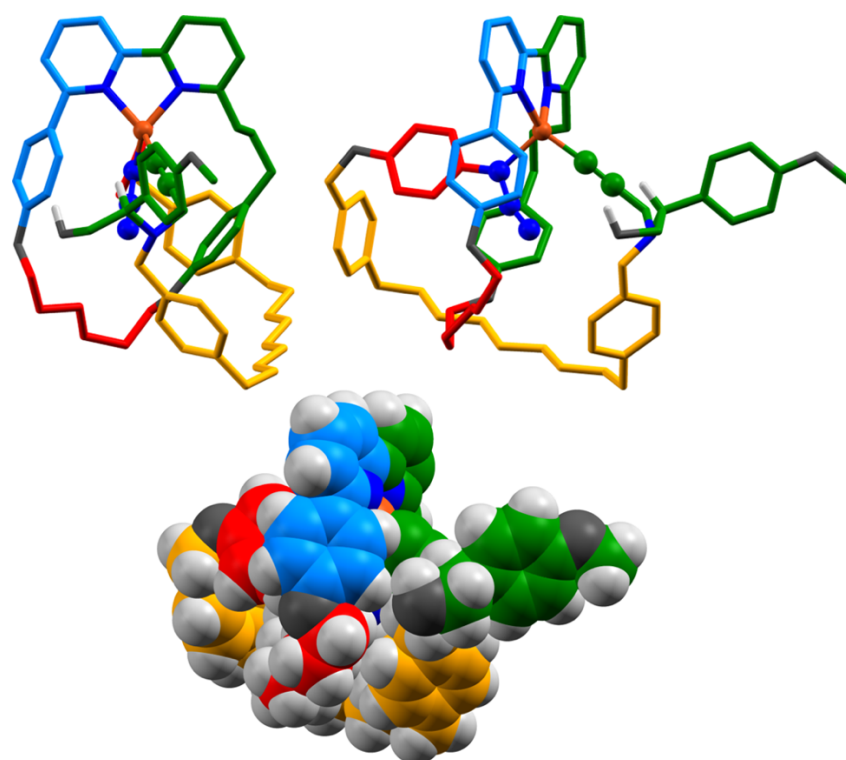


Figure S108. DFT (B3LYP, 631G, gas phase) model of intermediate (*R,S*)-**1a** viewed from the front and side in capped sticks representation, and from the side in space-filling representation.

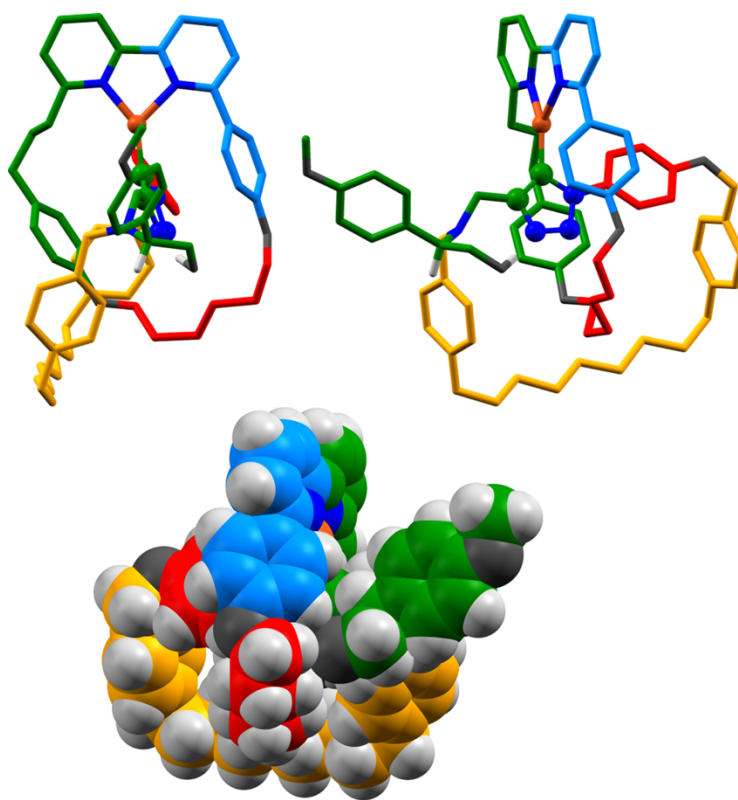


Figure S109. DFT (B3LYP, 631G, gas phase) model of intermediate (*R,S_{mt}*)-IIb viewed from the front and side in capped sticks representation, and from the side in space-filling representation.

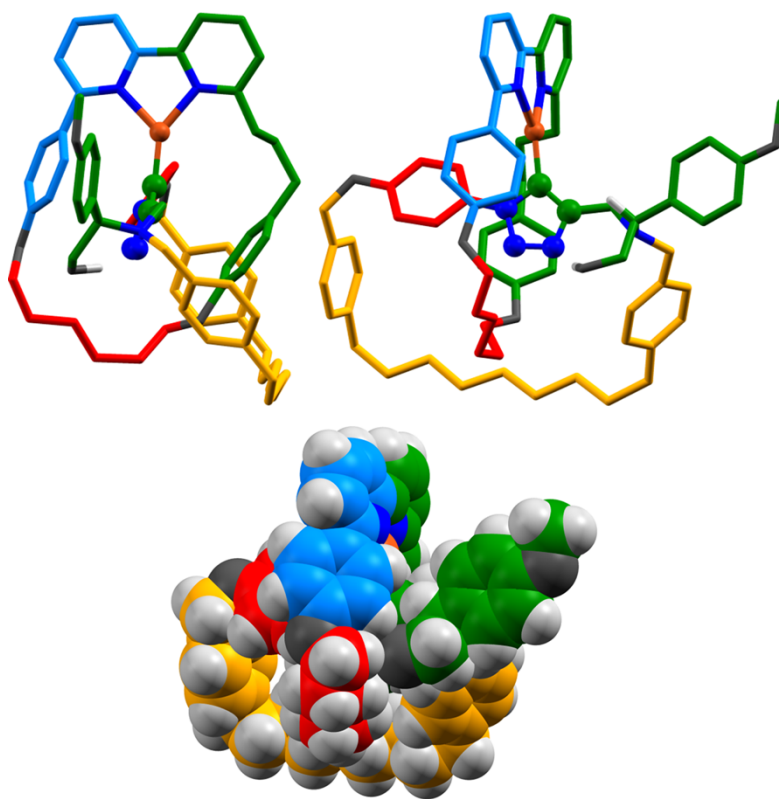


Figure S110. DFT (B3LYP, 631G, gas phase) model of intermediate (*R,R_{mt}*)-IIb viewed from the front and side in capped sticks representation, and from the side in space-filling representation.

9. Supplemental References

1. Lewis, J.E.M., Bordoli, R.J., Denis, M., Fletcher, C.J., Galli, M., Neal, E.A., Rochette, E.M. and Goldup, S.M. (2016). High yielding synthesis of 2,2'-bipyridine macrocycles, versatile intermediates in the synthesis of rotaxanes. *Chem. Sci.* **7**, 3154–3161.
2. Ravi Kumar, A., Bhaskar, G., Madhan, A. and Venkateswara Rao, B. (2003). Stereoselective Synthesis of (–)-Cytoxazone and (+)-5-Epi-cytoxazone. *Synth. Commun.* **33**, 2907–2916.
3. Lewis, J.E.M., Modicom, F. and Goldup, S.M. (2018). Efficient Multicomponent Active Template Synthesis of Catenanes. *J. Am. Chem. Soc.* **140**, 4787–4791.
4. Neal, E.A. and Goldup, S.M. (2016). A Kinetic Self-Sorting Approach to Heterocircuit [3]Rotaxanes. *Angew. Chem., Int. Ed.* **55**, 12488–12493, (2015). Competitive formation of homocircuit [3]rotaxanes in synthetically useful yields in the bipyridine-mediated active template CuAAC reaction. *Chem. Sci.* **6**, 2398–2404.
5. Please note: for convenience, diastereomeric intermediates leading to (*R*,*R*_{mt})-**3b** and (*S*,*R*_{mt})-**3b** were modelled as these can be obtained by manually inverting the covalent stereocenter. Given that the intermediates *en route* to (*S*,*R*_{mt})-**3b** are enantiomeric to those leading to (*R*,*S*_{mt})-**3b** (i.e. have identical properties) the results presented here are valid for the (*R*,*S*/*R*) manifold. The coordinates of the modelled structures are available as supporting information for the manuscript (Data File 2).
6. M. J. Frisch, G. W. Trucks, H. B. Schlegel, G. E. Scuseria, M. A. Robb, J. R. Cheeseman, G. Scalmani, V. Barone, B. Mennucci, G. A. Petersson, H. Nakatsuji, M. Caricato, X. Li, H. P. Hratchian, A. F. Izmaylov, J. Bloino, G. Zheng, J. L. Sonnenberg, M. Hada, M. Ehara, K. Toyota, R. Fukuda, J. Hasegawa, M. Ishida, T. Nakajima, Y. Honda, O. Kitao, H. Nakai, T. Vreven, J. A. Montgomery, Jr., J. E. Peralta, F. Ogliaro, M. Bearpark, J. J. Heyd, E. Brothers, K. N. Kudin, V. N. Staroverov, R. Kobayashi, J. Normand, K. Raghavachari, A. Rendell, J. C. Burant, S. S. Iyengar, J. Tomasi, M. Cossi, N. Rega, J. M. Millam, M. Klene, J. E. Knox, J. B. Cross, V. Bakken, C. Adamo, J. Jaramillo, R. Gomperts, R. E. Stratmann, O. Yazyev, A. J. Austin, R. Cammi, C. Pomelli, J. W. Ochterski, R. L. Martin, K. Morokuma, V. G. Zakrzewski, G. A. Voth, P. Salvador, J. J. Dannenberg, S. Dapprich, A. D. Daniels, Ö. Farkas, J. B. Foresman, J. V. Ortiz, J. Cioslowski, and D. J. Fox, Gaussian 09 (Gaussian, Inc., Wallingford CT, 2009).
6. Sheldrick, G. M. (2015). Crystal structure refinement with SHELXL. *Acta. Cryst.* **C71**, 3-8.
7. Dolomanov, O. V., Bourhis, J. L., Gildea, J., Howard, J. A. K., and Pushmann, H. (2009). OLEX2: a complete structure solution, refinement and analysis program. *Appl. Crystallogr.* **42**, 339-341.